DEPARTMENT OF MECHANICAL & AEROSPACE ENGINEERING

University of Strathclyde Engineering

FINITE ELEMENT ANALYSIS AND STRUCTURAL OPTIMISATION OF A CONCRETE MIXER

PETER MACDONALD

A thesis submitted in partial fulfillment

of the requirements for the degree of

Master of Philosophy (Mechanical and Aerospace Engineering)

University of Strathclyde

2017

Abstract

The UK concrete transport industry desires low weight concrete mixers in order to maximise payload. To investigate the potential for weight reduction of the mixer unit itself, three key structures of a particular mixer have been analysed using Finite Element Analysis; the front drum support structure, rear drum support structure, and the sub-frame.

A full scale 'dynamic load test' has been documented. This involved recording data from 20 strain gauges and 2 accelerometers attached to a concrete mixer. The three main load cases investigated during this test were bump/pothole loads, braking loads, and 'downhill' loads. The results are presented and discussed with a view to understanding the load paths through the whole structure. The data has provided a solid foundation for future work which could focus on specific areas. A test to investigate the differences in elastic properties of holding down U-bolts versus straight bolts has also been documented as these components facilitate the main load path between the supports and the chassis. Recommended practices for implementing a Design by Analysis process are discussed.

A redesign of the front drum support has allowed two sub-frame stiffening plates to be removed. This revised front support is 21% lighter than the combination of the existing front support and the stiffening plates. An optimisation study of the existing rear drum support has resulted in a reduction in the weight of this structure by 26%. The sub-frame was not lightened due to this being difficult to achieve without decreasing stiffness, which is already relatively low. However, some basic analysis has been done to examine the design of the brackets that secures the sub-frame to the chassis.

This work has shown that there is scope to reduce the weight of truck-mounted concrete mixers. In this industry, applying a comprehensive Design by Analysis process would significantly increase the profits achievable by companies involved in the transport of concrete. Concrete mixer manufacturers and similar SME's should consider this approach; however it must be ensured that the capabilities of FEA are fully understood before making a business case. Furthermore, it is vital to the success of the process that the engineers using the software are suitably trained or experienced.

Declaration of Authenticity

This thesis is the result of the author's original research. It has been composed by the author and has not been previously submitted for examination which has led to the award of a degree.

Signed:

Date:

Table of Contents

List of Figures

List of Tables

Abbreviations

DBA – Design by Analysis

FEA – Finite Element Analysis

SME – Small and Medium Enterprises

HGV – Heavy Goods Vehicle

HSLA – High-Strength Low-Alloy

OE – Original Equipment

SAE – Society of Automotive Engineers

HAZ – Heat Affected Zone

TIG – Tungsten Inert Gas (Welding)

MEMS – Microelectromechanical Systems

ABS – Anti-lock Braking System

RHS – Rectangular Hollow Section

Nomenclature

Hz – Hertz

N - Newton

MPa – Mega-Pascal (N/mm^2)

m – Mass

g – Acceleration (G-force)

1. Introduction

1.1 Concrete Mixer Functionality and Key Industrial Challenges

The main components comprising the structure of a typical concrete mixer are illustrated below.

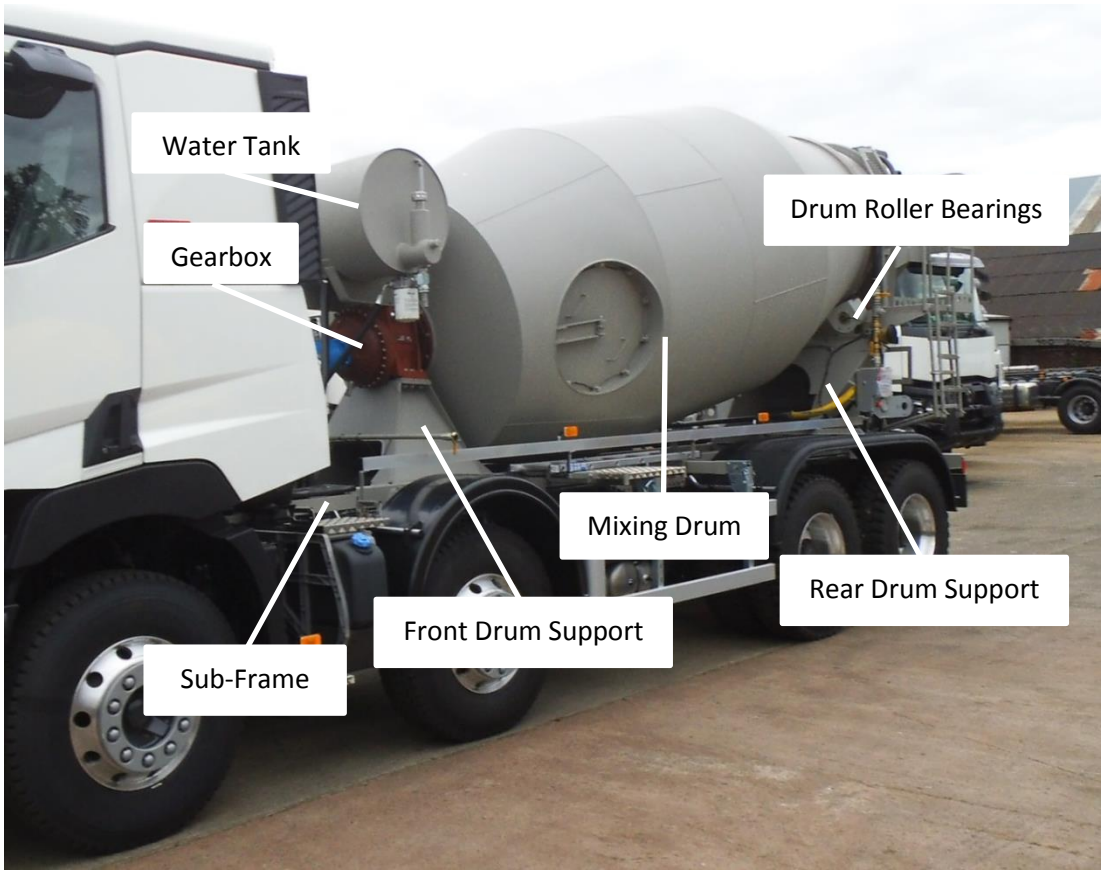

Figure 1-1 - Concrete Mixer Schematic

Truck-mounted concrete mixers, or transport mixers, are designed to transport large volumes of wet concrete whilst agitating the contents. Most concrete types used in the UK are effectively mixed before being loaded into a concrete mixer, and therefore there is a decreased requirement for the mixing drum to provide strong mixing characteristics. The drum contains a helical spiral blade arrangement, as illustrated below. When the drum is 'charging', it rotates anti-clockwise and therefore pushes the contents towards the front of the drum, and when 'discharging' the drum rotates clockwise thus pushing the concrete out the rear of the drum.

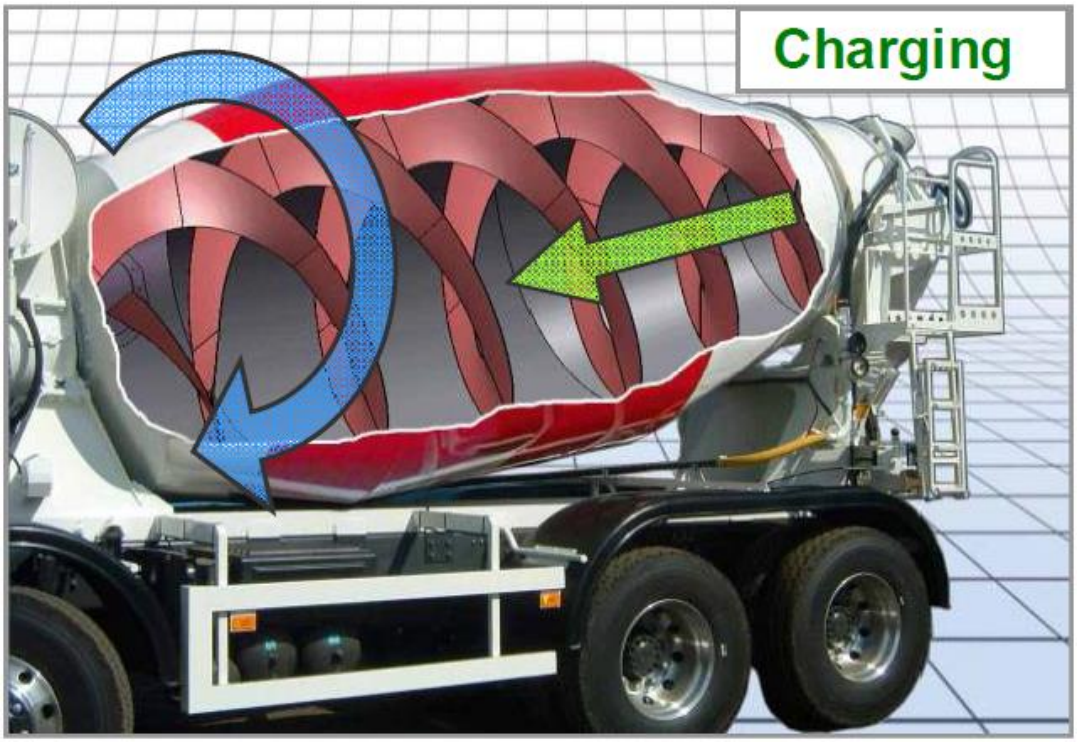

Figure 1-2 – Helical Blade Arrangement

Concrete consists of cement, water, and aggregates. Aggregates (gravel, sand etc) make up approximately 60-75% of the mixture. This high volume of aggregates leads to extensive wear occurring inside the mixing drum, and indeed on the chutes used to direct the concrete in and out of the drum. Mixing drums and blades are now typically made of high strength wear-resistant steels such as Hardox made by SSAB. These high strength steels can serve two purposes; to reduce weight and to increase lifespan.

Weight is a great consideration in the industry of concrete transport. In the UK, 4-axle rigid trucks (non-articulated) are limited to 32 tonnes as per Road Vehicles (Construction and Use) Regulations 1986 (SI 1986/1078). 4-axle rigid trucks are typically the type of truck used for concrete mixers, and the most common mixing drum size is $8m^3$. This drum can carry an $8m^3$ volume of concrete; however the trucks reach the 32 tonne limit with approximately $7.5m^3$ of concrete on-board. There is a relatively large amount of revenue to be gained from carrying a larger volume of concrete; hence the desire for low weight concrete mixers. Financially it often works out best for the concrete transport companies to purchase more expensive lightweight mixing drums despite the fact that they may require replacement after a few years.

Corrosion is a significant issue in the industry which also has an impact on weight. As well as the damage caused by concrete, acidic cleaning fluids are sometimes used on concrete mixers. These acids damage the paint and the zinc coating on fasteners. Steel parts must therefore be of suitable thickness to help prevent them from rusting through within the normal lifespan of the mixer.

In the search for existing similar research, it was found that few experiments and research papers have been shared on the subject of loadings in the structure of a concrete mixer. Little information can be gained through the vehicle manufacturers regarding truck dynamics due to data secrecy. The loadings need to be determined before any design optimisation can be performed. The majority of structural failures in the industry take the form of cracks starting at or near welds. One of the aims of this study has been to gain an understanding as to the cause of these cracks. As part of this, dynamic load testing has been performed using strain gauges and accelerometers.

There can be an adverse reaction to change in the industry of concrete transport equipment. This impact needs to be considered as part of the business-decision when making design changes. Due to the number of concrete plants in existence (stations where concrete is loaded into mixers), any drastic changes to the loading system would have a huge impact. A concept was theorised recently whereby the loading chute and the ladder/platform would be permanently removed in favour of a radical new loading system. The new system would have a chute at the plant that would direct the concrete straight into the rear of the drum. This would significantly reduce the weight of the mixers. The foreseeable problem is with the implementation of such a large scale change.

1.2 Preface & Scope

This thesis investigates the loadings in the structure of a concrete mixer, discusses the use of high-strength steel in such structures, discusses the Design by Analysis (DBA) approach, and provides case-studies in which key parts of a concrete mixer have been optimised using the DBA approach. Comments on the use of the approach for concrete mixers and other heavy transport vehicles are also presented as is the wider impact of the work on the SME sector.

The author is not aware of any published research analysing the structure of concrete mixers to this extent. Research in this area is limited. Some research exists on the design of

the front drum support and the sub-frame cross members, Li et al (2014). This author examined torsional loadings in a concrete mixer, but no other load cases were considered. In the present work, a variety of load cases have been investigated. The scope of this structural analysis includes the two drum support structures and the sub-frame. The concrete mixer manufacturer collaborating in this research felt that their mixing drum was already well optimised; hence the mixing drum has not been included.

This work was made possible through a Knowledge Transfer Partnership arrangement between the University of Strathclyde and a concrete mixer manufacturer. Two years were spent working with the manufacturer to implement a Design by Analysis process and to reduce the weight of their concrete mixers. Various parts were analysed during this time, however case studies have only been presented for the three most important structures; the front and rear drum support structures and the sub-frame. The analysis and redesign of the front drum support required the largest amount of work due to its complexity and structural importance.

2. Literature Review

For the purposes of this research, the literature available for the following three areas has been studied; dynamics of heavy goods vehicles, performance of high-strength steels in welded sheet metal structures, and connection methods of mounting bodies on chassis.

2.1 Dynamics of Heavy Goods Vehicles

Before FEA studies can be performed, the loadings that trucks experience on the road must be known. Three worst case scenarios were identified for the structure of a concrete mixer; braking whilst on a downhill slope, hitting a large bump or pothole, and the chassis torsionally twisting over rough undulating terrain. Concrete mixers are most commonly built on 3-axle and 4-axle chassis. The dynamics of such trucks is complicated. Aurell (2013) points out that heavy goods vehicles have relatively flexible chassis in comparison to passenger cars. Due to the flexible chassis, it can be challenging to design the truck and its body in a way that prevents the structure's natural frequencies from falling within the range of typical road excitation frequencies. In the study by Fui & Rahman (2007) the first 6 natural frequency modes for a particular 4.5 tonne truck chassis were found to be in the range of 12.68 to 61.64Hz. The frequencies resulting from road roughness tend to be in the region of 0-100Hz. It is therefore possible for this type of truck chassis to experience resonant conditions due to road roughness. It was also found that the excitations caused by the engine and gearbox are less likely to create resonance in the chassis than excitations caused by road roughness. The higher the speed, the less likely it is that engine and gearbox excitations could contribute to resonance in the chassis.

There are no published studies measuring the extent of chassis twist for this type of truck, so a figure has been estimated for the analysis. It is thought that over the entire length of the chassis, a maximum twist of around 10° would be possible before the resistive forces in the chassis would begin to match the load applied by the vehicle's own weight, potentially lifting the wheels off the ground at one of the lower corners. This value is purely an estimation made by an engineer with significant experience in the manufacture of concrete mixers. Li et al (2014) studied strains in a mixers structure resulting from torsional twist; however the maximum possible twist was not tested. For the literature review, braking loads and bump/pothole loads have been investigated. The load cases ultimately used in the FEA studies are described in sections 5.1.2 and 5.1.3 for the front drum support and section 5.2.2 for the rear drum support.

2.1.1 Longitudinal/Braking Loads

In this section, the word 'acceleration' always refers to a negative acceleration, i.e., decreasing velocity. Under braking, the front drum support provides an equal and opposite force to that created by the acceleration of the drum and its contents. The approximate direction of the reaction force is illustrated below.

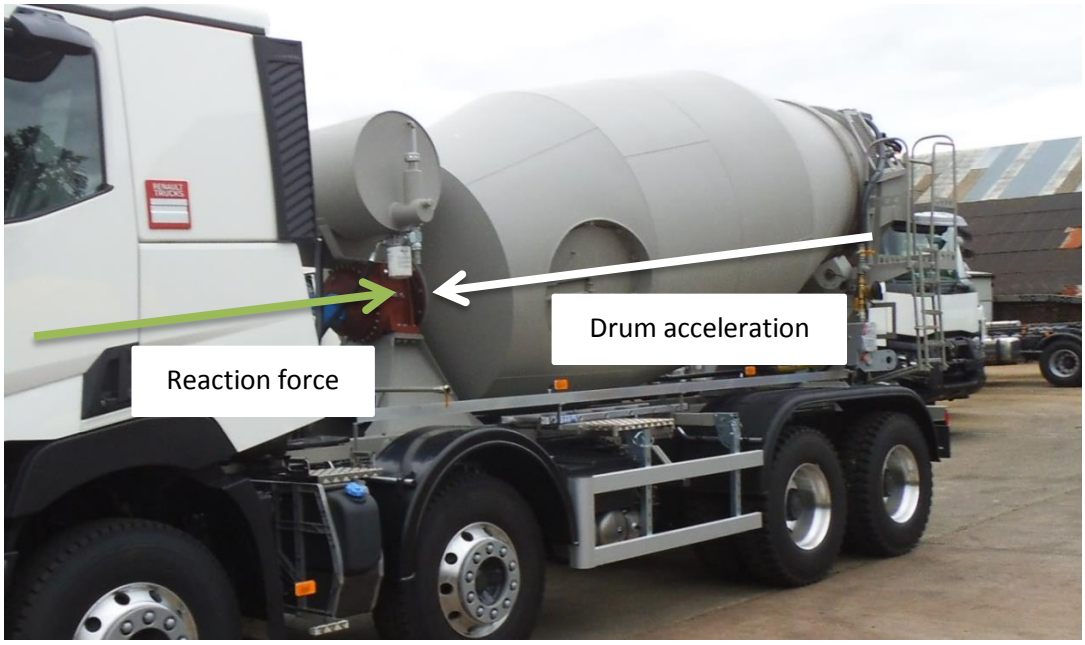

Figure 2-1 - Braking Load Illustration

A North American study by Dunn and Hoover (2004) tested 5 trucks in both LLVW and GVWR configurations (lightly loaded vehicle weight (not specified) and tractor gross vehicle weight rating – 22.7t). The shortest overall stopping distance recorded from 60mph on a surface with a high coefficient of friction in the LLVW configuration was 53m, and 66.4m in the GVWR configuration. This translates to average accelerations of 6.78m/s^2 (0.69g) and 5.42m/s^2 (0.55g) respectively. Another North American study in 2007 conducted by the National Highway Traffic Safety Administration, author unknown, performed extensive testing to compare OE and after-market brake shoe linings in a variety of test environments. The track-based tests were performed to the standards set by FMVSS 121 and involved braking from 60mph with maximum pedal pressure, therefore relying on the trucks ABS system. A variety of trucks and brake shoe linings were tested. The highest acceleration recorded for a fully loaded truck ("WC Class-8 Tandem-Axle") was 22 ft/s^2 (0.68g). The highest acceleration recorded for an unloaded truck ("W Class-8 Tandem-Axle") was 36.3 ft/s^2 (1.13g). For the unloaded truck, it was pointed out that such a high

acceleration seemed abnormal, but no issue was found with the equipment or the testing process.

Apart from the aforementioned US-based studies, little published data exists for the braking distances of trucks manufactured in the last 10 years or so. Birch (2001) reports that a Volvo FL12 (model year 1995) can stop from 30mph in 14.53m. Assuming a constant rate of acceleration, this equates to 0.63g. Since the acceleration would not be constant in reality, it could be assumed that the peak acceleration would be marginally greater. With the advances in tyre and braking technologies, one would imagine that the latest generation of HGV's (as of 2015) would be capable of achieving stopping distances in the region of 5-15% shorter than trucks manufactured 10 years ago.

In the finite element analysis of a truck trailer, Eckerlid et al (date unknown) used a longitudinal/braking acceleration of 0.65g. When running fatigue studies the longitudinal acceleration was changed to 0.25g (0.05g acceleration, 0.2g braking). George et al (1997) measured the "braking in a curve" capabilities of a number of heavy goods vehicles with trailers of combined weights between 40.9t to 66.1t. The curve had a 44.3m radius, and the truck was required to avoid locking its wheels and stay within the lane. The maximum longitudinal acceleration achieved was 0.54g. It was also pointed out that another author, Jarvis 1994, found that the peak braking acceleration for normal everyday driving is in the region of 0.17g for heavy vehicles.

For braking in a straight line and on flat ground, each source provides similar accelerations. The peak accelerations range from 0.55g to 0.69g for a variety of heavy goods vehicles, with the exception of that abnormal 1.13g achieved by an unloaded truck in the 2007 US study. Data for loaded trucks is of greater interest, since the peak stresses in the supporting structure will occur with a full load on-board.

2.1.2 Vertical/Bump Loads

For the following data, note that a vertical acceleration of 1g means there is 1g being added to the original weight. I.e. a body will double in weight when a vertical acceleration of 1g is applied. Under a vertical/bump load, the acceleration of the drum and its contents is transmitted through the front and rear drum supports as illustrated below.

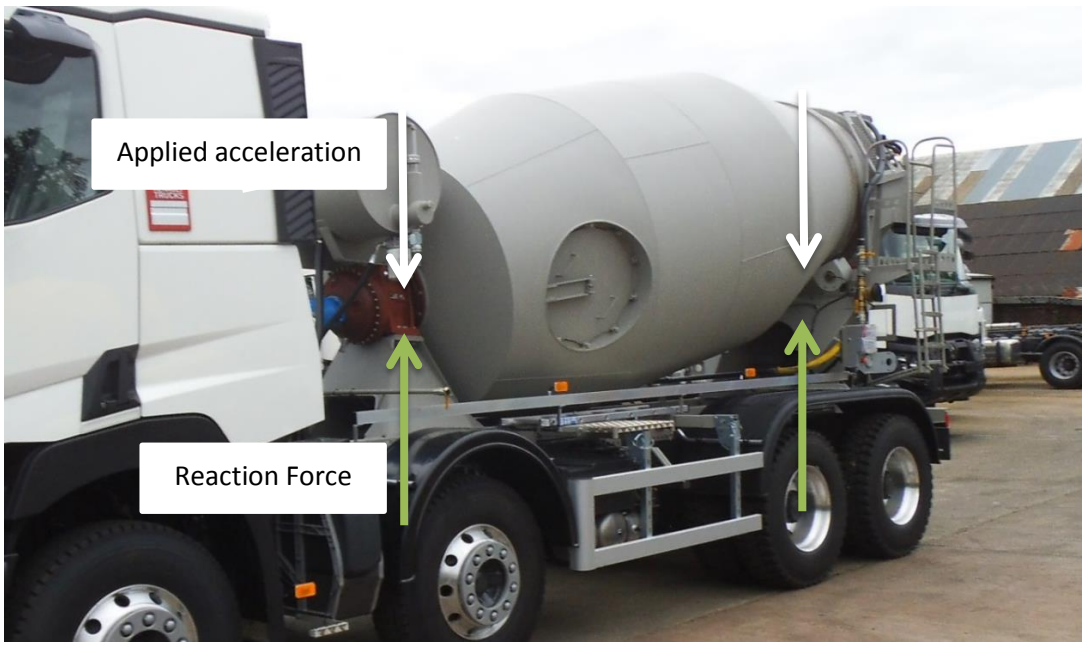

Figure 2-2 - Vertical Load Illustration

Kurdi and Rahman (2010) measured vertical acceleration of a truck chassis on a road of unstated roughness and found the max to be 1.5g. Eckerlid et al (date unknown) used a vertical acceleration of 1.7g as an estimated vertical load for the analysis of a truck trailer. To determine this load, Eckerlid consulted the manufacturer of the trailer and Epsilon High Tech Engineering. When running fatigue studies the vertical load was changed to 1.15g (±0.625g). In a report by students at Massachusetts Institute of Technology, a 1.5ft long and 4inch high speed bump provided an acceleration of 1.2g inside the body of a car travelling at 32mph. There is limited use in this data since the suspension on a car will almost certainly absorb such forces more effectively than the suspension on the rear of a HGV.

The above data is relevant for typical road bumps, but there is no suggestion as to the maximum vertical acceleration that a vehicle's body could be subjected to as a result of a particularly deep pothole, for example. There is no known published data pertaining to this subject. Whilst racing cars are not relevant to this area of study, it is interesting to note that in the analysis of a formula SAE car chassis, Riley & George (2002) found the maximum vertical acceleration to be 3.6g during a lap of their test track.

Excluding the data obtained for the SAE race car, the accelerations in the literature for vertical loadings are well matched. However, as mentioned previously this data does not

necessarily cover particularly large bumps/potholes. Therefore, a scaling factor will need to be used with these accelerations to represent a worst case scenario.

Incidentally, although this research is not concerned with lateral loadings, accelerations given in the literature for lateral loads are also well matched. George et al (1997) and Eckerlid et al (date unknown) both provide maximum lateral accelerations of 0.5g for HGV's.

2.2 Performance of High-Strength Steel in Welded Sheet Metal Structures

The supporting structure of a concrete mixer, largely a welded sheet metal structure, is subject to frequent large loadings. The use of high strength steel in such structures requires careful consideration. With or without high strength steel, weld fatigue strength is normally the determining factor for the life span of the structure. Therefore, designs previously using mild steel often need adjusted in order to take advantage of the benefits of high strength steel. Weld placement is the main consideration, another being the overall stiffness of the structure (if thinner material is used). Fatigue, weldability, formability, and the design of the structure itself need to be addressed in the process of determining whether high strength steel can provide sufficient benefit.

Costa et al (2010) found that the fatigue strength of Domex 600 (high-strength low-alloy steel with yield 600MPa) generally surpasses the recommendations given for conventional steels by the International Institute of Welding. This is particularly evident where the weld overfill has been removed and the toe has been smoothed off using a grinding disc, for which case the fatigue strength was shown to surpass the FAT 125 recommendations by up to 210% (FAT numbers are defined as the fatigue strength in MPa at $2x10^6$ cycles). This is also a 150% increase over the as-welded condition for which no weld treatment was applied. Given that the fatigue strength of the specimen with the treated weld was within 60MPa of that of the base material, it is clear that toe and near toe defects are the primary cause of crack propagation.

Billingham et al (2003) reviewed fatigue data for parent and welded high strength steels. It was concluded that the general fatigue performance of high strength steels is as good as that of conventional steels. A table was also developed to provide the mean improvement factors for various types of weld treatment:

Table 2-1 Weld Fatigue Improvement Techniques (Billingham 2003)

Improvement Technique	Steel Type	Yield Strength (MPa)	C/V	S/N	Mean Improvement Factor (%)	Ref
Tig dressed	DOMEX 590	615	CV	N	42	7.17
Tig dressed	WELDOX 700	780	CV	N	73	7.17
Tig dressed	WELDOX 900	900	CV	N	89	7.17
Shot peened	E550	640	C	S*	78	7.13
Hammer peened	HY80	-	-	-	175	7.12
Shot peened	Q&T	730/820	-	S*	70	7.11
Ultrasonic peening	WELDOX 700	780	CV	N	79	7.17
Tig dressed & ultrasonic peening	WELDOX 900	900	CV	N	104	7.17

Domex and Weldox are high strength low-alloy steels made by SSAB. The corresponding number defines the minimum yield strength. These studies prove the great extent to which weld treatments improve fatigue strength.

Residual stress and its effects on fatigue strength must also be considered. Clarin (2004) measured residual stress for three different strengths of welded box section; the first section used Domex 420, the second used Weldox 700 and third used Weldox 1100. It was found that the ratio of residual tensile stress to material strength decreases with increasing material strength. Therefore ultra-high strength steels do not experience residual stresses as close to their yield stress as standard strength steels. Note that the Domex section was welded using an electrode with yield strength of 470MPa, whereas a 690MPa electrode was used for the Weldox sections.

Eckerlid et al (date unknown) summarises the weldability of a particular High-Strength Low-Alloy (HSLA) steel; Domex 600MC made by SSAB. Domex 600MC is a low-carbon content thermo-mechanically hot-rolled steel with a minimum yield strength of 600MPa. Due to the lean chemical composition and very low amounts of non-metallic inclusions, Domex has good weldability and formability. Hot cracking and hydrogen cracking are not a concern due to the lean chemical composition and the microstructure in the Heat Affected Zone (HAZ) retaining good ductility. Low heat input is the key consideration when welding a HSLA steel

like Domex. This ensures that the width of the soft zone in the HAZ is kept to a minimum, and that the HAZ retains high toughness. Eckerlid et al also comments that a filler metal with high acicular ferrite content is recommended to achieve good strength and toughness when welding this type of steel.

2.3 Connection Methods of Mounting Bodies on Chassis

There are numerous types of bolted and welded connections that can be used for mounting a body on a truck chassis. All bodies are built onto sub-frames, independent from the chassis. The sub-frame is then connected to the chassis in a non-permanent fashion, should the body ever need to be removed for any reason. The sub-frame and the body it supports add to the stiffness of the chassis. Since there is flexibility in a truck chassis, the sub-frame and its connections must be designed to allow or restrict this movement accordingly. A concrete mixer body interacts differently with the chassis to a tipper body, for example. The sub-frame connections must be tailored for each application.

Most of the literature available on these connections and the sub-frame's interaction with the chassis comes from the truck manufacturer's body building guidelines. Since these are purely design guidelines, they do not provide extensive detail. There is no detailed research examining the interaction between a typical sub-frame and a 3 or 4-axle truck chassis.

Zoran et al (2010) performed a basic analysis of connection types and their positioning for a number of different superstructures. This research was based on manufacturer guidelines and was performed primarily to summarise differences in connection types and the basic reasons for their design and positioning. Due to be being based on manufacturer guidelines, there is limited detail provided. It is reiterated that "the stiffer the superstructure is, the more elastic the connection must be." A stiff superstructure can create high stress in the connections unless they have enough elasticity. Zoran also explains that chassis twist is most predominant in the region just behind the cab. This is also the foremost point at which the body's sub-frame attaches to the chassis. It is suggested that the sub-frame and its connections in this region should not be rigid; otherwise a stress concentration is created in the chassis. The increase in stiffness over this first section of the sub-frame should be gradual.

To determine whether any significant discrepancies exist between the various manufacturers body building guidelines, the guidelines for the following manufacturers

have been compared: Volvo, Renault, MAN, Scania, Mercedes, and DAF. General sub-frame recommendations do not deviate significantly. The main difference found is in the recommended connectors for concrete mixer bodies. It seems likely that each manufacturer's chassis interacts with the sub-frame in a similar way. Therefore the reason for these differences is unknown.

Scania's guidelines suggest using longitudinally flexible brackets in front of the front drum support and rigid brackets rearwards from this region (see Figure 2.1).

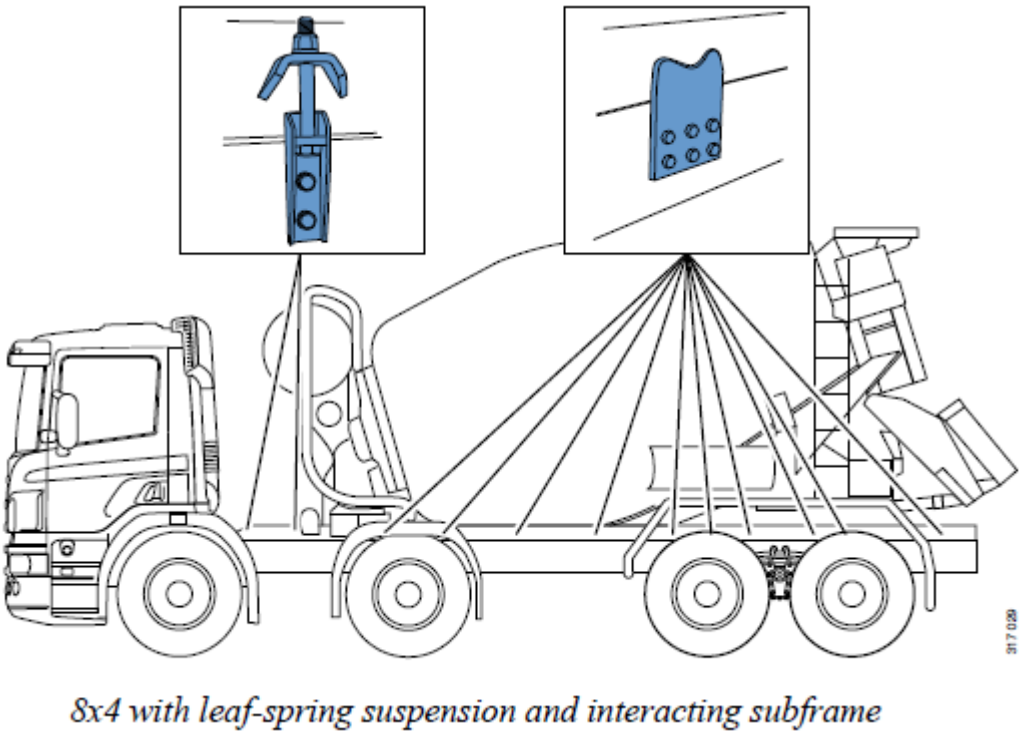

Figure 2-3 - Scania Mixer Mounting Guidelines - 4-axle Truck

Volvo, Renault, and MAN provide similar recommendations in terms of using flexible bracketry near the front and rigid brackets for the middle and rear. There is some variation in where these manufacturers suggest the rigid brackets should begin. For the rigid brackets, Volvo recommends bolting to both the sub-frame and the chassis, whereas Scania, Renault, and MAN suggest plates that are bolted to the chassis but welded to the sub-frame (see Figure 2.2).

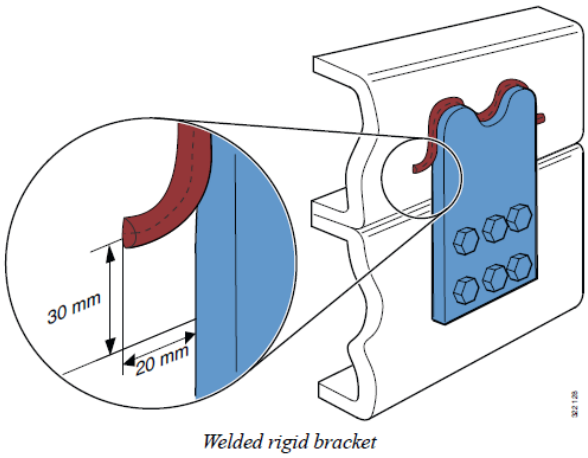

Figure 2-4 - Scania Rigid Bracket Welding Recommendation

DAF and Mercedes are the exceptions in the sense that they suggest using rigid brackets along the entire length of the sub-frame. Mercedes provide uniquely shaped brackets designed to minimise stress concentrations (see Figure 2.3). This design has been verified in section 5.3.3 of this thesis.

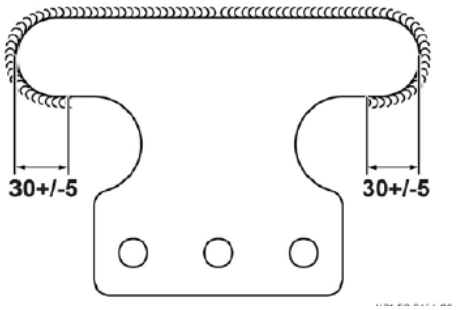

Figure 2-5 - Mercedes Attachment Bracket with Welding Guidelines

DAF and Mercedes state that when using fully rigid attachments, the material of the sub-frame should have a yield strength of at least 500MPa or be at least the same quality as the chassis. The recommendations of DAF and Mercedes would suggest that there is not a problem with using rigid connectors near the front of the sub-frame, which was expressed as a concern by Zoran et al (2010). It is thought that a well-designed rigid connector that spreads the load will avoid creating stress concentrations in the chassis. Perhaps it has also been found that using rigid connectors and high-strength materials benefits other areas of the structure. One possible benefit is that by restricting torsional movements in the region just behind the cab, the stress where the sub-frame contacts the front drum support may

be reduced. This may be at the expense of ride comfort, however. In section 5.3, some basic analysis has been done to compare rigid and flexible sub-frame connectors.

3. Experimental Work

The secondary research performed did not yield sufficient data to base 'worst-case' FEA studies on. To confirm worst-case loadings for the FEA studies, it was necessary to execute primary research. This took the form of two experiments. Whilst confirming the worst-case loads, the findings have also increased the understanding of how loads are transmitted through a mixer's structure.

The first experiment was a full scale dynamic load test on a concrete mixer. The primary intention of this experiment was to confirm the load cases used in the analyses. This large-scale experiment produced stress and strain data for various areas of the mixer's structure, and has therefore created a foundation for future work which could focus on specific areas. The second experiment was a tensile test comparing U-bolts with normal straight bolts. This was done to determine what bolting method should be used in the design of the front drum support. The analysis and redesign of the front drum support is covered in Chapter 5, as are the final load cases. A further experiment comparing the strength of the existing and redesigned front supports under a vertical load has also been included in Chapter 5.

3.1 Dynamic Loadings in the Structure of a Concrete Mixer

3.1.1 Background and Test Aims

From the literature review in Chapter 2, there was not a sufficient amount of loading data found to base FEA studies on. Braking accelerations for heavy goods vehicles made before 2005 are relatively well covered in the literature by Dunn and Hoover (2004), National Highway Traffic Safety Administration (2007), Birch (2001), Eckerlid et al, and George et al (1997). However, bump or pothole accelerations have not been reported in great detail for HGV's, hence the requirement for experimental testing.

To understand the nature and magnitude of these loadings, strain was measured at eight positions on the mixer's structure using a series of strain gauges; for six positions the gauges were arranged in rosette form, and the two remaining positions used single gauges (twenty strain gauges in total). Two rosettes and one single gauge were positioned on the rear drum support as illustrated in Figures 3-4, 3-5, and 3-6. Three rosettes and one single

gauge were positioned on the front drum support, as shown in Figure 3-3. The final rosette was positioned on the offside leg of the sub-frame just in front of the front drum support as illustrated in Figure 3-3. Additional images of the installation of these strain gauges are given in Appendix A.

The front drum support takes the majority of the loadings resulting from the mass of the concrete inside the drum and the drum itself, via a heavy duty planetary gearbox. The front drum support is the only structure fully restraining the drum longitudinally. The forward sloping angle of the rear roller bearings provides limited longitudinal restraint. Therefore the loadings through the front support structure can be very large, potentially in the magnitude of 265kN (as per the calculated braking load applied during the FEA study, Chapter 5). The rear drum support primarily restrains the drum vertically and laterally via the roller bearings. Refer to Figure 1-2 to view the positions of the drum supports and the gearbox.

Two sensing units each containing a 3-axis accelerometer and a gyroscope were also attached to the truck; one positioned on a section of the chassis just behind the cab and the other positioned on a section of the sub-frame just in front of the rear drum support. The sensing units measured acceleration in the vertical, longitudinal, and lateral axes, as well as angles of pitch, roll, and yaw. This combination of sensors made it possible to learn about the strains in the mixer's structure that result from given accelerations. Suitable commercially available sensing units with data logging capability were not found within the desired price range. Instead, a specification was written, and an Electrical Engineering student provided assistance in the assembly and programming of the sensing units.

One of the complications of measuring strain on the structure of a concrete mixer is that the movement of the wet concrete inside the drum causes constantly fluctuating strains. The mixing blades draw the concrete up one side of the drum where it then 'folds' over. This not only causes a lopsided centre of gravity, but with a low slump or dry mixture the movements of the contents can be felt throughout the truck.

One other author is known to have applied numerous strain gauges to the structure of a concrete mixer and compare the results to FEA studies (Li et al, 2014). However this comparison was specifically for a static torsional load case.

3.1.2 Equipment

The strain gauges were connected to a VPG System 5000 data logger using StrainSmart software. Arduino software on a laptop was used to record the data from the two sensing units via 2x10m Ethernet cables. Each sensing unit contained an MPU 6050. The MPU 6050 combines a MEMS (Microelectromechanical systems) accelerometer and a MEMS gyroscope in a single chip. The sensor unit data was sampled at a rate of 70Hz. The strain gauge data was sampled at a rate of 100Hz. In hindsight, the sensor unit should have been designed for a rate of 100Hz for consistency. This equipment, excluding the sensors, was located inside the truck's cab and powered by the 12V auxiliary supply, via an inverter. The strain gauges and the sensing units were covered to protect against poor weather. The strain gauges were of type CEA-06-250UN-120. The truck was a 2013 DAF CF85 4-axle with an $8m^3$ mixer unit.

Figure 3-1 - In-cab Data Logging Equipment

Figure 3-2 - Test Truck - DAF CF85 with 8m^3 Mixer Unit

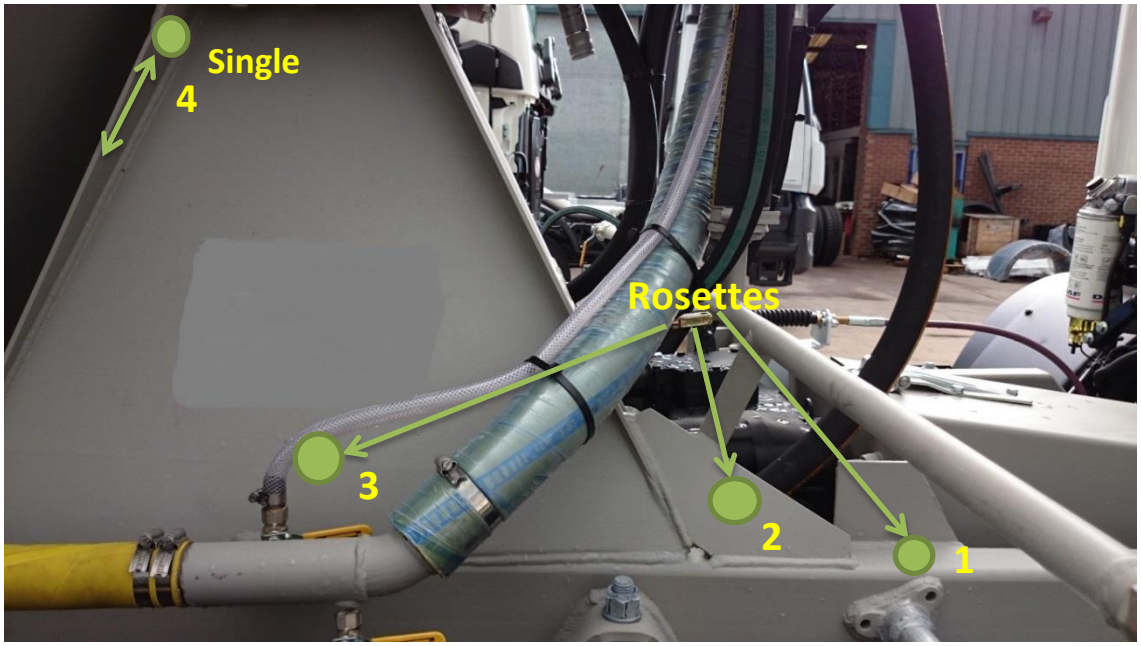

Figure 3-3 - Schematic of Strain Gauge Positions 1,2,3,4,8

Rosette 8 is positioned as rosette 2 but on the opposite side of the truck. The arrow beside position 4 indicates the direction of the single strain gauge. Gauge 1 is on the top surface of the sub-frame. Gauges 2, 3, 4, and 8 are on the front drum support – an important load bearing structure.

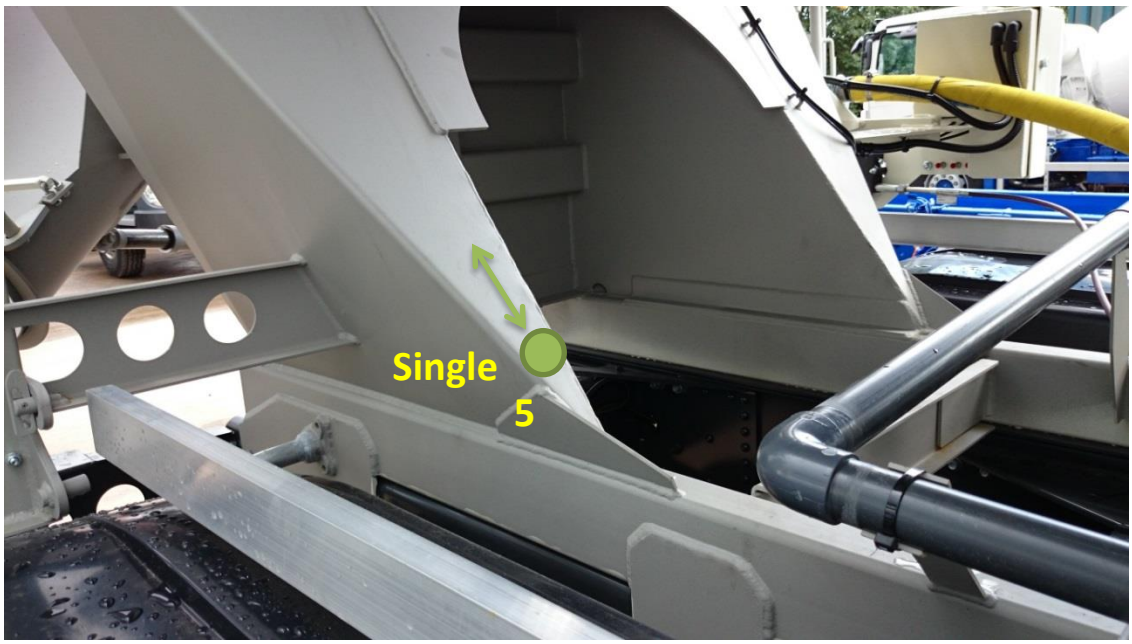

Figure 3-4 - Schematic of Strain Gauge Position 5

Gauges 5, 6, and 7 are on the rear drum support.

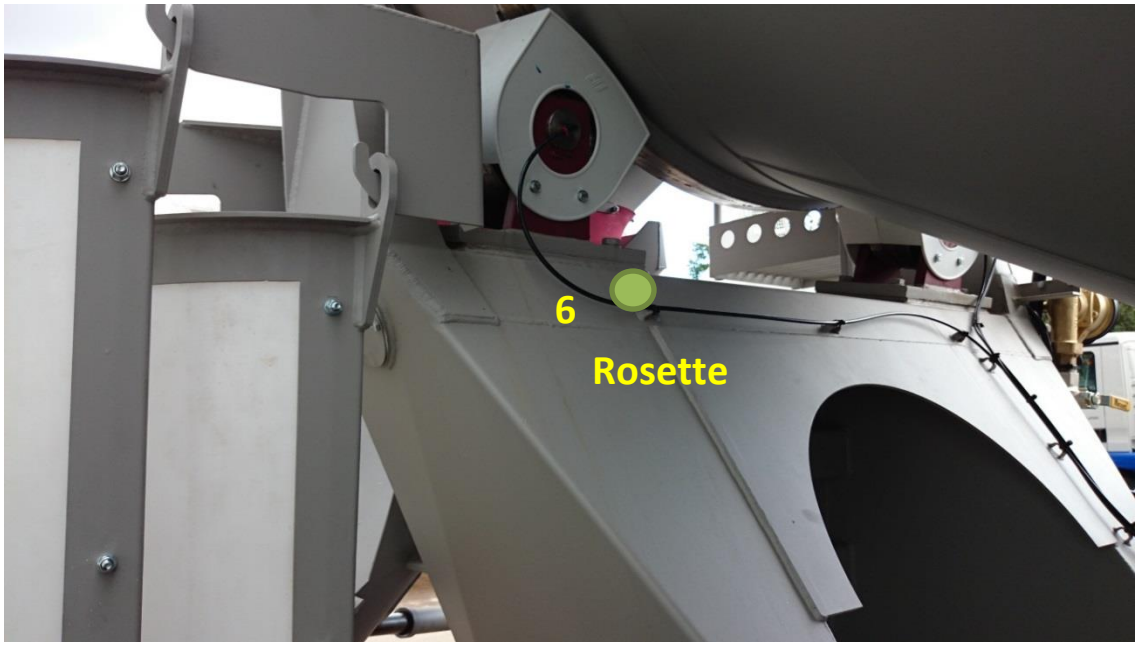

Figure 3-5 - Schematic of Strain Gauge Position 6

Figure 3-6 - Schematic of Strain Gauge Position 7

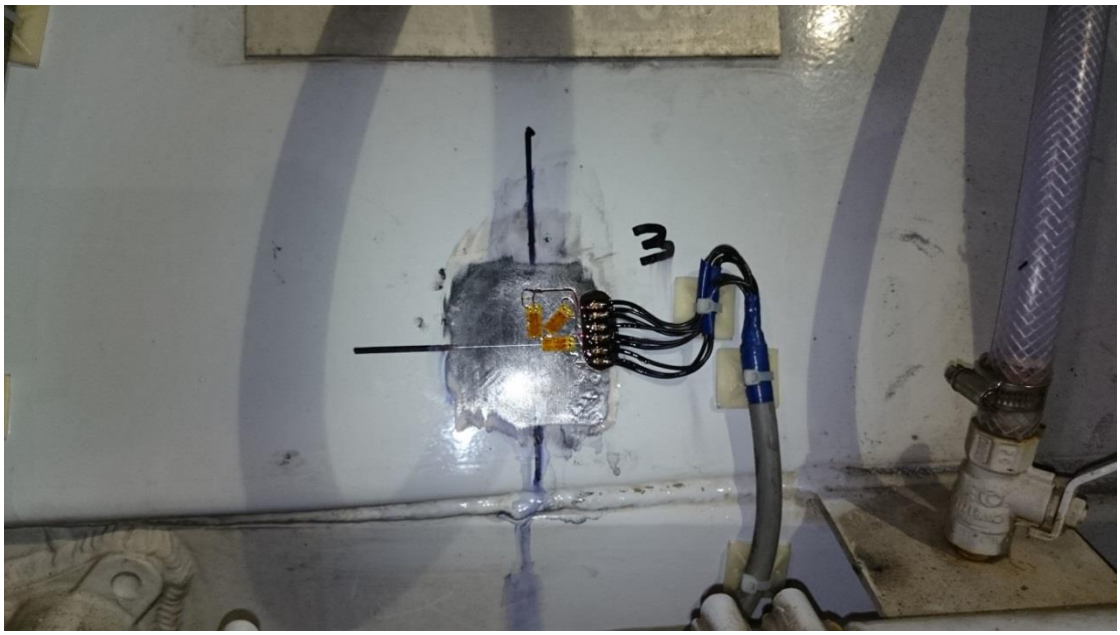

Figure 3-7 - Strain Gauge Rosette No.3 – Uncovered

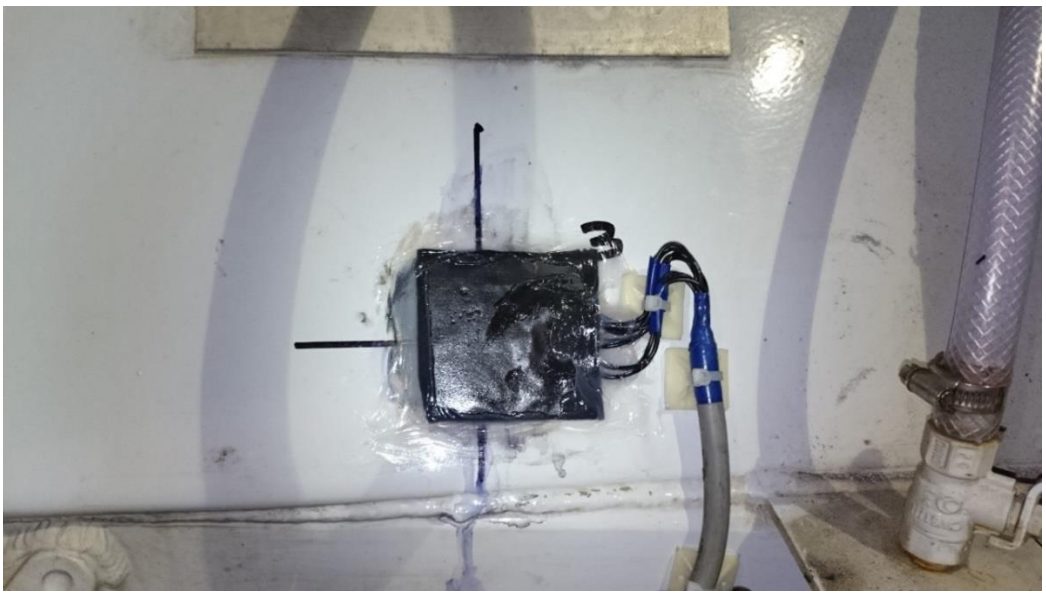

Figure 3-8 - Strain Gauge Rosette No.3 – Covered

More images of the strain gauge positions are given in Appendix A.

3.1.3 Test Procedure

With the sensors attached, the test protocol was such that the driver went about his normal duties delivering concrete to a variety of local construction sites over the period of 4 days. A number of loads can be delivered each day depending on the distances involved. This arrangement allowed for the truck to remain in service whilst the tests were carried out, thus minimalizing cost. An equipment operator was required to sit in the passenger seat to operate the data logging equipment. The routes involved a variety of road surfaces including speed bumps, raised platforms, relatively steep slopes, and some off-road tracks. The driver was also asked to brake relatively heavily on a straight section of road. Unfortunately on the day of the test, the job the truck did not often have a full load on-board. Financial constraints meant that it was not possible to ask the driver to focus on jobs involving full loads.

The data logging systems were normally only active for periods of 1-5 minutes to minimise the influence of drift and ‘random walk’. Such issues can occur with both accelerometers and gyroscopes, particularly with low cost MEMS units. The strain gauging system was not susceptible to significant errors; however leaving it running for too long can amass unwieldy data files. The data loggers were activated prior to key events. This meant that it was necessary to stop the truck on level ground and zero the sensors before such events.

Unfortunately, this complicates the process of analysing the data, because the strains recorded for certain events do not include the strain that exists due to the mass of concrete inside the drum (since the sensors have been zeroed after loading the concrete).

To combat this, the strains were measured during the loading process of a full 7.5m^3 load. This data can to some extent be used in combination with the 'event' data to estimate what the actual strains during these events would be, had the sensors not been zeroed after loading. In hindsight, it may have been reasonable to only zero the sensing units prior to events, due to the low-error nature of the strain gauging system. Furthermore, note that the strains due to the mixing drum's mass are unaccounted for in this test.

3.1.4 Results

The strain gauge system performed reliably, and the acceleration data from the sensing units appeared realistic. However the pitch, roll, and yaw data from the sensing units seemed to show high levels of drift. It is possible that the high vibration environment in which the sensing units were being used had not been fully realised during the design of the sensing units. Ultimately the pitch, roll, and yaw data was discarded. Slope angles are therefore unknown. One intention of this data had been to measure angles of chassis twist, since one sensor was near the cab and the other towards the rear end.

A considerable amount of valuable information was still gained from the remaining data. Strains resulting from given accelerations have been recorded for key events such as braking and hitting a bump in the road. The measured strains can also be used in fatigue analysis.

3.1.4.1 Bump/Vertical Load

In the following discussion, the data from the strain gauging system has been presented as principal stress, since stress is a more relevant measurement than strain for failure analysis. Also note that the direction of the principal stress has not been discussed due to this being difficult to convey without several images and illustrations. The additional images of strain gauge positions in Appendix A may be of interest. For this event, the strain gauges were zeroed before the concrete was loaded so no correction needs to be applied to the data. The largest vertical acceleration occurred when driving over a raised platform with a full load on board (7.5m^3) at around 7mph.

Figure 3-9 – Raised Platform Creating High Vertical Acceleration

The plot of the vertical acceleration is given in Figure 3-11. No filtering has been applied to either the acceleration or strain plots. For an unknown reason, the front sensor unit effectively sampled at 7Hz rather than the intended 70Hz. This reduces the validity of the peak accelerations recorded by this sensor. The effect of this fault can be seen in Figure 3-11 where the plot for the front sensor has a linear appearance. The sensing unit just behind the cab recorded a peak acceleration of 1.31g. The sensing unit towards the rear recorded a peak acceleration of 1.73g. This difference can be explained by the rear suspension being stiffer than the front. These accelerations match well with the limited data in the literature. Given that this bump is only of moderate severity and that the truck's speed was only around 7mph, it could be estimated that accelerations of at least 2g would occur for the most severe bumps and potholes.

The single strain gauge in position 4 reached a maximum stress of 120MPa compressive – 146% greater than the static stress with a full load on board. The largest principal stress was measured by the rosette in position 8; 164MPa compressive – 129% greater than the static stress.

As predicted, the largest stress in the rear drum support was measured at position 7: 79.8MPa compressive. This was the largest stress recorded at position 7 throughout the test. Position 1, on top of the sub-frame near the front drum support, experienced a maximum stress of 60.4MPa compressive. Interestingly this is only marginally greater than the static stress.

The stress plot for gauges 2, 4, 7, and 8 is shown in Figure 3-12. The remaining positions experienced lower stresses and have been excluded to prevent overcrowding the graph. Only the 'minimum' principal stress has been shown in the graph since this shows the compressive stress (generally speaking the minimum principal stress is compressive and the maximum principal stress is tensile). See appendix B for the maximum and minimum principal stresses at all positions. It can be seen that at virtually the same time, position 8 experiences a peak in compressive stress whilst position 2 experiences a trough (near 1912s). Positions 2 and 8 are symmetrically placed on opposite sides of the front drum support. Quite how this extreme variation can occur between the two sides has not been fully understood. If the truck had driven onto the platform at an angle, then it may be possible to achieve this type of loading due to the chassis 'pushing' one side of the drum support up and 'pulling' the other side down. However it is thought that the truck was driving head-on to the bump when this peak occurred.

For this loading, the peak compressive stress experienced in position 8 is 53% greater than the peak in position 2. These peaks are around 2s apart. This trend of position 8 experiencing greater stresses than position 2 is also recognised for the longitudinal/braking loading and the 'downhill' loading. The gearbox on top of the front drum support transmits a large torque in order to rotate the drum. Therefore the reaction torque applied through the gearbox casing causes the front drum support to be loaded unevenly. There is also the effect of the concrete mass having an offset centre of gravity. Other condition-specific factors could also be contributing to this difference in stress.

The two largest shear stresses calculated from the strain data for this event were 19.6MPa and 21.7MPa at positions 1 and 8 respectively. Position 2 experienced a shear stress of only 9.5MPa.

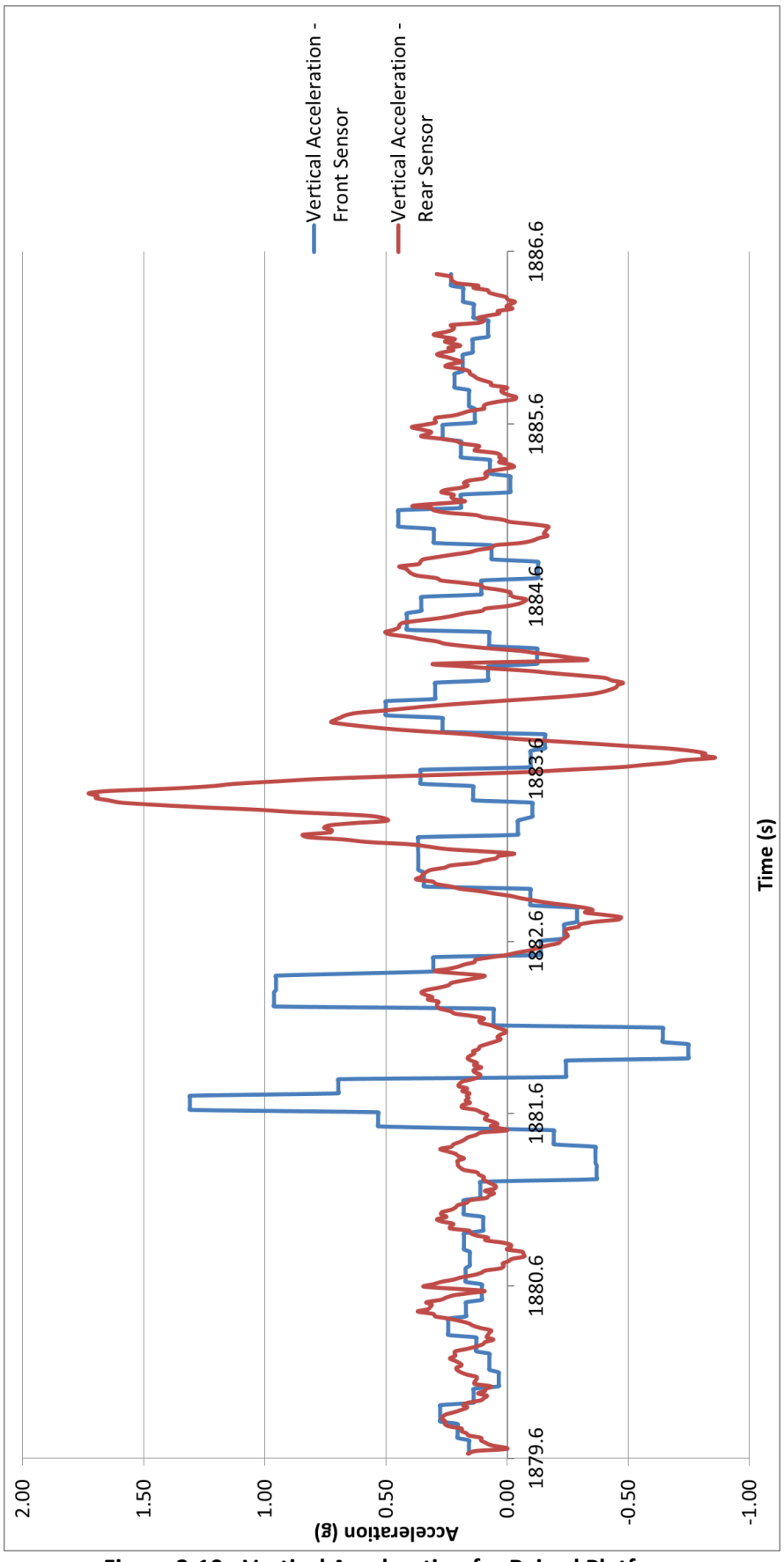

Figure 3-10 - Vertical Acceleration for Raised Platform

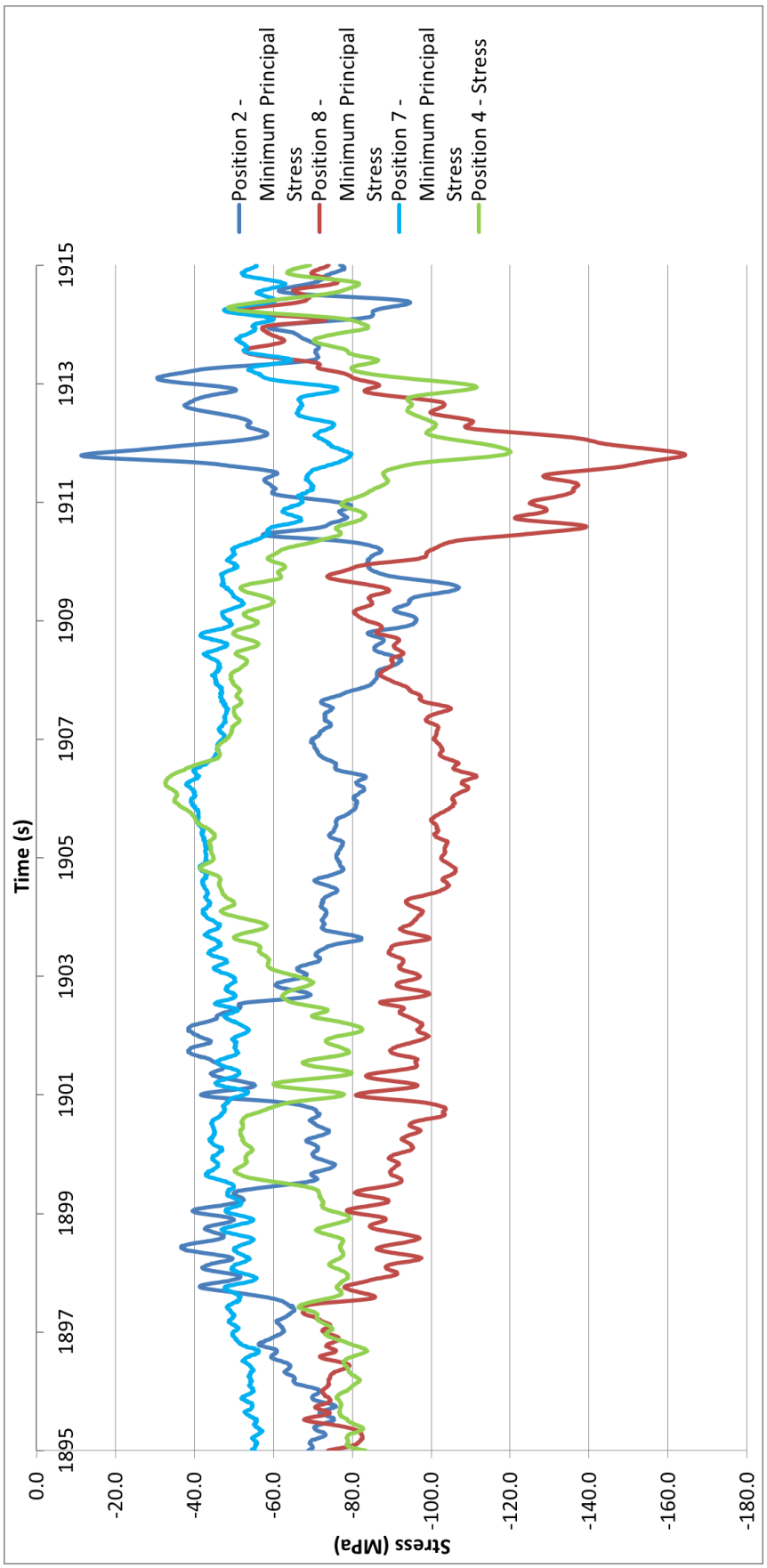

Figure 3-11 - Bump Stress Plot for Positions 2, 4, 7, 8

Most of the positions fluctuate between tensile and compressive stress depending on the loadings. The majority experience mostly compressive stress as would be expected. The exceptions being positions 5 and 6 which predominantly remain in tension. In fact, the greatest overall tensile stresses measured throughout the entire test occurred at positions 5 and 6 whilst driving over this raised platform; 31.5MPa and 38.9MPa respectively. These peaks in the rear support may in-part be due to the drum lifting off and then landing with force on the roller bearings. This is a known problem with concrete mixers. The solution thus far has typically been to strengthen this area, however it would be ideal to either have a form of shock absorption under the roller bearing or a method of preventing the drum from lifting. Certain trucks with particularly stiff rear suspension have developed cracks at the base of the rear drum support. The shock-loadings from the drum bouncing on the roller bearings are thought to be the primary cause of failures in this region. Overall, failures in the region of the rear drum support are rare.

The vast majority of this mixer's structure is made with S355 type steel. The large panels that make up the front and rear drum supports tend to be 4-5mm thick. Smaller parts on the mixer range from 3-20mm thick. Parts with thickness greater than 8mm are made from S275. The gussets that rosettes 2 and 8 are attached to are 8mm thick. The sub-frame legs have a cross-section of 120x60x6.3mm, and are also made of S355. S355 has yield strength 355MPa. One type of weld wire is used for the majority of the welding; G 38 4 M G3Si1. The minimum yield strength of the weld wire is 380MPa, therefore the welds are overmatched. This theoretically makes it possible for the parent material to yield before the weld, depending on the quality of the weld and the residual tensile stress.

For this loading there are no tensile principal stresses great enough to cause yielding. However, fatigue is the primary consideration, and even compressive stresses can contribute to fatigue. For example, the residual tensile stress in a weld will fluctuate along with the fluctuating compressive stress in the parent material. The literature shows that a great improvement in fatigue life can be achieved by simply smoothing the toe of the weld. No such treatment was applied to this particular mixer during the production process. The fatigue life of this structure therefore depends heavily on the quality of the welds and their geometry.

Whilst driving over this raised platform the greatest stress range in one particular principal direction was measured at position 8; 50MPa to 164MPa compressive, a range of 114MPa.

Despite the relatively low compressive stresses measured for this event, a frequent change in the order of 114MPa combined with an imperfection in an area of tensile residual stress could contribute to a low fatigue life.

See Appendix B for a summary of the strain gauge data for driving over a raised platform.

3.1.4.2 Braking/Longitudinal Load

The driver was asked to brake moderately hard on a straight piece of road in slightly damp conditions. Given that the test was performed on a public road, it was ensured that the braking manoeuvre was performed safely and that the truck's ABS system was fully functional. The short braking manoeuvre was initiated at around 45mph. The driver applied a moderate pressure to the brake pedal and then briefly relieved pressure at around 30mph. Then he applied a greater braking pressure to bring the speed down to 15mph, at which speed the brakes were fully released. ABS did not initiate, suggesting that the truck could have achieved greater braking forces. Given the acceleration felt inside the cab by the driver and the equipment operator, it could be estimated that this braking manoeuvre was around 75-80% of the truck's braking capabilities. The mixer contained 5m^3 of high slump (high viscosity) concrete.

Figure 3-12 - Hard Braking Manoeuvre on Approach to Roundabout

The plot of the longitudinal acceleration for both sensors is given in Figure 3-14. Again, the front sensor sampled data at 7Hz rather than 70Hz. The front sensor recorded a

longitudinal acceleration of 0.81g, the rear 0.83g. Given that the driver felt the braking was performed to around 75-80% of the truck's capabilities, these accelerations seem high in comparison to the data in the literature. In the literature, 0.7g appeared to be the maximum for many HGV's. One possible explanation is the advancement in tyre and heavy vehicle braking technologies, since no data was given in the literature for trucks manufactured after 2005. The truck used in this test, a DAF CF85, was manufactured in 2013. It could also help that the braking force was relieved part way through the manoeuvre, so that when the peak pedal force was applied the truck was only doing around 30mph. It may have been harder to achieve this acceleration had the brakes been applied with the same force at 50mph. If the data is taken as being accurate, and the truck did indeed have greater braking capabilities than tested, then accelerations approaching 1g may be possible. This would place the truck's braking capabilities surprisingly near that of a modern passenger car, which can typically achieve around 1g in braking.

For this manoeuvre, the strain gauging system was zeroed after loading the concrete. Figure 3-15 shows the stress at positions 2, 4, and 8. For positions 4 and 8, both the maximum and minimum principal stresses have been given. The braking manoeuvre began around 542s and ended at 546s. The dip at 544s is in response to the driver briefly relieving pressure on the brakes. The largest overall 'tensile' principal stress occurred at position 2 during the second phase of the braking manoeuvre; 52.6MPa. However, the static stress at this position with a full concrete load was 79.6MPa compressive. It could be loosely estimated that with just $5m^3$ of concrete on-board, this static stress would be around 53MPa. Therefore the true stress would be roughly in the region of 0.4MPa compressive (53 - 52.6 = 0.4). At the exact same time, position 8 had a far greater compressive stress (around 63.7MPa after accounting for the concrete load). However, just one second prior to this, position 8 did experience a trough in compressive stress (around 11.5MPa after accounting for the concrete load) which appears to coincide with the time at which the driver briefly relieved braking pressure. Bear in mind the 'correction' applied to these stresses lacks accuracy.

The largest overall compressive stress during this manoeuvre occurred at position 8; 85MPa (after accounting for concrete load). This is 18.2MPa greater than the peak at position 2. Before and after the braking manoeuvre, these two positions are loaded somewhat more evenly. It is clear that the front drum support is frequently loaded unevenly, which is not

an easy characteristic to replicate in FEA. It is difficult to find a reason as to why this difference suddenly increases during the second phase of the braking manoeuvre. With the irregular loadings from the secondary sources such as concrete moving around and the torque transmitted by the gearbox, no two braking manoeuvres produce the same stresses.

After 'correcting' the data for the concrete load, the largest tensile stress occurred at position 6; 26MPa.

It was predicted that the single gauge in position 4 would experience a tensile stress under braking due to the moment applied through the gearbox. In actual fact, increased compressive stress was recorded during braking. The peak, after accounting for the concrete load, was around 70MPa. It seems that the force going into the gearbox is not transmitted in such a way that applies a significant moment to the drum support. The force must have a larger vertical component than expected. Furthermore, the braking force may cause the proportion of concrete gathered at the front of the drum to increase. This will contribute to the increased compressive stress observed at position 4.

See appendix B for a summary of the strain gauge data for this braking manoeuvre.

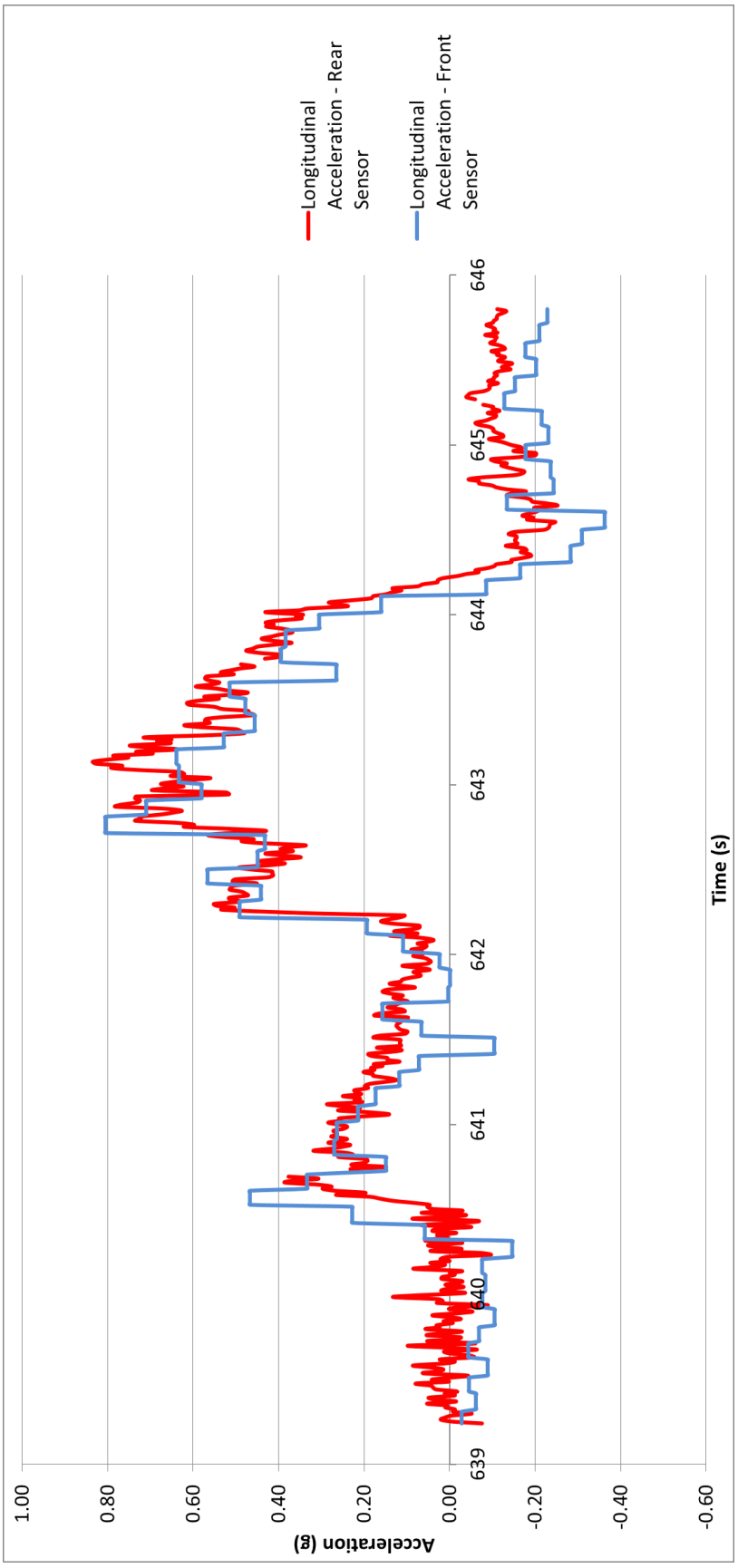

Figure 3-13 - Longitudinal Acceleration for Braking Manoeuvre

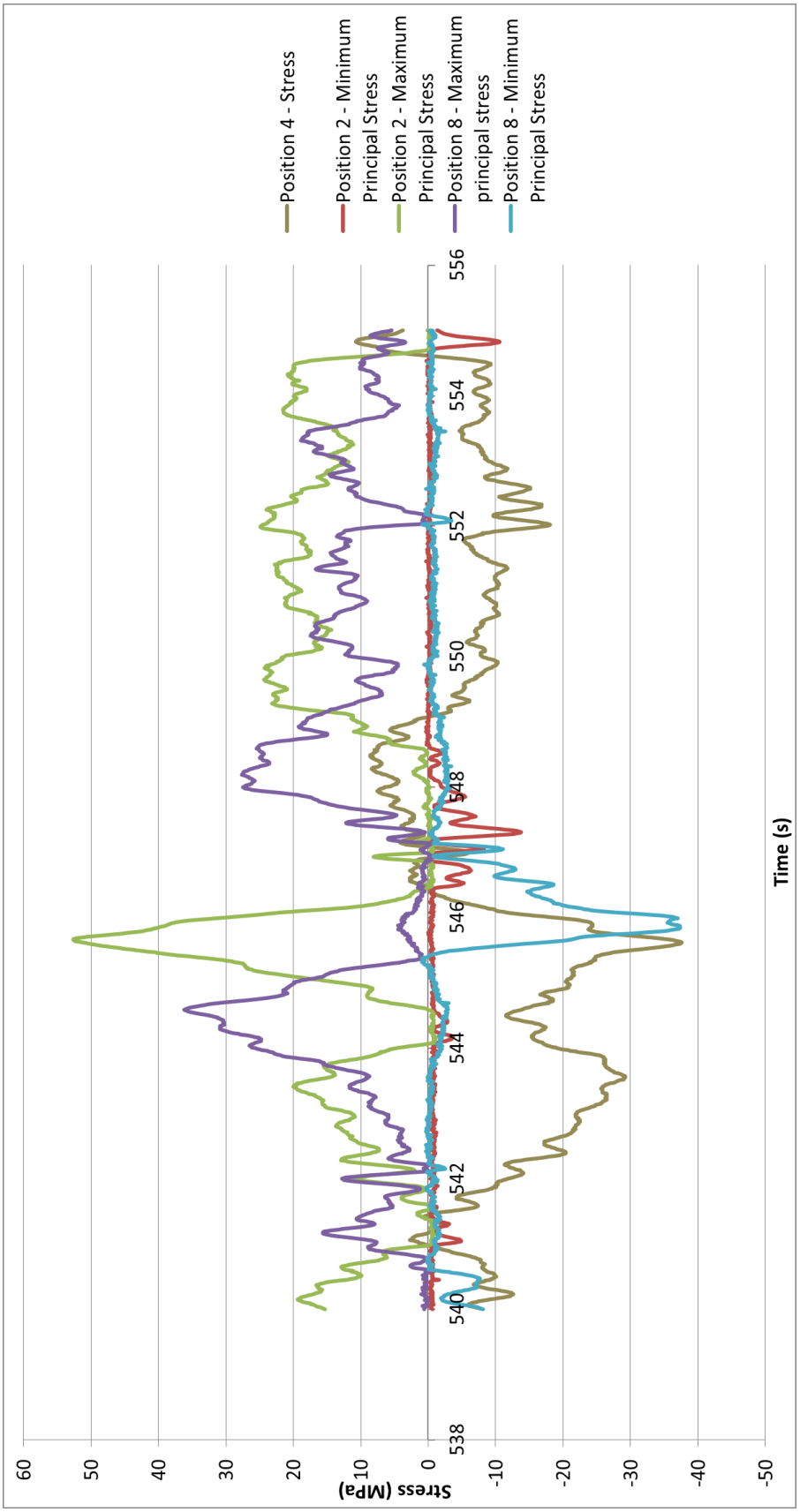

Figure 3-14 - Braking Stress Plot for Positions 2, 4, 8

3.1.4.3 Downhill Load

A short but relatively steep slope was part of most of the routes due to being on the entrance to the main concrete plant. This particular event was recorded as part of the same session as the bump load, therefore the mixer contained a full 7.5m^3 load of 50-90 slump (low viscosity) concrete. The truck's speed was around 6mph. As mentioned previously, the pitch, roll, and yaw data was discarded since it appeared to suffer from drift. However, since the sensors were zeroed just seconds before the truck drove onto the slope, there may be some relevance in this data.

The front sensor recorded a pitch angle of 6.2°, the rear 7.7°. A difference of 1.5° suggests that the accuracy of this data is poor. 7° does not sound like a particularly steep slope, but in actual fact it is close to the typical ramp angle in multi-story carparks (these ramps tend not to exceed 10°). To add further context, the steepest public road known in the UK is said to reach around 18° (Hardknott Pass).

The strain gauging system was zeroed before the concrete was loaded. The stress plot for positions 1, 2, 4, and 8 is given in Figure 3-16. Most of the plots shown are for minimum principal stress which provides the compressive stresses, however both the maximum and minimum have been given for position 2 to show where it briefly experienced a tensile stress (1455s). This tensile stress peaked at 23.3MPa. The largest overall tensile stress recorded for this event was 33.8MPa at position 6.

The peak compressive stress at position 8 was 207.7MPa. This is in fact the largest compressive stress measured throughout the entire test. Position 2 reached a peak compressive stress of 115.9MPa. The peak compressive stresses at positions 1 and 4 were 77.5MPa and 82.7MPa respectively. It had been predicted that positions 2 and 8 would experience increased compressive stress whilst the truck was on the slope. The data shows that position 2 actually experiences reduced compressive stress whilst the truck is on the slope, and position 8 experiences increased compressive stress. Momentary reductions in compressive stress might result from the water and concrete loads moving around, however an explanation has not been found for this sustained reduction.

Position 4 on the rear panel of the front drum support experiences increased compressive stress at the same time as the reduction at position 2. This suggests that the load transferred to the rear of the support at this moment. However, on the other side of the

support position 8 experiences a peak in compressive stress, suggesting a load transfer to the front. This complex load path seems to describe a torsional load, whereby the support is being ‘twisted’ around a vertical axis.

The two largest shear stresses were measured at positions 1 and 8; 26.3MPa and 25.4MPa respectively.

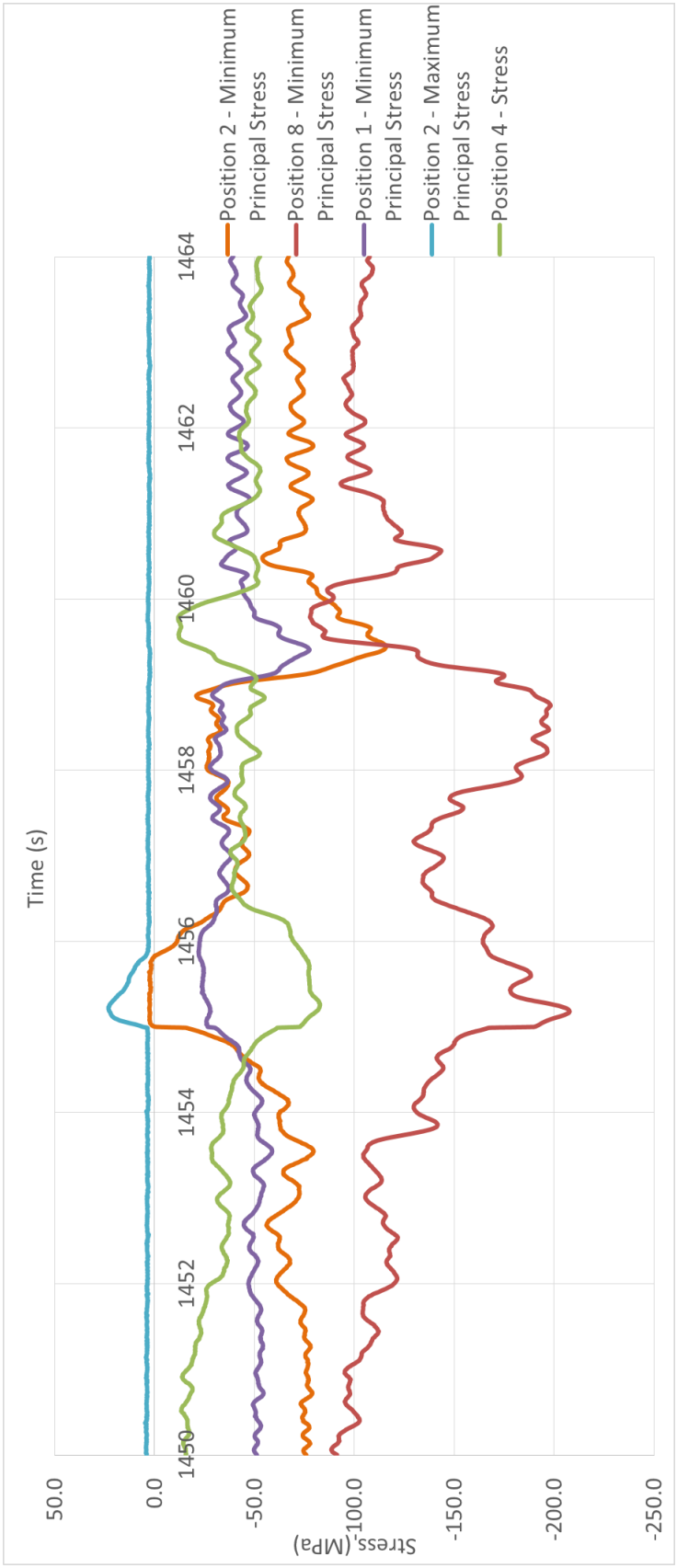

Figure 3-15 – Downhill Stress Plot for Positions 1, 2, 4, 8

3.1.4.4 Summary

The overall maximum tensile and compressive stresses measured throughout the test for each position are summarised in table 3-1. The max tensile stress is the upper number given for each position. Note that S4 and R7 never experienced a tensile stress so the upper numbers given for these two are the minimum compressive stress. The 'loading scenario' column describes which event caused the peak.

Table 3-1 - Table of Maximum Tensile and Compressive Stresses

Gauge type & Position	Max Shear Stress (MPa)	Max Tensile and Max Compressive Principal Stresses (MPa)	Loading Scenario (for principal stress only)
R1	26.3	7.4	Downhill
		-77.5	Downhill
R2	12.2	23.2	Downhill
		-115.9	Downhill
R3	6.8	24.3	Bump
		-30.2	Downhill
S4	-	-11.8	Downhill
		-120.1	Bump
S5	-	31.5	Bump
		2.9	Downhill
R6	12.7	38.9	Bump
		8.5	Downhill
R7	10.6	-20	Downhill
		-79.8	Bump
R8	25.4	18	Bump
		-207.7	Downhill

The bump event features in 4 max tensile stresses, and 2 max compressive stresses. The downhill event features in 4 max tensile stresses and 6 max compressive stresses. The braking event does not feature at all. This reflects the fact that the truck did not have a full load on board for this event. On top of this, the strain data from the braking event was generally of less relevance due to having an inaccurate correction applied to it.

The largest tensile stress of 38.9MPa occurred at position 6 during the bump event. The largest compressive stress of 207.7MPa occurred at position 8 during the downhill event. The largest range of stress at one position occurred at position 8 which ranged from 50.1MPa in compression to 207.7Mpa in compression – a difference of 157.6MPa.

3.1.5 Reflective Conclusion

More testing should have been done with the sensing units to check the consistency and reliability of the data in high vibration environments. An oversight led to the strain gauging system often being zeroed after the loading the concrete. It should have been zeroed before loading the concrete and then left running for as long as necessary. It is true that this would amass very large data files but that would have been more productive than gaining data for which the gauges have been zeroed after loading. In the ideal situation, the loading events would have been arranged to occur soon after the concrete was loaded. For example, by placing an object on the road just outside the concrete plant to act as a large bump, and then performing the hard braking manoeuvre soon after leaving the plant. Since the steep downhill was on the entrance to the plant, this arrangement would have allowed all three of these events to be executed in a far shorter period of time.

For the last day of testing, a video camera was positioned inside the cab to capture the events. The importance of recording the events on video had not been realised before. The footage proved useful for later confirming things like speed and sizes of bumps. It would have been beneficial to have video recordings from all 4 days of testing.

The load paths through the front support in particular are far more complex than expected. As such, tests like this are the only way to gain an understanding of the loads transferred through the drum supports. Having said that, understanding these loadings to the extent where they can be accurately replicated in FEA would be challenging even with another 20 strain gauges installed.

The uneven loading of the front drum support has made it harder to compare estimated loadings with the measured loadings. The largest stress in the front drum support was found in position 8 which is on the nearside of the structure. However the other three strain gauge positions on the front drum support are on the offside. The extent of the variation between the two sides was not anticipated. Replicating each gauge position on both sides would have provided a more complete understanding of the load paths through the structure. Unfortunately the data logger had no remaining unused channels to allow for more gauges, not to mention the additional costs involved.

The lesson for the future is to avoid attempting to measure strains over the entire structure unless time, finances and equipment allow for a very large number of gauges. In this

instance, it would have been more productive to focus efforts on the front drum support, since it is a particularly important part of the structure.

See section 5.1.3 for a discussion on how these measured loadings compare with previously estimated loadings based on the literature.

3.2 Tensile Test - U-Bolts versus Straight Bolts

3.2.1 Background and Test Aims

U-bolts are commonly used for attaching front and rear drum supports on concrete mixers. To understand if there is a practical reason for this trend, a test has been constructed to determine whether U-bolts offer benefits over straight bolts in this type of application.

The aim of this test is to determine the characteristic differences between U-bolts and straight bolts when a tensile load is applied. Of particular interest is their extension throughout the application of an increasing tensile load.

In this test, two bolting methods have been compared. The first method uses one semi-round U-bolt of specification M20 grade 8.8. The second method uses two straight bolts of the same specification.

If the U-bolt has significantly greater elastic extension under working loads then there will be a good case for using U-bolts on the front support. If the extension of the straight bolts is comparable to the U-bolts (within 25%) then there will be a good case for using the straight bolts, since they cost significantly less. The importance of the elastic extension is that it relates to the fatigue life of the structure, particularly the sub-frame which has been a known failure region. A connection with greater elasticity will improve the fatigue life of the surrounding structure.

3.2.2 Test Procedure

Each bolting method was subjected to a constantly increasing tensile load until failure occurred. As well as measuring the load, the extension of the bolts was measured using a transducer and strain gauges were positioned as shown below.

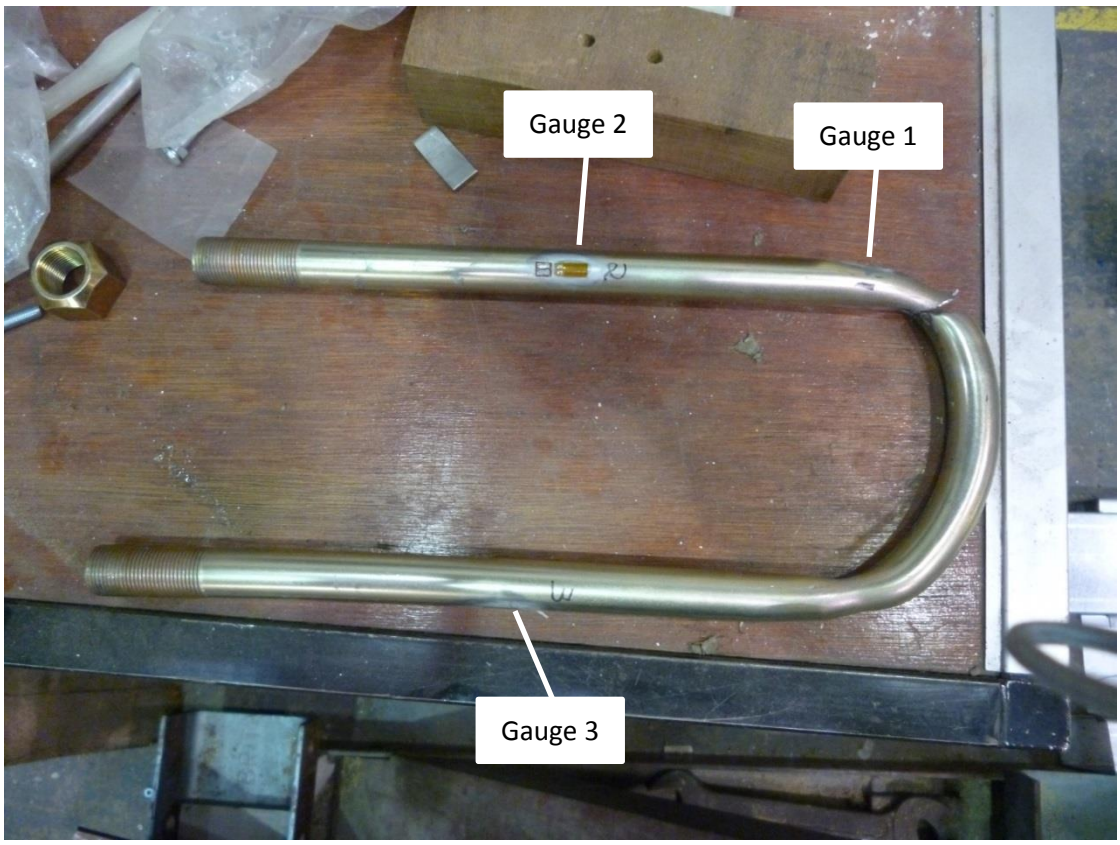

Figure 3-16 – U-Bolt Strain Gauge Positions

Note that Gauge 1 is positioned where there is a slight reduction in the diameter of the U-bolt due to the manufacturing process. This was a suspected failure region. Interestingly, the main region of yielding was actually just beyond this thinner section. This is discussed in more detail later in the report.

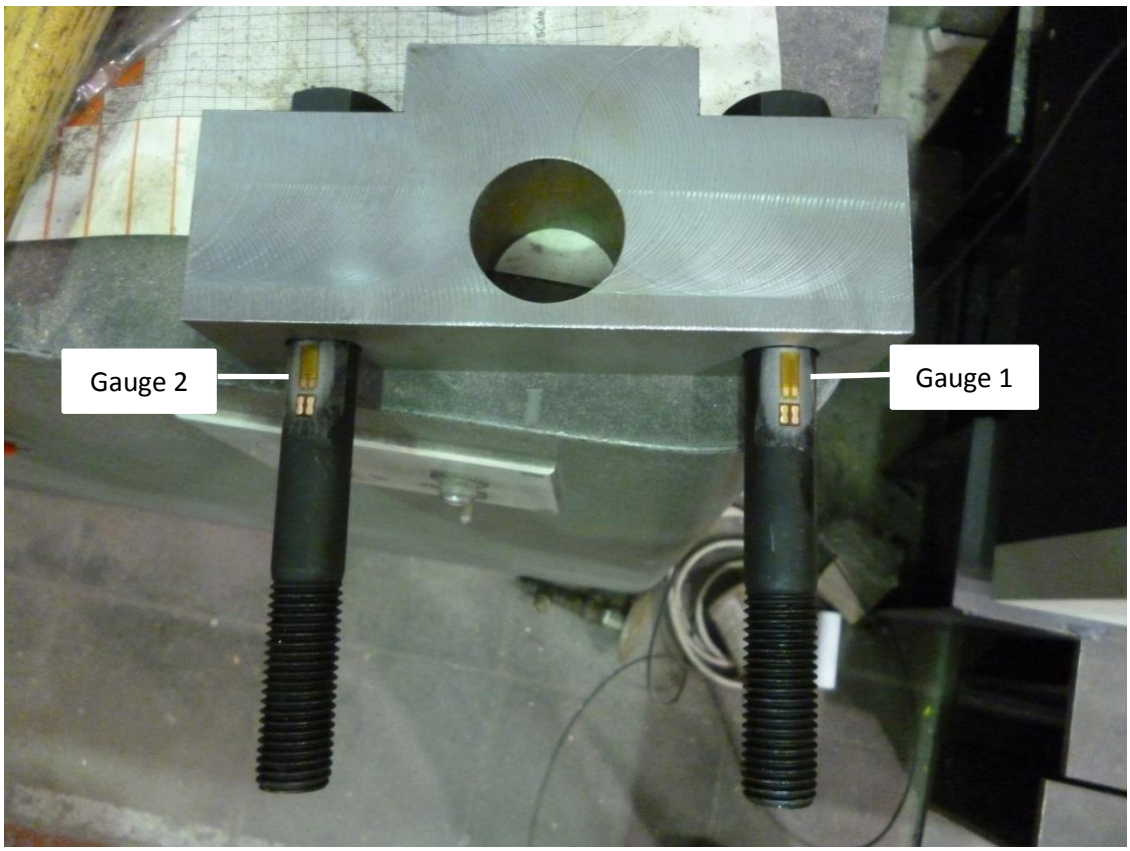

Figure 3-17 - Straight Bolt Strain Gauge Positions

Note that the nuts on both the straight bolts and the U-bolts were positioned such that they were fully on the threads with only a few threads extending past the nut.

A Tinius Olsen press with the capability of exerting around 90 tonnes was used for the test. The blocks that secure the bolts are made of mild steel. A section of bright bar was used to hold the bolting blocks to the securing jaws. See below.

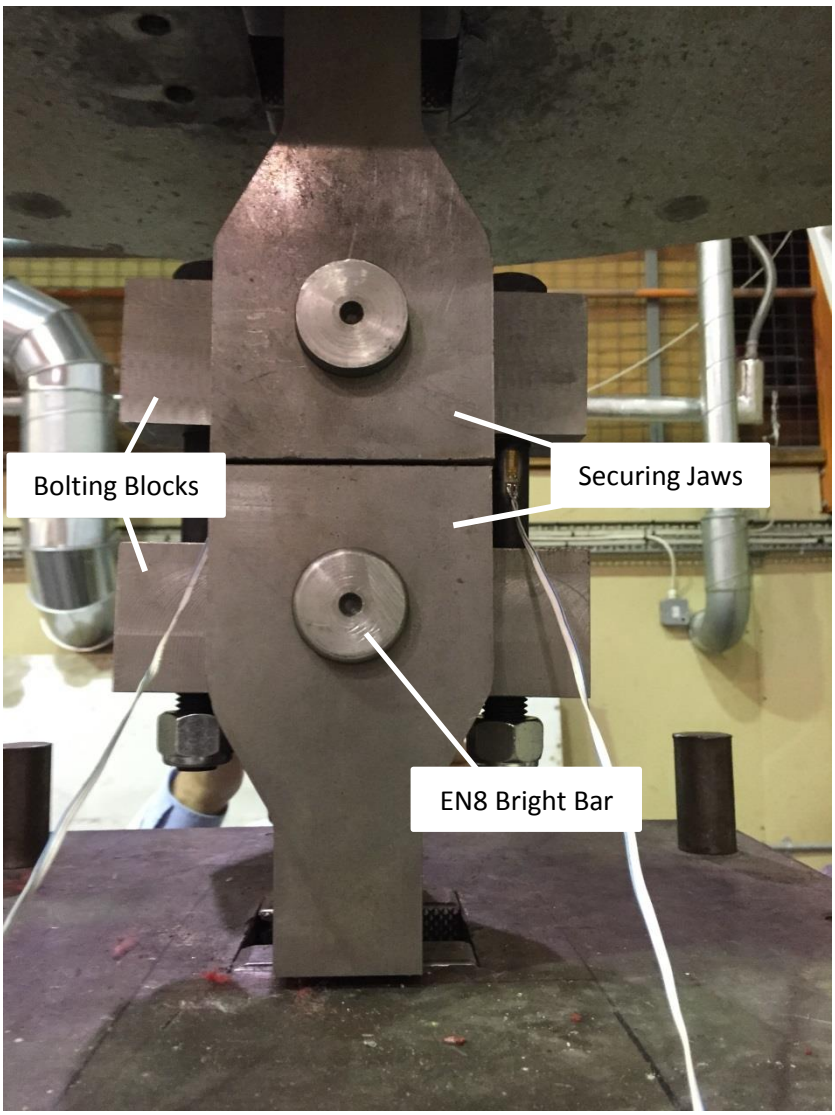

Figure 3-18 - Main Test Components

The bar allows the blocks to rotate, therefore evenly spreading the load between the bolts. The upper bolting block for the U-bolt was machined to closely match the bolt's inner radius. The pictures below show more clearly that the bolting blocks fit inside the securing jaws. Note that the lower platform of the press is fixed. The upper platform is moved by 4 rotating threaded shafts.

Figure 3-19 – Installing U-Bolt Upper Bolting Block into Securing Jaw

Figure 3-20 - Setting up U-Bolt Test

3.2.3 Results

3.2.2.1 Strain

"Strain 1" and "Strain 2" listed in the graph's legend refer to the gauge numbers displayed in Figures 3-22 & 3-23. Gauge 3 on the U-bolt did not produce meaningful results and has therefore been excluded.

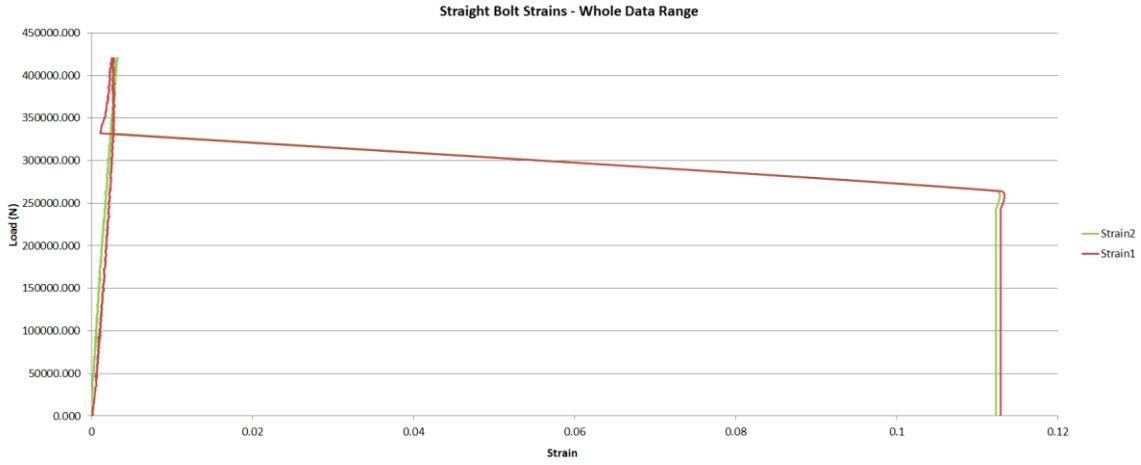

Figure 3-21 - Straight Bolt Strain - Whole Data Range

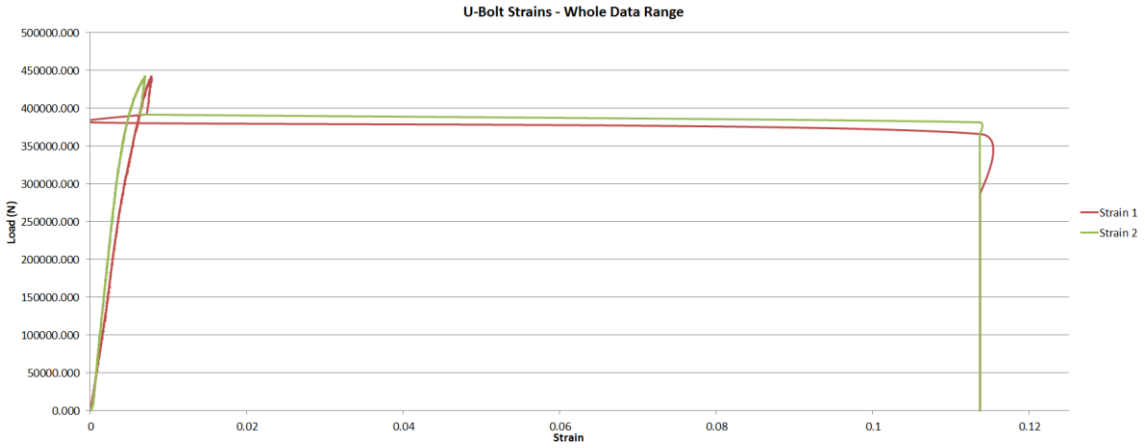

Figure 3-22 - U-Bolt Strain - Whole Data Range

The maximum tensile strength of the two straights bolts is 420kN (42t). The maximum tensile strength of the U-Bolt is 442kN (44.2t). Beyond the point of failure, where the strains suddenly increase dramatically, the values are of no interest (The wires most likely

broke off the gauges at this point due to the shock upon failure). The following graphs show the useful part of the strain data in more detail.

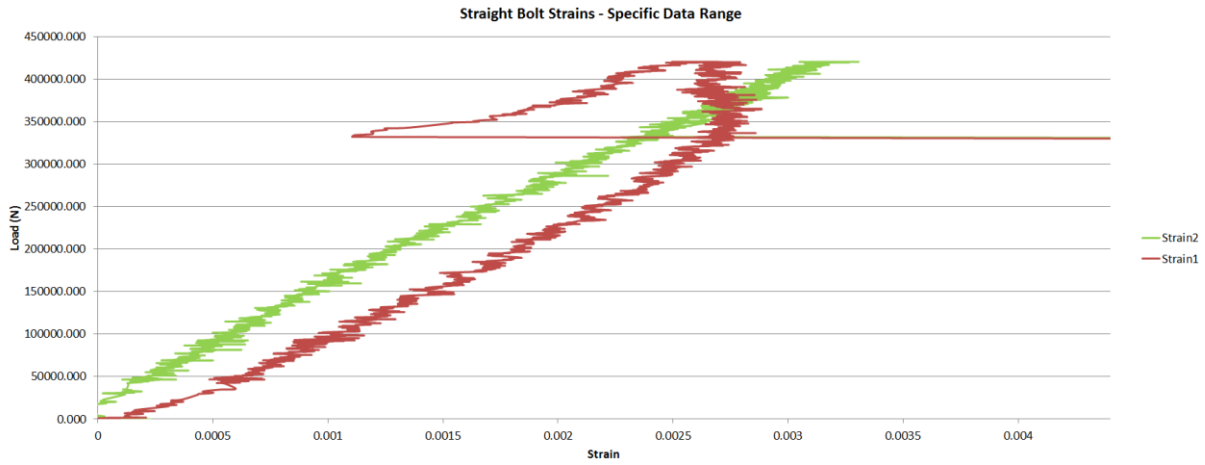

Figure 3-23 - Straight Bolt Strain - Specific Data Range

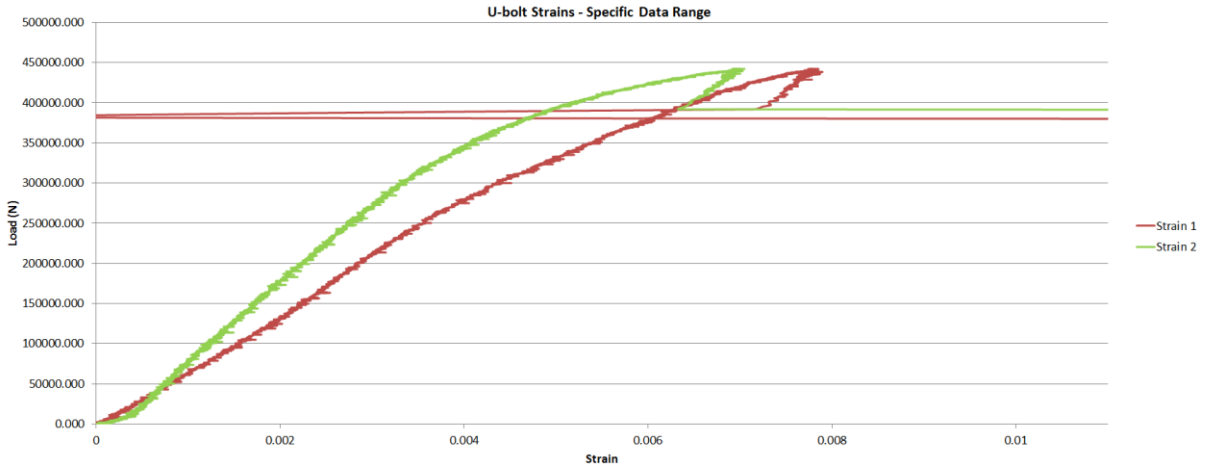

Figure 3-24 - U-Bolt Strain - Specific Data Range

Table 3-2 Strain Data - Comparing Straight Bolt vs. U-Bolts

Load Range	Straight Bolt		U-Bolt	
	Change in Strain 1	Change in Strain 2	Change in Strain 1	Change in Strain 2
From 50 to 250kN	0.001544	0.001468	0.002000	0.002760
From 50 to 350kN	0.002132	0.002322	0.003310	0.004588
From 50 to 410kN	0.002059	0.002786	0.004730	0.005918

From reading the above strain values it is clear that the strains in the U-bolt shanks are significantly greater than the strains in the shanks of the straight bolts. An explanation is given in the Discussion of Results. The U-bolt shanks appear to begin to yield around 300kN. The straight bolt shanks do not appear to yield; however the decreasing strain observed in the "Strain1" plot suggests that another area of this bolt starts to extend significantly at around 330kN. The yielding of the U-bolt occurs in a more gradual fashion.

3.2.2.2 Extension

3.2.2.2.1 Measured Values

The following graphs must be read from right to left (extension appears reversed due to equipment setup). The change in extension is the important factor.

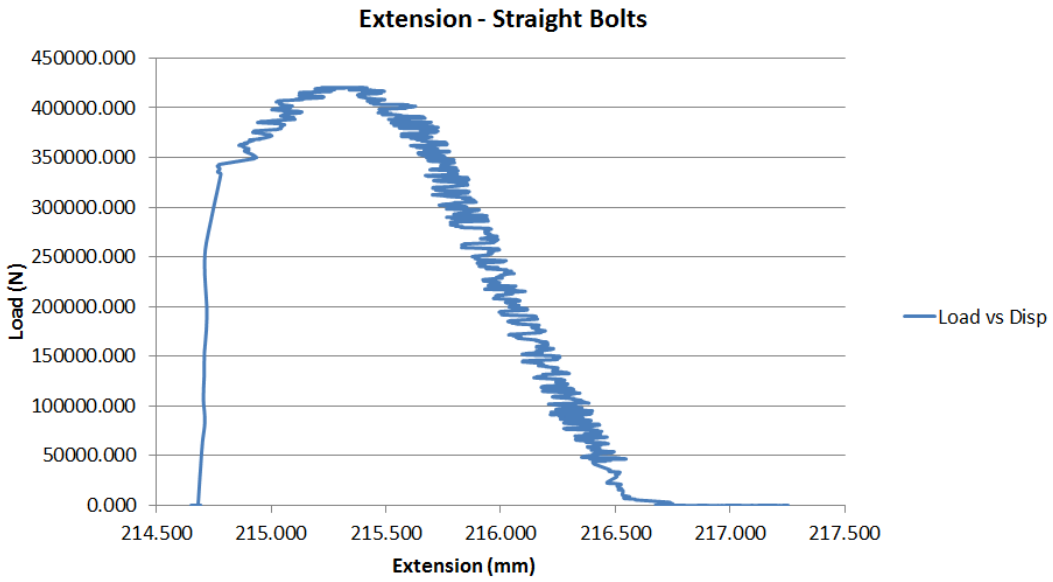

Figure 3-25 - Straight Bolt Extension

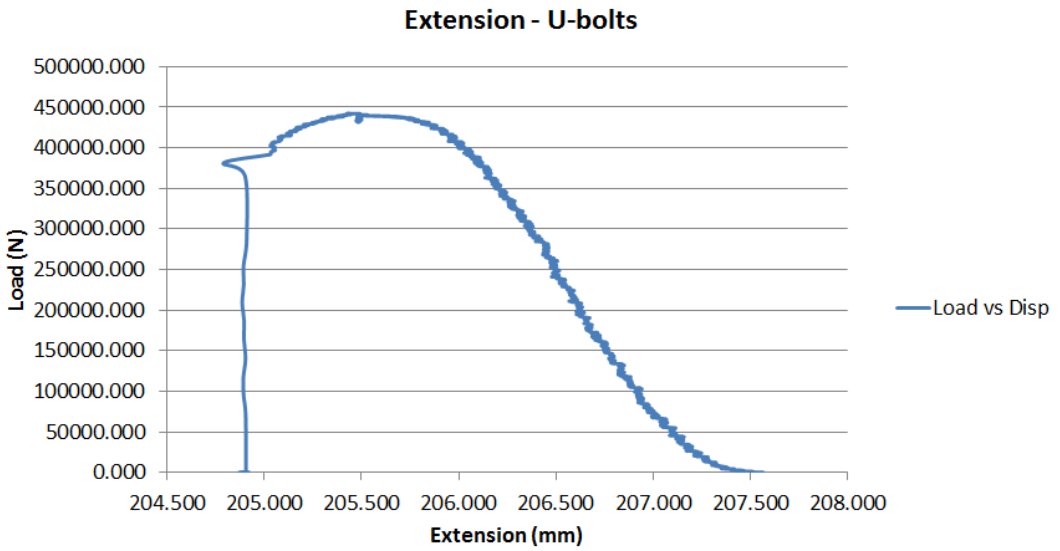

Figure 3-26 - U-Bolt Extension

Table 3-3 Extension Data - Comparing Straight Bolts vs. U-Bolts

Load Range	Straight Bolt Change in Extension (mm)	U-Bolt Change in Extension (mm)	Difference in Extension
From 50 to 250kN	0.514	0.602	0.088
From 50 to 350kN	0.689	0.903	0.214
From 50 to 410kN	0.990	1.136	0.146

The fourth column gives the difference in extension between the straight bolts and the U-bolt for given load ranges. A normal working load would not exceed 200kN. For the load range of 50 to 250kN, the extension of the U-bolts is only marginally more than that of the straight bolts. For the load range of 50 to 350kN, this difference increases as the U-bolt starts to form and stretch around the curved support block. The difference in extension for the highest listed load range is smaller than the middle load range. This is largely because the straight bolts have yielded more extensively than the U-bolt at 410kN.

3.2.2.2.2 Corrected Values

The above statements concern the *measured values*. However, in order to compare the bolts in a like-for-like scenario, there is a need to correct the values. This need arises because the U-bolts are longer than the straight bolts. Elongation is proportional to length. The straight bolts are 73% of the length of the U-bolt, and therefore the U-bolt elongates

27% more for a given load. To correct the values, 27% has been taken off the U-bolt extension values.

Table 3-4 Corrected Bolt Extension Values

Load Range	Straight Bolt Change in Extension (mm)	U-Bolt Change in Extension (mm)	Difference in Extension
From 50 to 250kN	0.514	0.440	0.074
From 50 to 350kN	0.689	0.660	0.029
From 50 to 410kN	0.990	0.830	0.160

These corrected values show that the straight bolts actually extend marginally more than the U-bolt under normal working loads. See below for an explanation.

3.2.4 Discussion of Results

It has been discussed that the shanks of the U-bolt experience significantly higher strain than the shanks of the straight bolts. The reason for this is also the main reason for the straight bolts extending more than the U-bolt in this test. From looking at the bolts (see Appendix C for a variety of pictures) there are a few dimensional differences in the threaded sections. The shank of the U-bolt is actually 19mm in diameter. It can be seen that the M20 thread sticks out further than the shank. The thread is also a fine thread. Little thickness is lost due to the thread depth. The threaded sections and the shanks of the U-bolt are therefore closely matched in terms of cross sectional area.

The standard straight bolts do not have the same characteristics. Their shank diameter is 20mm. The thread is a course thread, whereby the inner diameter of the threaded section is ~17mm. There is therefore a mismatch between the load carrying capacity of the threaded section and the shank.

It can be concluded that the reason for the significantly lower strain in the shanks of the straight bolts is because the threaded section elongates and yields before high strains can develop in the shank. It is likely that the threaded section of the U-bolt extends similarly to its shank. The straight bolt shanks do not appear to yield before the bolt breaks, whereas the U-bolt shanks do experience yielding.

The reduced effective diameter of the threaded section of the straight bolts is the main reason for the straight bolts extending more than the U-bolt in this test (considering the

corrected values). Ideally, for a more accurate comparison, the tested straight bolts should have had the same length and thread dimensions as the U-bolt.

Note that the bolting blocks and securing jaws may account for a very small amount of the measured extension values.

3.2.5 Conclusion

It was stated in the "Test Aim" section that there would be a good case for using straight bolts if the extension under normal working loads is within 25% of that of the U-bolts. For these particular bolts, it has been found that the straight bolts actually extend more per length than the U-bolt, due to the weaker threaded section. Over a load increase of 50 to 250kN the straight bolts extend 14.4% more than the U-bolt. This difference would likely be significantly reduced if the straight bolts had fine threads.

This test has highlighted the importance of a bolt's dimensions and thread type. A fine thread results in the load being spread more evenly throughout the bolt. A suitably long bolt should be used where elasticity is required.

From these results it can be concluded that U-bolts offer no benefit over straight bolts in terms of their elasticity under tensile loading.

4. Implementing a Design by Analysis Process

As part of this work, it was necessary to examine how a Design by Analysis (DBA) approach would be integrated into a manufacturer's existing design process. The integration of a DBA process is briefly discussed in this chapter, followed by comments on the integration and impact with regards to this particular concrete mixer manufacturer. To provide a foundation for this discussion, a concise explanation of Finite Element Analysis has also been given.

4.1 Finite Element Analysis

Simply put, Finite Element Analysis is a numerical method of approximating the response of a body to a load or thermal input. This numerical method involves discretizing the body into numerous simple shapes known as elements. The resulting arrangement of connected elements is known as a mesh. An element is defined by a number of nodes and connecting edges. For example, a linear tetrahedral element has 4 corner nodes and 6 connecting edges. A parabolic tetrahedral element has 4 corner nodes, 6 mid-side nodes, and 6 edges.

Figure 4-1 - Illustration of Linear and Parabolic Tetrahedral Elements

Equations known as shape functions describe the response of each element. A method developed by Richard Courant around 1950 allowed these functions to be combined into matrix format and solved algebraically. This development made it possible to calculate the response of complicated structures that could not be solved through differential equations alone.

For every Finite Element Analysis study there is a series of specifications and conditions that must be controlled:

- Creation of suitable geometry (it is often beneficial to modify or simplify the model)
- Study parameters/solver type (linear static, non-linear dynamic etc)
- Material specifications
- Boundary conditions; fixtures, contacts, connections, loadings
- Mesh specifications & convergence

In the last 15 years or so, the accessibility of FEA has dramatically increased now that personal computers have the power to perform complicated analyses. With this increased accessibility comes an increasing concern that less qualified users may misuse this powerful design tool.

4.2 Impact & Integration of a Design by Analysis Process

The implementation of a Design by Analysis process, or even just the purchase of FEA software, must be justified. This first requires an understanding of the capabilities of FEA as a design tool, and then an estimation of the impact it will have on the product and the company. An important realisation for companies investigating the benefits of FEA is that it is merely a tool for use during the design process, and not a means of checking the suitability of a final or near-final design. All designs with any level of safety or structural consideration should undergo practical testing.

Companies looking to develop a competitive advantage often find that focusing on the process by which innovation is generated provides greater benefit than focusing on the search for technological advancements. Advantages are typically gained through novel utilisation of known technologies rather than through breakthroughs in the technologies themselves, Adams (2006).

The potential benefit of FEA is therefore heavily affected by the design process. Adams (2006) states that an implementation plan should consider:

- Goals and business expectations
- Periodic re-evaluation of the implementation
- Process for initiating an analysis (the interaction between analysts and the engineering team)
- Documentation for analyses and practical test results
- Time spent on validation activities
- Continuous development and education (strong technical skills must be developed both with the software and in the understanding of materials and mechanics etc – the expertise of the user is vital to success)

This is a dynamic and changeable plan which must be documented and understood by all those involved with FEA. The design team should meet and check over the results of every analysis for verification and sense-checking purposes. Validation can be in the form of hand calculations, expected results based on historic data, or practical testing. Results of validation activities should be documented, as well as the methods used and any assumptions made. Strong documentation of the design, analysis, and validation allows new or outside users to quickly interpret the results and understand why certain assumptions were made.

In the case of this particular concrete mixer manufacturer, the company did not have any experience with FEA prior to the project. The decision was made to use the Solidworks Simulation package since the company already had Solidworks Premium. It was expected that the vast majority of the analyses would suit a 'linear static' solver. The capabilities of the Solidworks Simulation package were seen as being suitable for this application. The primary goal set during the implementation of FEA was to reduce the weight of the mixer. Without much historic design data to use for approximation of results, validation was mainly achieved through practical testing. For companies that desire to use FEA to reduce weight, it is necessary to carefully consider what factor of safety should be adhered to. A factor of safety of 1.5 was set as the intended minimum for this work.

The impact of this particular implementation was moderately beneficial given the two year period, however only a relatively small weight reduction was achieved as a direct result of analysis work. The mixing drum was excluded from the project. Since the mixing drum accounts for roughly 50% of the weight of a mixer unit, this exclusion decreased the potential weight reduction. A secondary benefit of the implementation was the improved documentation created for each design. This not only allows new users to understand previous work but also provides 'proof of design' – a necessity for companies adhering to ISO procedures for design and quality.

In summary, SME's must fully understand the capabilities of FEA before a business case can be made. During this process, it is beneficial to speak to an experienced FEA user in the industry. It is also highly important that the engineers using the software are suitably trained or experienced. When implemented under the right conditions, FEA can provide a market advantage for SME's.

5. Design of an Optimised Support Structure for a Concrete Mixer

With a box style body, the body itself contributes to the stiffness of the chassis. However, with a concrete mixer the bulk of the body is supported at two specific points; the front and rear drum supports. The sub-frame is therefore the main contributor to the stiffness of the chassis. The flexibility of the chassis results in misalignment of the two supports, thus misalignment of the drum. Hence why sub-frames with high torsional rigidity are recommended for concrete mixers. Typical mixer gearboxes use large spherical roller bearings that can cope with drum misalignment angles of up to 6°. The two drum supports create high localised rigidity, particularly with the designs that have been assessed in this study. The problems associated with this are discussed below in section 5.1.

The front and rear drum supports are the most significant parts of the structure that were optimised during the project. Some analysis has been done to assess the sub-frame's interaction with the chassis and the drum supports, however time and hardware constraints have limited the work in this area. There have been issues when running large complex sub-frame interaction analyses which appear to be caused by either hardware or software deficiencies.

5.1 Front Drum Support – Design & Analysis

As discussed in Chapter 3, the front drum support carries the majority of the drum and concrete mass due to the way that the mixing blades gather the wet concrete towards the front of the drum. Since the rear drum support does not restrict the drum longitudinally, the front drum support can take large loadings under heavy braking manoeuvres. It could be said that its design requires more consideration than any other part of a mixer's structure. On top of the support is a gearbox, and on top of the gearbox is a water tank. Loadings from the drum and concrete are transmitted through the gearbox to the support. As well as the concrete moving around inside the drum, the water moving around in the water tank also creates significant loadings. The tank size typically varies from 200-600 litre. As discussed in Chapter 3, large torque forces are transmitted to the support via the gearbox.

Clearly the front drum support receives a variety of large loadings and plays an extremely important part in the mixer's structure.

5.1.1 Design of Existing Front Drum Support

Figure 5-1 shows the existing front drum support on a sub-frame and chassis. This view shows the front of the support. The rear panel is closed off just like the side panels.

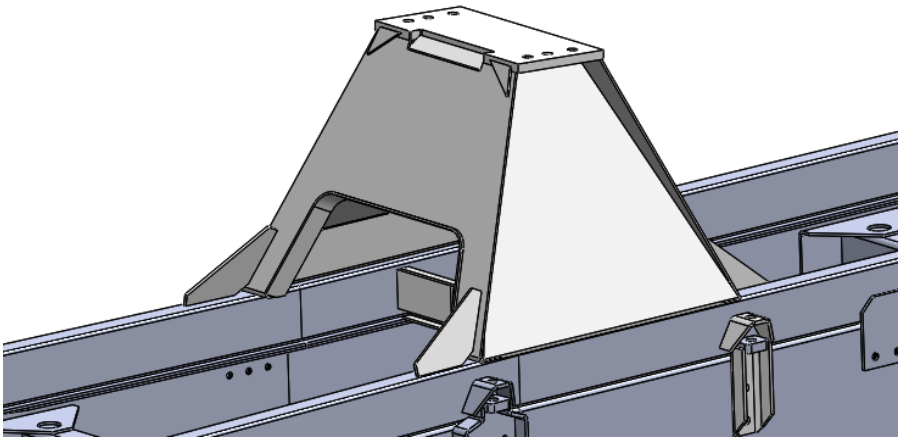

Figure 5-1 - Existing Front Drum Support on Sub-Frame

The front drum support is a fully welded steel structure with 4 separate main panels making up the shell of the structure, to which numerous other parts are welded. It is welded to the sub-frame along its full length on both sides. Six bolts are used to attach the gearbox. The 4 main panels are 5mm thick. The majority of the structure is made from S355 grade steel. The thick 20mm plate on the top uses a lower grade; S275.

Welded box structures like this are inherently rigid. The support therefore resists any twist occurring in the chassis. Should the chassis be flexible enough to twist in this region, high stresses will occur in the support and in the welded connection to the sub-frame. To successfully use this type of structure, the sub-frame needs to be suitably stiff to control the flexibility of the chassis. However, the weight of the structure would be significantly affected by increasing the size of the sub-frame legs. Taller sub-frame members also raise the centre of gravity of the structure. For these reasons, the existing design of this particular mixer uses a relatively small hollow section for the sub-frame legs (120x60x6.3mm).

This miss-match between the rigidity of the support and the sub-frame is a contributory cause of a failure that has occasionally occurred with this structure. The sub-frame occasionally cracks at or near the foremost point of contact with the support, where the triangular gusset is welded to the top of the sub-frame. The area just behind the cab is

known to be the most flexible section of the chassis. Another contributing factor in this failure is the way that the support is welded to the sub-frame. It is welded along its full length in one weld pass. This continuous weld puts a large amount of heat into the sub-frame legs. Upon cooling, shrinkage occurs and causes the sub-frame to develop an upwards bend. Then, when the sub-frame is attached to the truck, it is clamped down forcing the hollow section legs to become straight again. The sub-frame legs are therefore under significant stress before any external loads are applied. To combat this, the manufacturer now heats up this region of the sub-frame and bends it in the opposite direction so that after welding they are close to being straight again.

A few other design tweaks were made over a number of years to combat this failure; the sub-frames were stiffened in this region by welding additional plates to it, the gussets on the front of the support were moved so that they are welded nearer the outer edge of the sub-frame (rather than being positioned centrally across the width), and a different manufacturing process was employed to create the kink in the sub-frame. A truck chassis typically has a 'kink' towards the front where the chassis legs spread further apart for packaging reasons. Originally, to create this same profile in the sub-frame, it was cut and then welded back up at the correct angle. This weld became one of the occasional failure areas since it was often near the front of the front drum support. The revised manufacturing process was to create this bend by heating up the hollow section and then press-bending to the desired angle.

These changes drastically reduced failures, however the addition of the sub-frame stiffening plates adds weight and the process of 'pre-bending' the sub-frame adds time. Hence Finite Element Analysis has been performed on this structure to learn more about the cause of this failure and furthermore to design an improved structure that will allow the removal of the sub-frame stiffening plates.

The weight of the existing front drum support for an $8m^3$ mixer is 81.8Kg.

5.1.2 Initial FEA Load Cases for Front Drum Support

Prior to performing the dynamic test on the structure of a concrete mixer (section 3.1) a set of worst-case loading scenarios were calculated based on information from the literature. These comprised of; a braking whilst going downhill load (longitudinal), a bump load (vertical), and an experimental twist load to replicate the chassis twisting over rough

ground. These initial calculations will be discussed first, followed by the changes made after the dynamic testing. Other significant load cases include driving along a slope (perpendicular to the slope) and hard cornering. These were predicted to be less severe than the chosen 3 scenarios.

5.1.2.1 Calculation of Longitudinal/Braking Load

The worst-case longitudinal load on the front drum support occurs when the truck is braking whilst going downhill. The braking data in the literature suggests maximum accelerations in the region 0.6-0.7g. Whilst travelling down a steep slope there is a significant transfer of weight towards the front of the truck. This weight transfer, combined with the effect of gravity, results in a decrease in peak acceleration. The extent of this decrease has had to be estimated. A 0.5g braking force was chosen (4.9m/s^2) for braking on a steep slope.

It was also required to determine the maximum slope angle that a truck may have to traverse. For UK roads, the recommended maximum gradient is 1 in 12 (5°) according to the Health and Safety Executive. However, there are roads in the UK that supposedly reach a gradient of 1 in 3 (18°), such as the Hardknott Pass in England.

To add a factor of safety to the calculation, an extreme gradient of 1:1.7 (30°) was chosen for use in the calculation.

A mixer with capacity 8m^3 has been chosen for the sake of this calculation. This particular mixer manufacturer has found that orders for mixers larger than 8m^3 are extremely rare due to weight legislation. The mass of an 8m drum containing 8m^3 of wet concrete is 22540Kg (Taking wet concrete density as 2500kg/m^3). Normally only 7.5m^3 can be loaded before the truck reaches the weight limit of 32t, however 8m^3 is used here to account for an operator overfilling the drum.

Applying an acceleration of 4.9m/s^2 (0.5g) to the drum creates the following longitudinal force:

$$F = ma$$

$$F = 22540 * 4.903$$

$$F = 110513.6\ N$$

When going down a slope of 30°, the drum is at an angle of 44.2°. The theoretical axial force on the gearbox due to this angle is:

$$F = mg\ sin\theta$$

$$F = 22540 * 9.81 * sin44.2$$

$$F = 154983.2\ N$$

Applying both the horizontal and axial forces above gives the worst case longitudinal load.

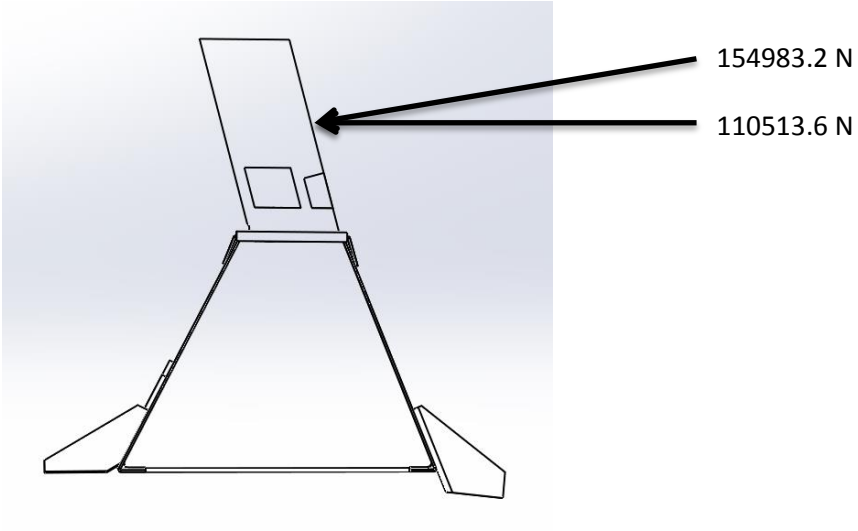

Figure 5-2 - Illustration of Longitudinal Load - Side View

5.1.2.2 Calculation of Vertical/Bump Load

This load represents driving over a very large bump or pothole. From the literature, the most reliable sources suggest accelerations in the region of 1.5-1.7g. The severity of the bumps/potholes that provided such accelerations was not discussed by the authors. To account for potentially more severe bumps an acceleration of 2g has been chosen. Again, a concrete volume of 8m^3 has been used in the calculation.

The following equation gives the vertical reaction forces applied by the front and rear supports to suspend the drum when the truck is stationary:

$$Rear\ support\ force = \frac{(Drum\ mass * gravity) * distance\ between\ front\ support\ and\ drum\ C\ of\ G}{distance\ between\ front\ and\ rear\ supports}$$

$$Rear\ support\ force = \frac{221117.4 * 1.4535}{3.5527}$$

$$Rear\ support\ force = 90464.76\ N$$

Reaction force at front support is therefore:

$$Front\ support\ force = force\ exerted\ by\ drum - rear\ support\ force$$

$$Front\ support\ force = 221117.4 - 90464.76$$

$$Front\ support\ force = 130652.6\ N$$

To find the additional force resulting from a 2g bump, the reaction force at the front support is simply multiplied by 3 (the 2g acceleration does not account for 1g gravity):

$$130652.6 * 3 = 391957.9\ N$$

The centre of mass position was estimated by modelling the drum and concrete in Solidworks and then using the mass properties tool. The concrete mix gathers towards the front of the drum due to the spiral blade arrangement, hence why the front support takes significantly more load than the rear support.

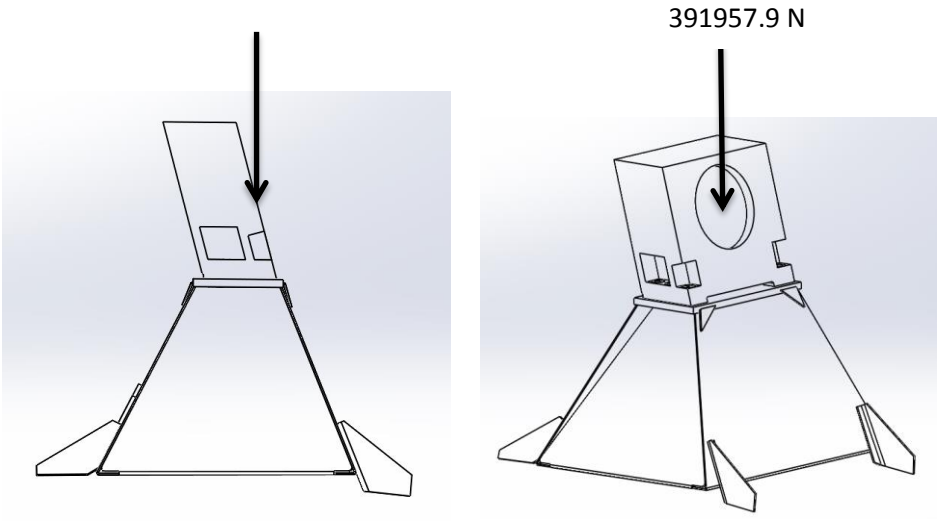

Figure 5-3 - Illustration of Vertical Load - Side and Rear Views

5.1.2.2 Chassis Twist Load

There was no literature available to base this load case on. Through discussions with an engineer at the mixer manufacturer, it has been estimated that the maximum 'twist' from one end of the chassis to the other is in the region of 8-10°. Since less than half of the length of the chassis & sub-frame was to be used in the analysis (for computational purposes), and that this frontal section of the chassis is the most flexible, the twist over this section alone was estimated to be around 5°. In this analysis, forces have been applied to the ends of the chassis rails to create this 5° misalignment. Using a 'forced displacement' on a face in SolidWorks restricts the movement of the face in a way that is unrealistic for this application. Using a simple force allows the faces to move with greater freedom. However, this meant applying a larger force to the model of the existing front support than the proposed support to achieve the 5° twist, since the existing design uses a sub-frame stiffening plate. This is illustrated in the results section.

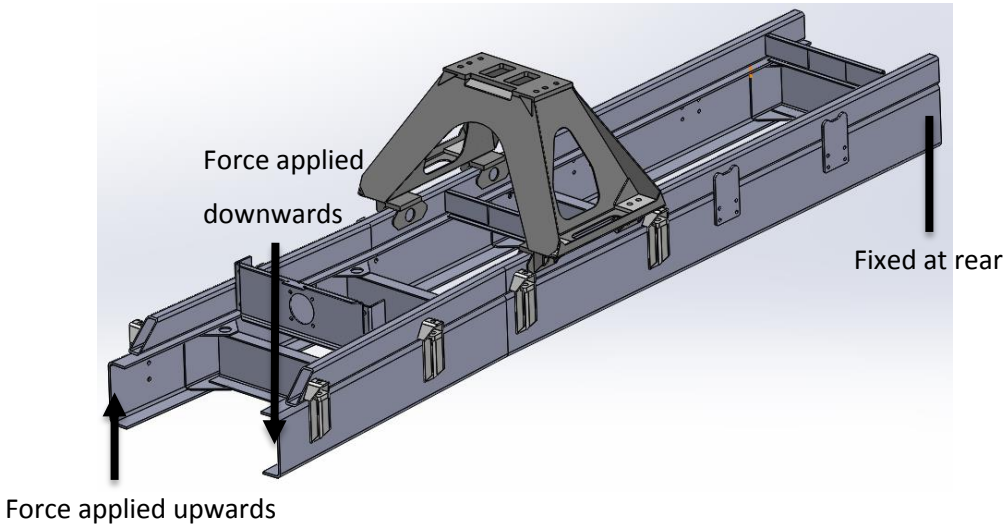

Figure 5-4 - Illustration of Twist Load

5.1.3 Changes Made to Load Cases after Dynamic Testing

The complexity of the measured strains has made it difficult to determine the way in which the loadings are transmitted through the gearbox, and therefore it is difficult to perform a comparison with the calculated loadings. One important finding was that under braking the force is not applied as longitudinally as expected. A greater vertical component needs to be accounted for. A new 'combination' load case has been created. This combination load combines both a longitudinal and vertical component, based on the maximum longitudinal

and vertical loads calculated previously. It effectively represents hitting a bump whilst braking on a hill.

It is thought to be impossible for the maximum vertical and longitudinal loadings to occur at the same time. Therefore each loading has been reduced. The slope on the longitudinal loading was reduced to 10°. This 10° angle causes an axial force of 91344N. A braking force of 0.5g has been used as before, giving a longitudinal force of 110513.6N. Since very high loads applied vertically through the support are unlikely to occur when going downhill, a vertical acceleration of 1g has been used in the analysis (261305N – remember this is 1g on top of gravity).

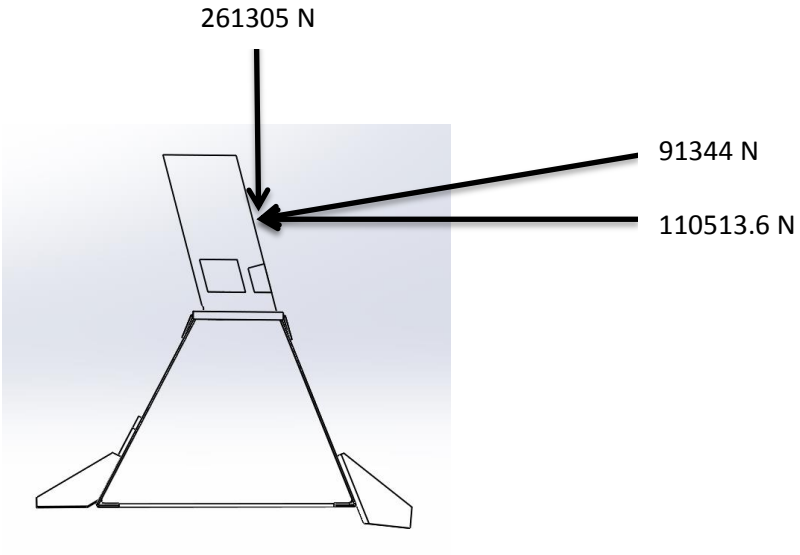

Figure 5-5 - Illustration of Combination Load - Side View

The majority of the measured stresses are slightly lower than the corresponding peaks computed in the FEA studies using the above load cases. There are few situations where the measured stresses exceed those computed by FEA. The main exception occurs at position 8 where a large compressive stress of 207.7MPa was measured, whereas the FEA study obtained a maximum of 130MPa at this position for the combination load case. Without fully understanding the cause of the measured peak, the best option when considering the redesign of the front support would be to ensure that a higher than normal factor of safety is employed for this region. The longitudinal load case is unrealistic, hence the creation of the combination load case. Other than this, it can be concluded that the

loadings applied in the FEA studies are suitable for design purposes. As always when designing by analysis, practical testing is required to validate the design.

5.1.4 FEA Results for Existing Front Drum Support

Regardless of the longitudinal load case being unrealistic, the results for all load cases are given below. All plots show Von-Mises stress on a colour scale set to a range of 0-355MPa to match with the minimum yield strength of the steel used in this structure. Von-Mises theorem is the accepted yield criteria for ductile materials. Although not shown in this thesis, principal stresses were also examined for the purpose of analysing and calculating weld strengths.

The support used in this analysis is the '8m' support. The sizes of these supports are matched to the drum sizes. Note that the model of the gearbox on top of the support has been simplified for simulation purposes. For accuracy in the region of the base of the support, the model includes a section of the sub-frame with two cross members. No weld geometry has been modelled so it is necessary to be wary of stress singularities arising at re-entrant edges. The upper edges of the 4 main panels were remodelled to sit flush with the thick top plate. This geometry enables a continuous/compatible mesh which helps to improve accuracy at this connection. The model is symmetrical from left to right. For the vertical, longitudinal and combination load cases the symmetry feature was employed. This allows only half of the model to be analysed, reducing computational efforts.

SolidWorks Simulation was used for all FEA, and all analyses were performed with static loadings. For the vertical, longitudinal and combination load cases the adaptive mesh feature 'h-adaptive' was used to ensure convergence. A solid mesh with parabolic tetrahedral elements was used. This was preferred over the use of a shell mesh for the improved accuracy at bonded/welded connections.

Vertical Load

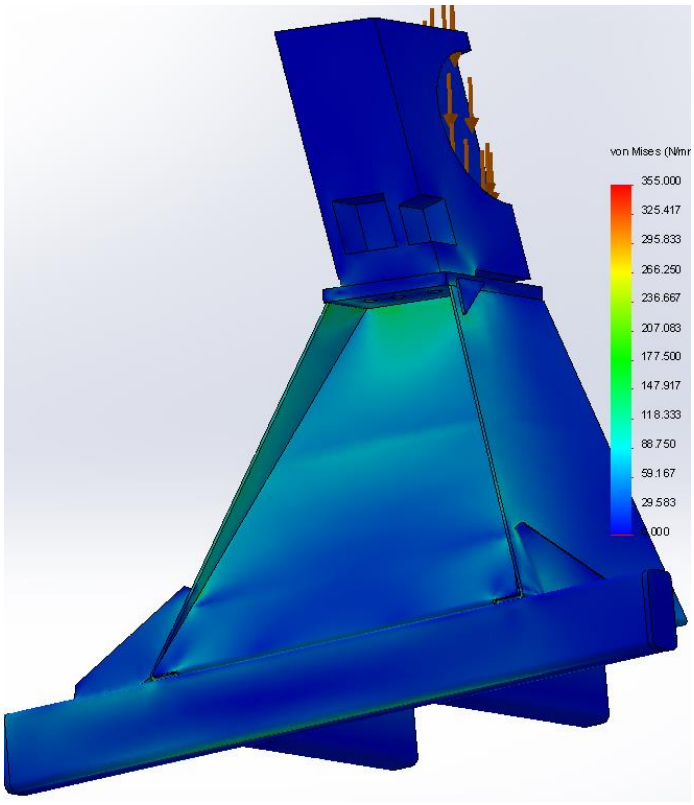

Figure 5-6 - Existing Front Support - Vertical Load - 1

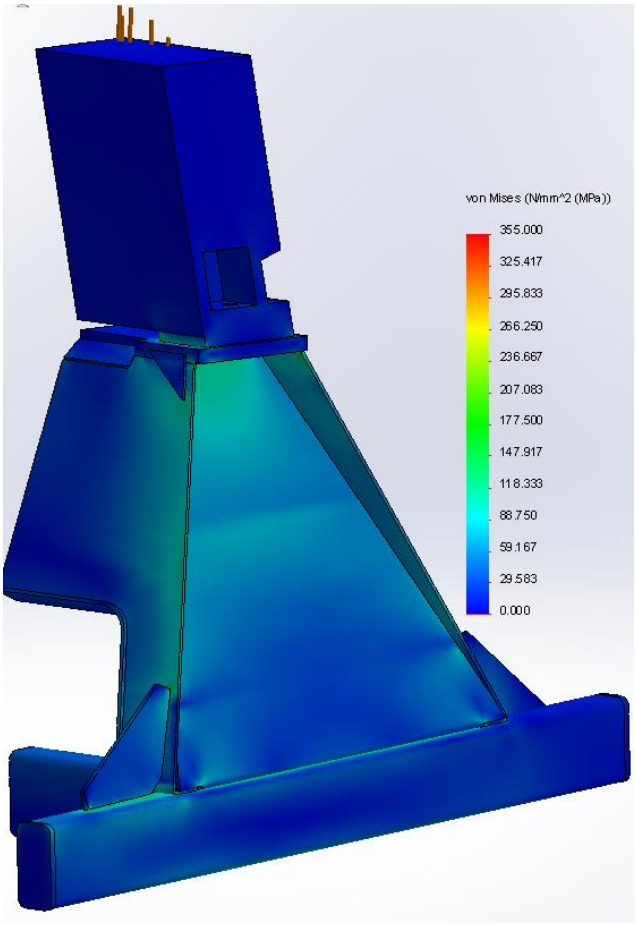

Figure 5-7 - Existing Front Support - Vertical Load - 2

Longitudinal Load

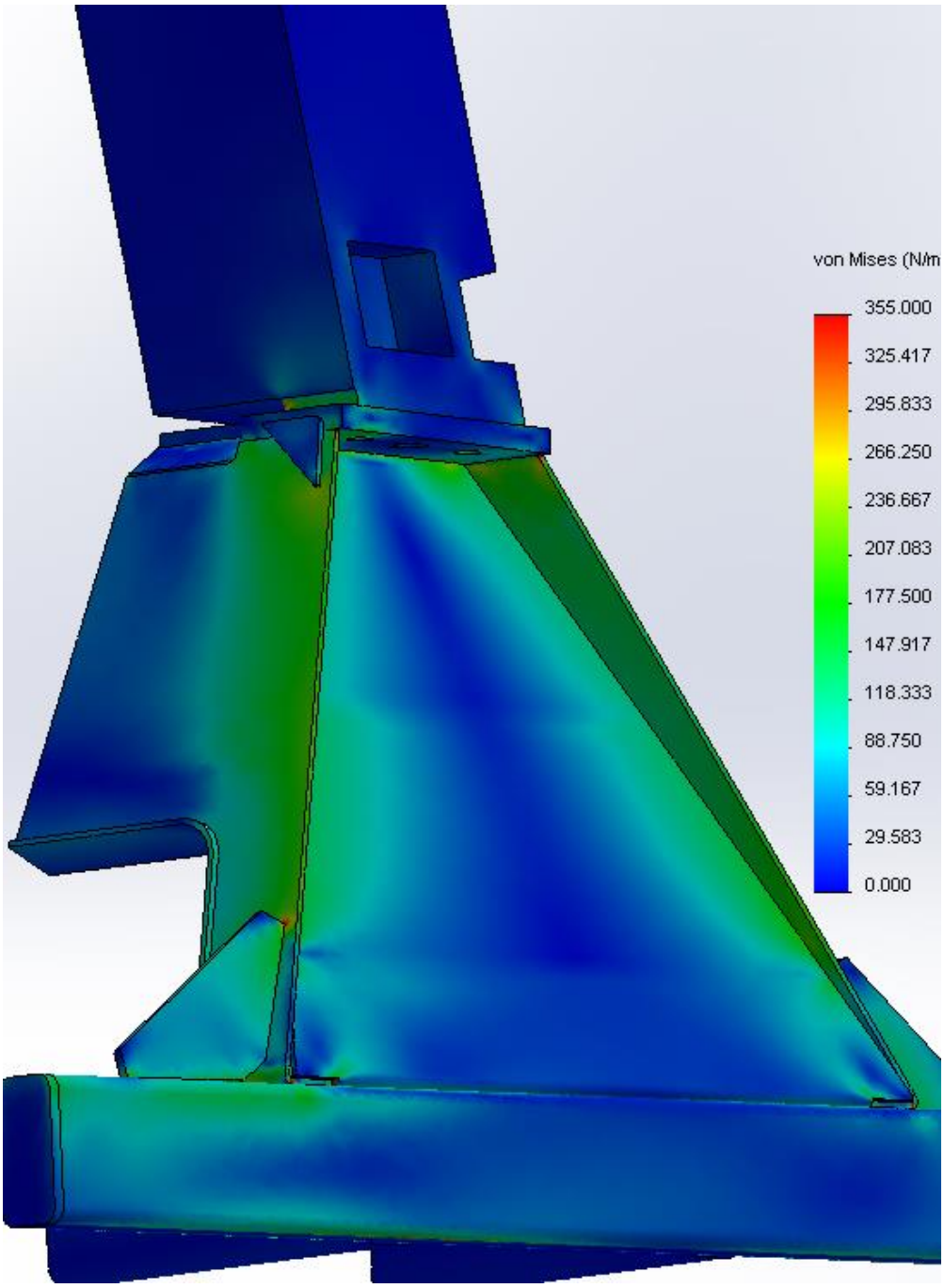

Figure 5-8 - Existing Front Support - Longitudinal Load

Combination Load

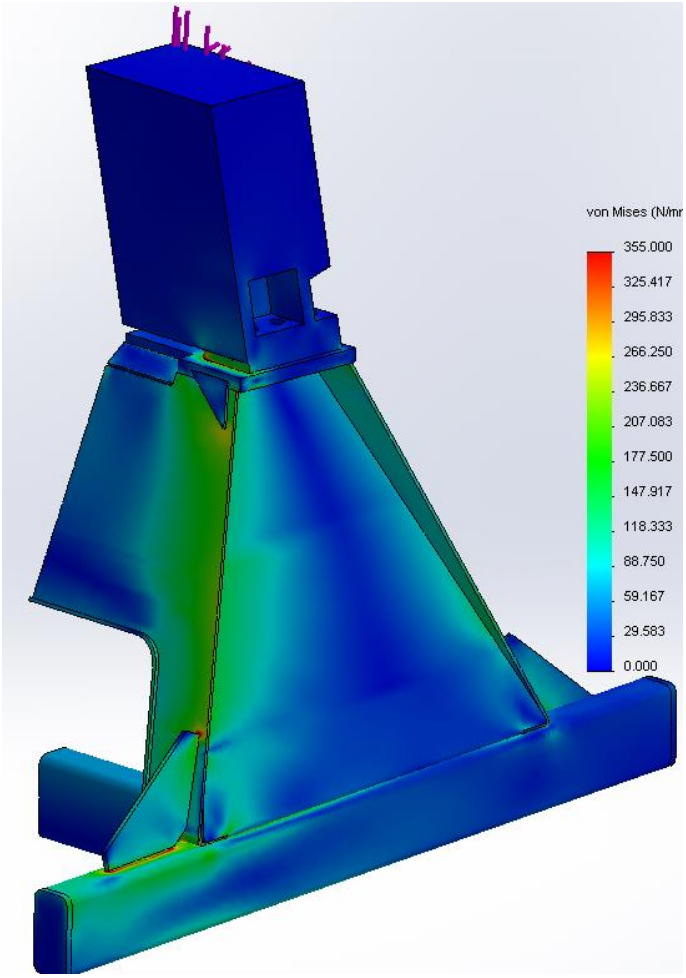

Figure 5-9 - Existing Front Support - Combination Load - 1

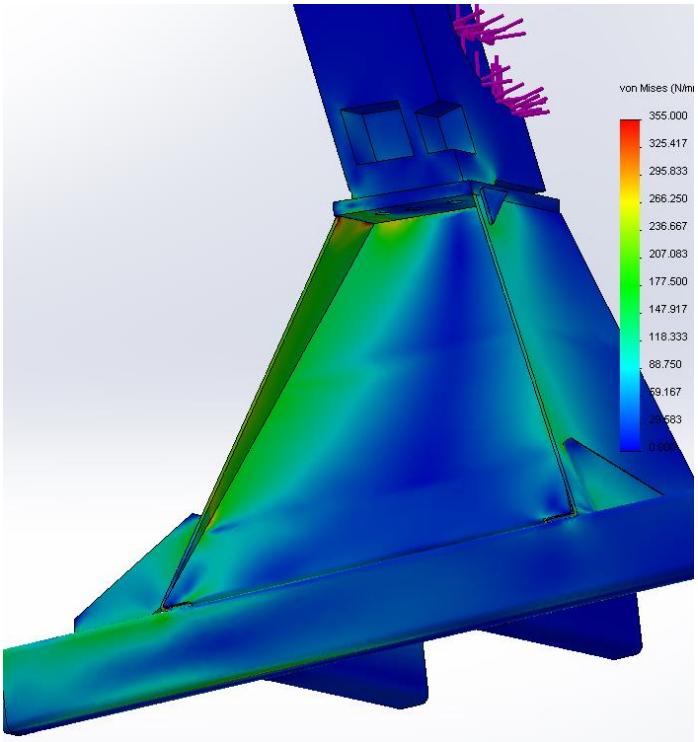

Figure 5-10 - Existing Front Support - Combination Load - 2

Chassis Twist Load

Unfortunately this study could not be completed using high quality elements, most likely due to hardware restrictions. It is a large and complicated model with various computationally intensive contacts. The study was therefore run using low quality first-order tetrahedral elements. Such elements only have 4 nodes connected by straight edges and as such they are not as good at representing curved boundaries (second-order tetrahedral elements have 10 nodes in total). The less effective shape functions of the first-order element cause under predicted displacements and less accurate stresses.

These results are therefore purely for comparison purposes. It is still possible to draw conclusions regarding the differences in the way that the existing and proposed supports interact with the sub-frame.

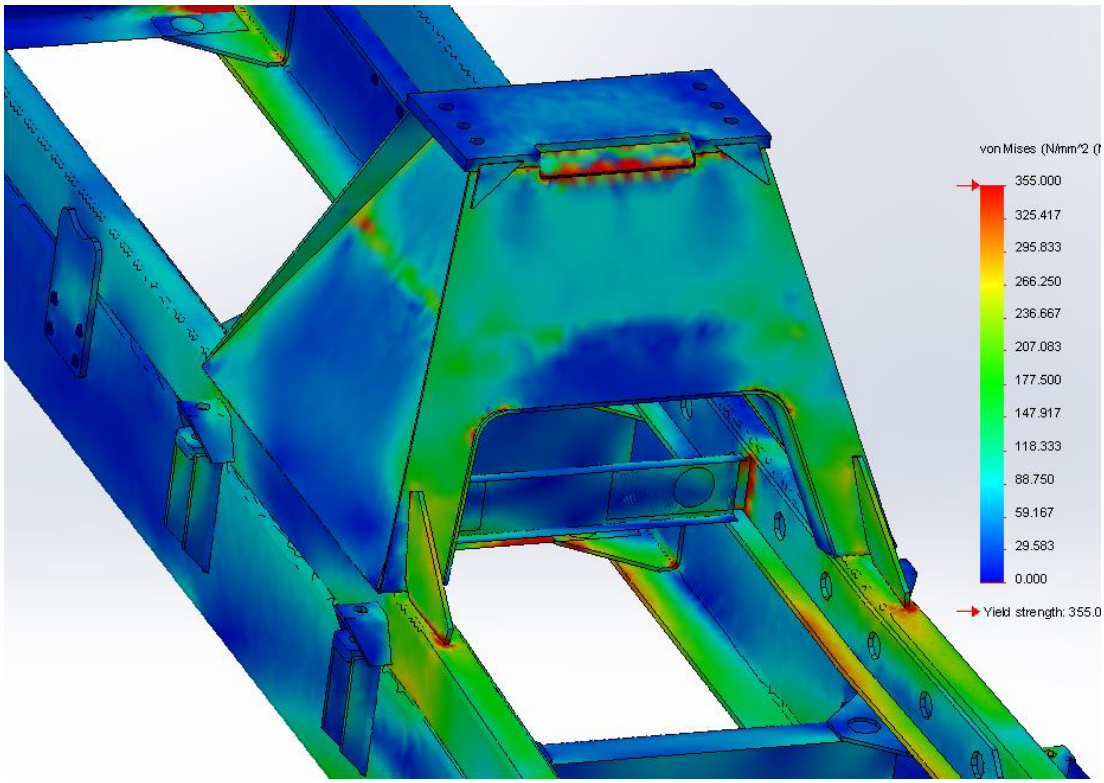

Figure 5-11 - Existing Front Support - Twist Load

5.1.4.1 Discussion of Results

The vertical load creates little stress in the structure which suggests that it could withstand far greater vertical loads. The combination load creates a relatively high compressive stress in the front panel. However, 280MPa is far from being great enough to cause buckling. The test in 5.1.7 confirms this. For the vertical, longitudinal, and combination loads, the existing support has a higher than necessary factor of safety. This suggests there is scope to reduce weight.

For the twist load, stress concentrations are visible at the front of the triangular gussets contacting the top of the sub-frame. It can be concluded that this is the most stressed region across the base of the support during a twist load. However, the stress in this region is affected by singularities. It should also be pointed out that the stresses in the structure would be different had loads been applied to the top of the support. Also note that the sub-frame stiffeners are present in this model (the plates with the series of holes on the inside of the sub-frame legs). It seems that the high rigidity of the existing front support results in poor stress distribution under such twist loads. One solution would be to use a very stiff sub-frame, but this would increase weight. Therefore the approach has been taken to design a support that interacts more effectively with the current sub-frame design. It is also intended that the sub-frame stiffening plates will no longer be required with the proposed front support design.

5.1.5 Design of Proposed Front Drum Support

It has been found that the existing design creates stress concentrations at its connection to the sub-frame. This area has been a known failure region. The proposed design has therefore been developed to interact more effectively with the sub-frame whilst keeping weight as low as possible within financial restrictions. A method of indirectly bolting the support to the sub-frame has been developed. Many mixer manufacturers use bolts in a similar fashion, but their designs are often heavy. As discussed before, one of the greatest selling points in the UK industry is low weight.

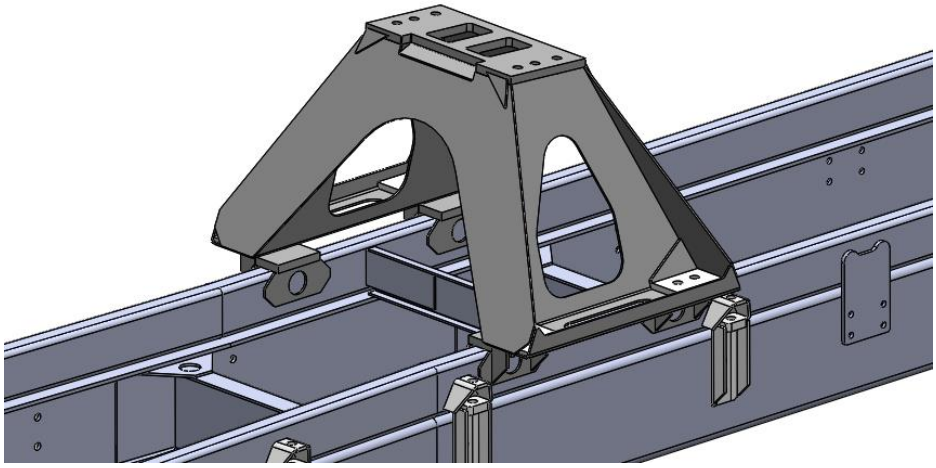

Figure 5-12 - Proposed Front Drum Support on Sub-Frame

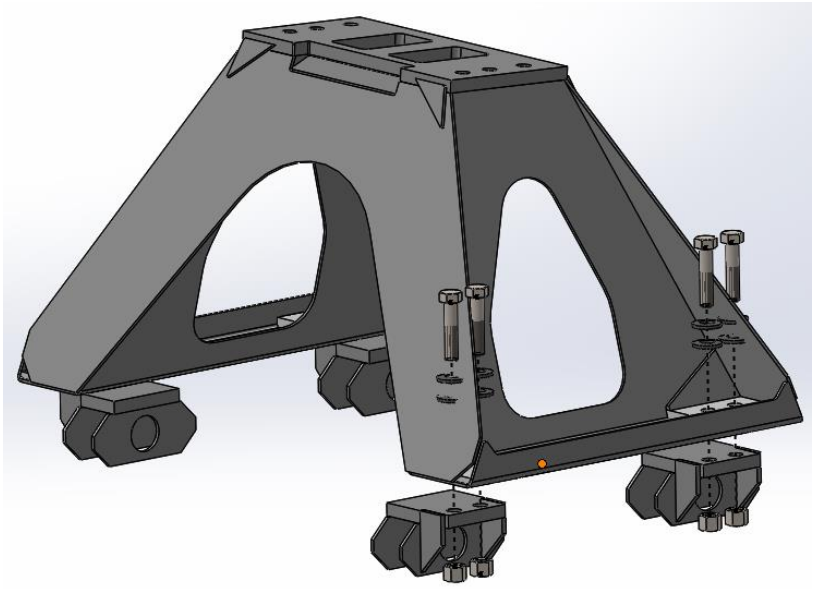

Figure 5-13 - Exploded View of Bolting Arrangement

It is a welded structure comprising of a main support structure and 4 ‘bolting blocks’. For each bolting block there are two plates welded to the sub-frame; one on each side to ensure that the loads are spread over a suitably large area whilst limiting the weld length in any one particular direction. These plates are plug welded (see the central hole on each of these plates) and also welded around their edge. The edge weld starts and finishes around 75% of the way up the sides of the plate. Above this point the sub-frame’s corner radius creates a gap. Attempting to weld this gap may yield poor weld geometry, hence the start and end positions. The material of these plates has been matched to that of the sub-frame (S355). The thick base plate on the bolting blocks simply rests on top of the sub-frame. It is best to weld to the sides of a hollow section arranged in this way since the top and bottom surfaces experience the largest stresses. The bottom corners of the front and rear panels have small cut-outs to allow water drainage from the bolting area.

Like the existing design, the main support structure uses 4 main panels to make up the shell of the structure, each of them 5mm thick. However, the proposed design uses Strenx 600MC for these panels, chosen for its combination of formability, weldability, and strength. The characteristics of this steel are discussed in section 2.2. The use of this high-strength low-alloy steel has allowed for material to be removed from the panels. One of the improvements delivered by this design is the ‘archway’ through the structure from front to rear. This shape allows a minute amount of flexibility in the structure which is apparent under torsional ‘chassis twist’ loads. This reduces stress in the sub-frame. Between this and the attachment design of the bolting blocks, the interaction between the support and the sub-frame is greatly improved.

The experiment in section 3.2 found that U-bolts offer no clear advantage over straight bolts for this application. The bolts selected are M20x90 grade 12.9 with corresponding grade 12 nylon lock nuts – two bolts per corner. Two heavy duty conical spring washers are used on each bolt. The purpose of these spring washers is to maintain preload in the connection. Each spring washer requires a force of approximately 93.2kN to flatten it. When arranged in parallel this force simply doubles (186.4kN). The proof load of an M20 Grade 12.9 bolt with a course thread is around 238kN. Flattening these spring washers therefore requires a force of 78% of the bolt’s proof strength. This ensures that a suitable level of preload will be maintained despite the relaxation that will occur in the connection over time. Preload helps to prevent vibration loosening. This is of particular consideration

where the bolts have a low length to thickness ratio, such as those used in this design. An alternative method would be to use longer bolts with spacers/packers. It would be possible to use one larger bolt per corner; however a company-led decision resulted in the use of two bolts per corner.

An undermatching weld wire was selected; G 38 4 M G3Si1 with minimum yield strength 380MPa. The strength of an undermatched weld has been shown to greatly exceed the strength of the welding wire, due to triaxiality and strain hardening, Collin et al (2007). A weld wire with yield strength closer to 500MPa would be a more suitable match for the base material; however the G 38 wire is of suitable strength for this application given the arrangement of the welds.

The weight of the proposed support for an $8m^3$ mixer is 79Kg including bolts. This is just 2.8Kg less than the existing support; however the intention is that the sub-frame stiffening plates can be removed with this design. This removes a further 18Kg. Weight could be further reduced by using just one bolt per corner.

5.1.6 FEA Results for Proposed Front Drum Support

Like the FEA results for the existing support, all plots shown are for Von-Mises stress. The symmetry feature has been used. The adaptive meshing tool 'h-adaptive' was not used for this model and therefore the convergence process was manual. The parameters of the automatic mesh were set to a max element size 18.6mm, min element size 1mm, and a size of 4.2mm was specified for a variety of surfaces where increased accuracy was required.

Like the existing support, this proposed support is an '8m' model, sized for an $8m^3$ drum. Two stress scales are given in the following results; one scaled to a max of 355MPa to match the yield strength of the parts made from S355, and the other scaled to 600MPa to match the yield strength of the parts made from Strenx 600MC. The icons at the bolted areas purely indicate that bolt connectors are present.

Vertical Load

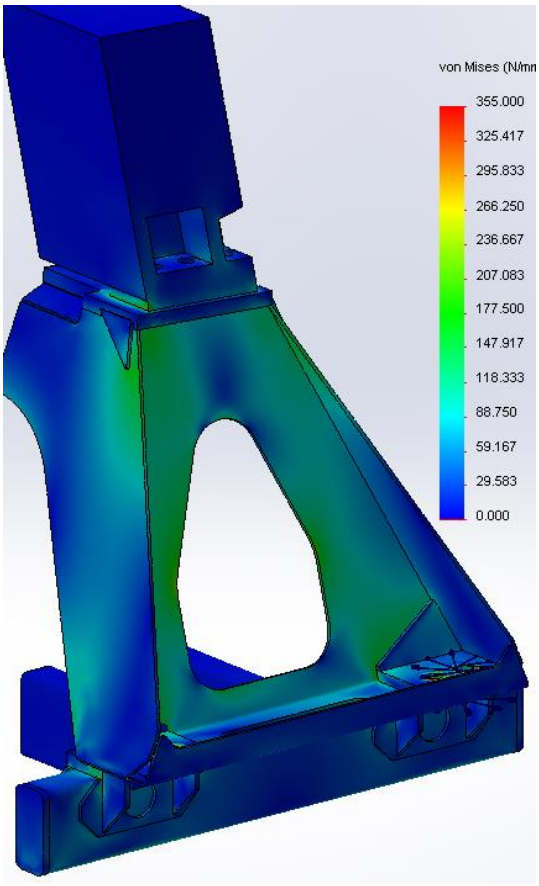

Figure 5-14 - Proposed Front Support - Vertical Load - Scaled to 355MPa

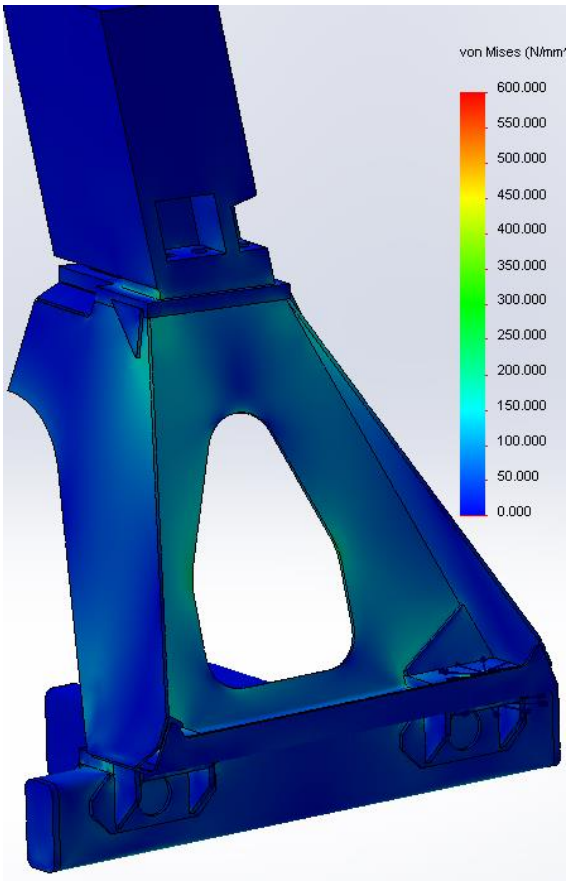

Figure 5-15 - Proposed Front Support - Vertical Load - Scaled to 600MPa

Longitudinal Load

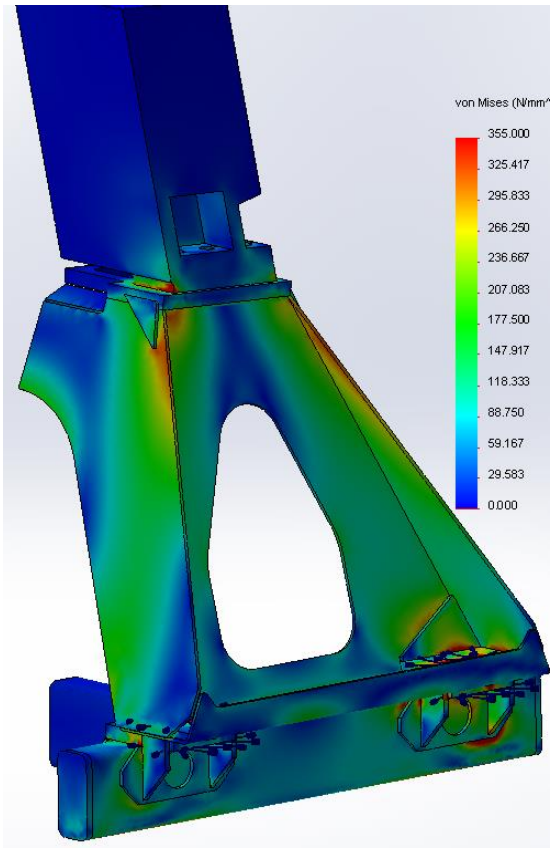

Figure 5-16 - Proposed Front Support - Longitudinal Load - Scaled to 355MPa

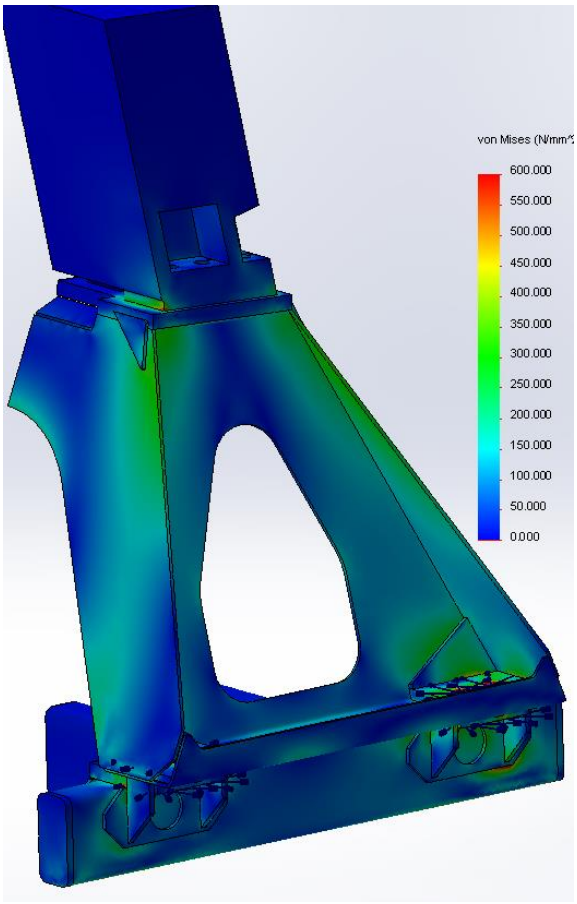

Figure 5-17 - Proposed Front Support - Longitudinal Load - Scaled to 600MPa

Combination Load

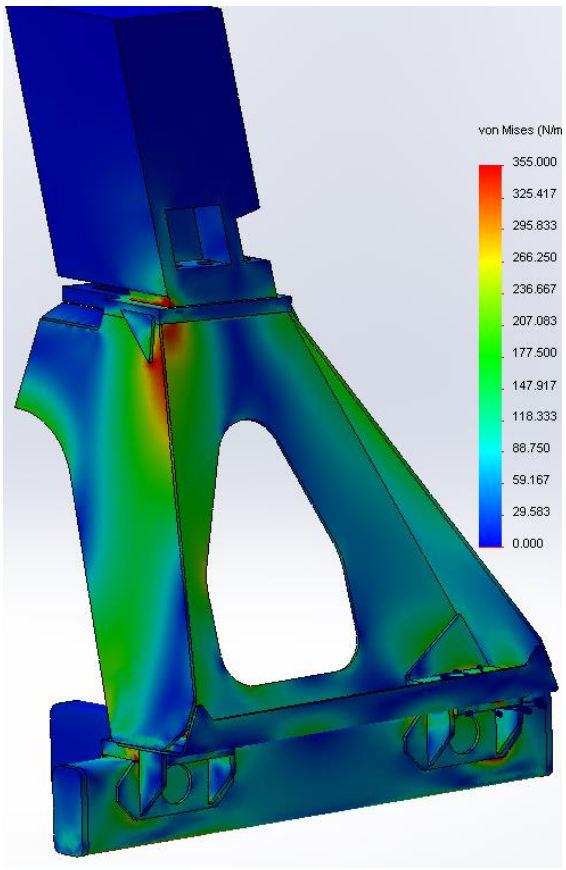

Figure 5-18 - Proposed Front Support - Combination Load - Scaled to 355MPa

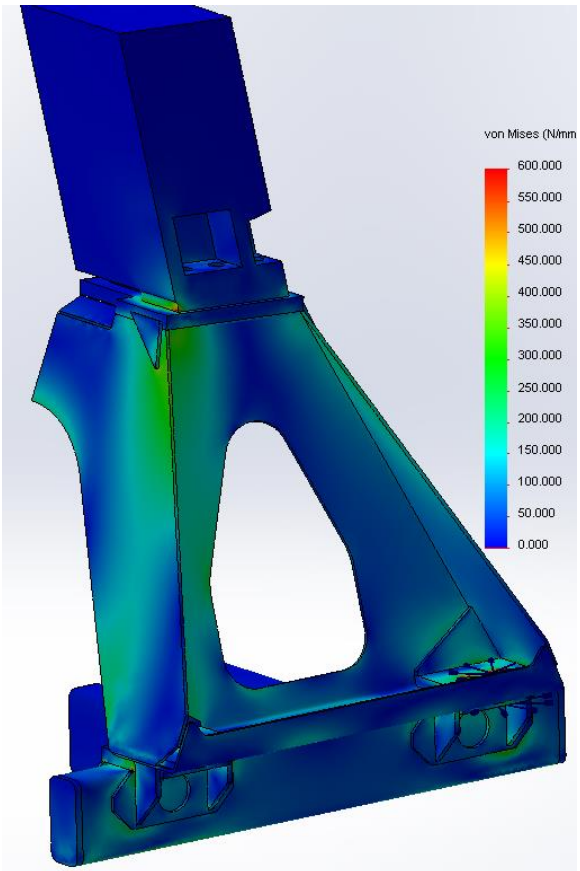

Figure 5-19 - Proposed Front Support - Combination Load - Scaled to 600MPa

Chassis Twist Load

As before, this study had to be completed using low quality first-order elements.

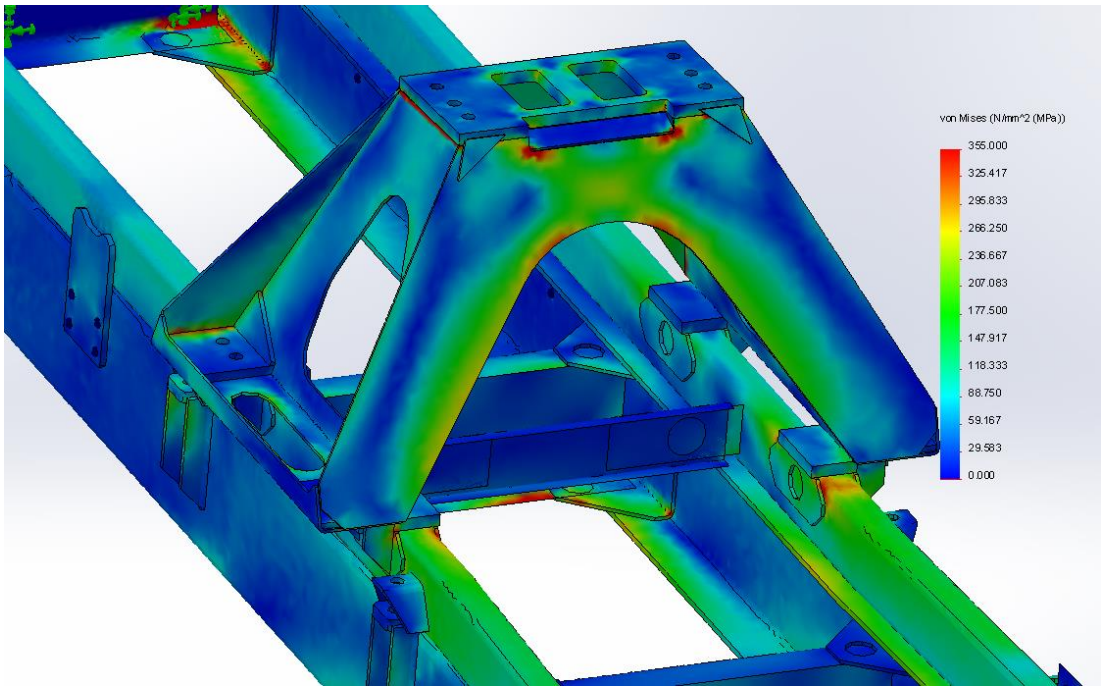

Figure 5-20 - Proposed Front Support - Twist Load - Scaled to 355MPa

5.1.6.1 Discussion of Results

Like the existing support, the proposed support withstands the vertical load without developing high stress. For the combination load, the compressive stress in the front panel reaches 350MPa, 70MPa more than on the existing support. Other than this compressive stress, the proposed support has no areas of concern. The test in 5.1.7 has proven that the buckling resistance of the proposed support is more than adequate.

For the twist load, an area of high stress does still occur in the sub-frame near the front of the support, particularly on the right side. However, the stress on top of the sub-frame legs is greatly reduced in comparison to the study with the existing support. The right side of the chassis is being forced downwards. The front corner on this side is therefore resisting and pulling upwards on the sub-frame. The region of the largest stress has been moved to the side of the sub-frame. The high stress region is less severe and spread over a larger area than with the existing support. It can be concluded that the proposed support does interact more effectively with the sub-frame; however, care must still be taken to achieve high quality welds. The weld toe near the highly stressed region should be ground smooth.

5.1.7 Further Testing – Press Test

As part of the Design by Analysis process, it is necessary to confirm the suitability of an optimised design by means of practical testing. It was found that high compressive stresses occur in the front drum support, particularly under the combination load. With the nature of this structure, it was difficult to accurately determine the buckling load using FEA. In order to determine the buckling load, the support has been tested in pure compression. It was too complicated to apply a loading similar to the combination load, hence using a simple vertical load in testing.

5.1.7.1 Equipment and Procedure

A Tinius Olsen press capable of exerting 90 tonnes was used for the test. Both the existing and proposed supports were tested. Each support was welded onto a hollow section frame using the same 120x60x6.3mm S355 hollow section as the sub-frame. The length of this frame was limited by the dimensions of the press bed which was only just large enough for the full scale supports. Four strain gauges were attached to the proposed support. Five strain gauges were attached to the existing support in similar positions (the different design meant that they could not be placed in identical positions). Two blocks were machined and bolted to the top plate of each support. These blocks closely replicate the two feet of a typical mixer gearbox.

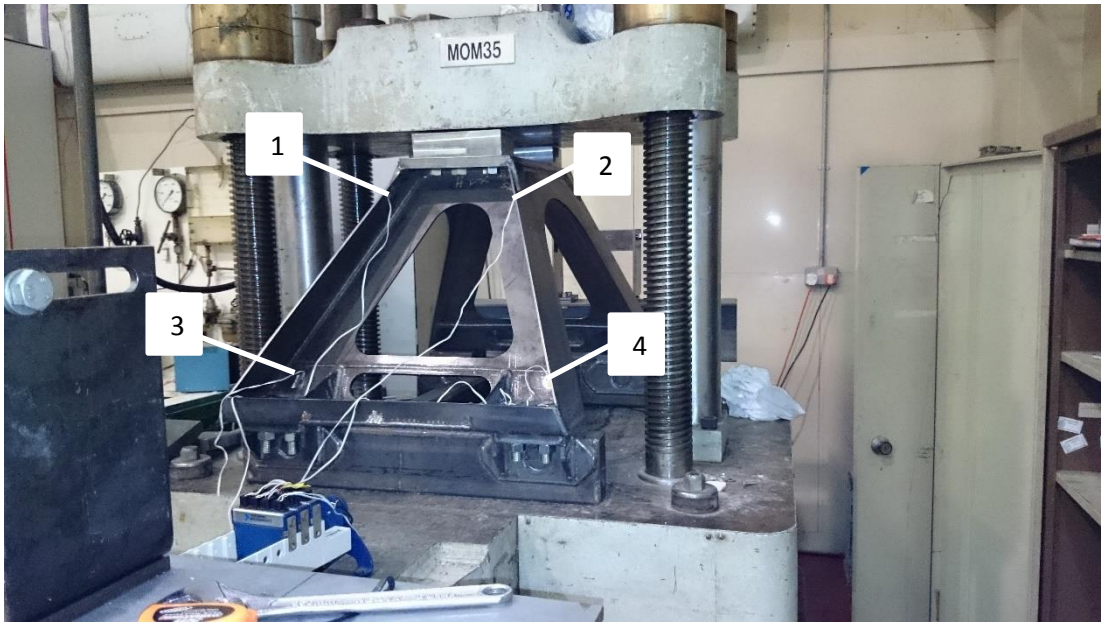

Figure 5-21 - Proposed Support Positioned in Press

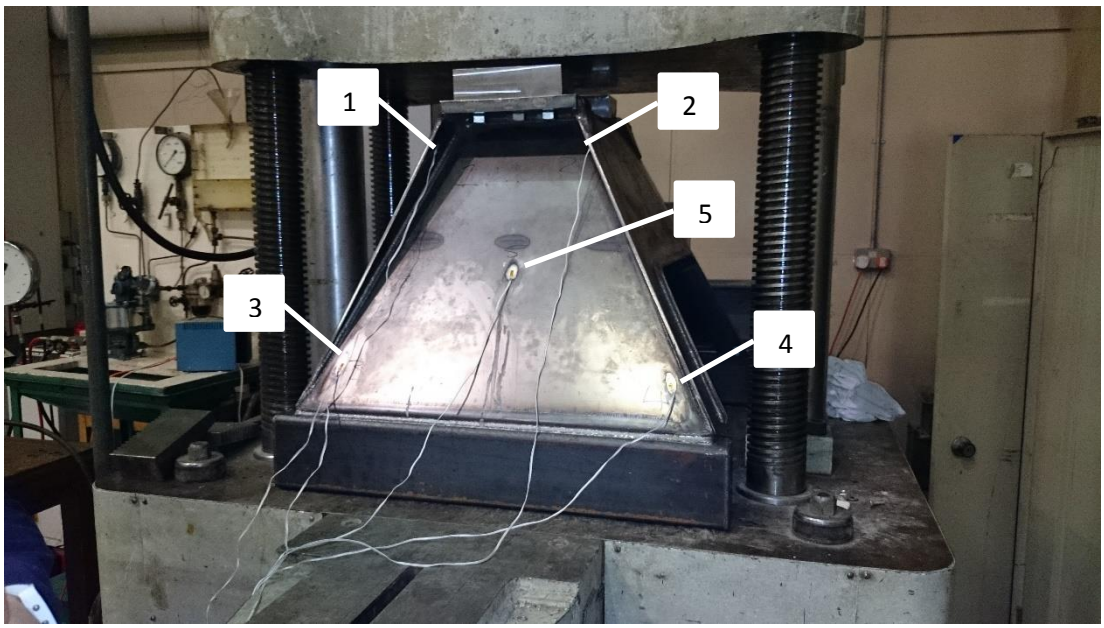

Figure 5-22 - Existing Support Positioned in Press

In Figures 5-21 and 5-22, the supports are shown positioned in the press ready for testing, and the strain gauge positions have been illustrated. Positions 1 and 2 are on the inside of the front and rear panels. Positions 3 and 4 are on the side panel.

It is important to note that there are some differences between the tested proposed support and the analysed proposed support presented previously. Revisions were made after testing to improve manufacturability. To clarify, the revised support is the one shown in the FEA results. The tested support primarily differs in that the side and rear panels are 4mm rather than 5mm, and that the side panels meet the top plate inwards from the edge like on the existing support. The side panels are also made using two separate parts. The lower flange section is 8mm thick. This caused manufacturing issues whereby part of the side panel was bending after welding. Hence the two parts of the side panels were combined into one 5mm thick panel. To keep the manufacturing process simple, it was then decided that the rear panel should be cut from 5mm steel so that all of the main panels can be cut from the same sheet of Strenx 600MC. Arranging the side panels so that they meet the top plate at the edge was done to further increase buckling resistance. Due to these changes, the revised version will exhibit a higher buckling resistance than the tested version.

Three loading runs were performed on each support. The first two loaded the support from zero to around 400kN, and then back to zero. This is practically the same as the vertical

load applied in the FEA study. The third run loaded the support until failure, i.e. buckling, visibly occurred. The top plate of the support is not level. It is angled upwards towards the front at around 3.6°. The two blocks bolted to the top plate were designed to provide a flat contact surface for the press. Unfortunately, due to manufacturing inaccuracies the press contacted the blocks unevenly, and also slightly differently for each support. With even loading the buckling resistances would have been greater. The tests were also recorded on video. The videos proved useful for confirming at what load the supports began to visibly deform, and for capturing the shape of deformation since the supports sprung back to their original shape when the load was removed.

5.1.7.2 Results

Only the stress plots for the high stress areas (strain gauge positions 1 & 2) are shown below. There is a separate graph for each of the three runs, and each graph shows the plots for both supports. The gauges were not zeroed between runs. On the first two runs, the stresses do not necessarily return to zero when the load is decreased to zero. Given that the supports experience no yielding or buckling at this load, it is unlikely that this residual stress is accurate. It may be due to poor attachment of the strain gauges. The peak stresses may therefore lack accuracy, particularly for position 2 on the proposed support which appeared to experience a large 'drift' during Run 1. There is also a spike during run 2 on the proposed support at around 125kN, the cause of which is unknown.

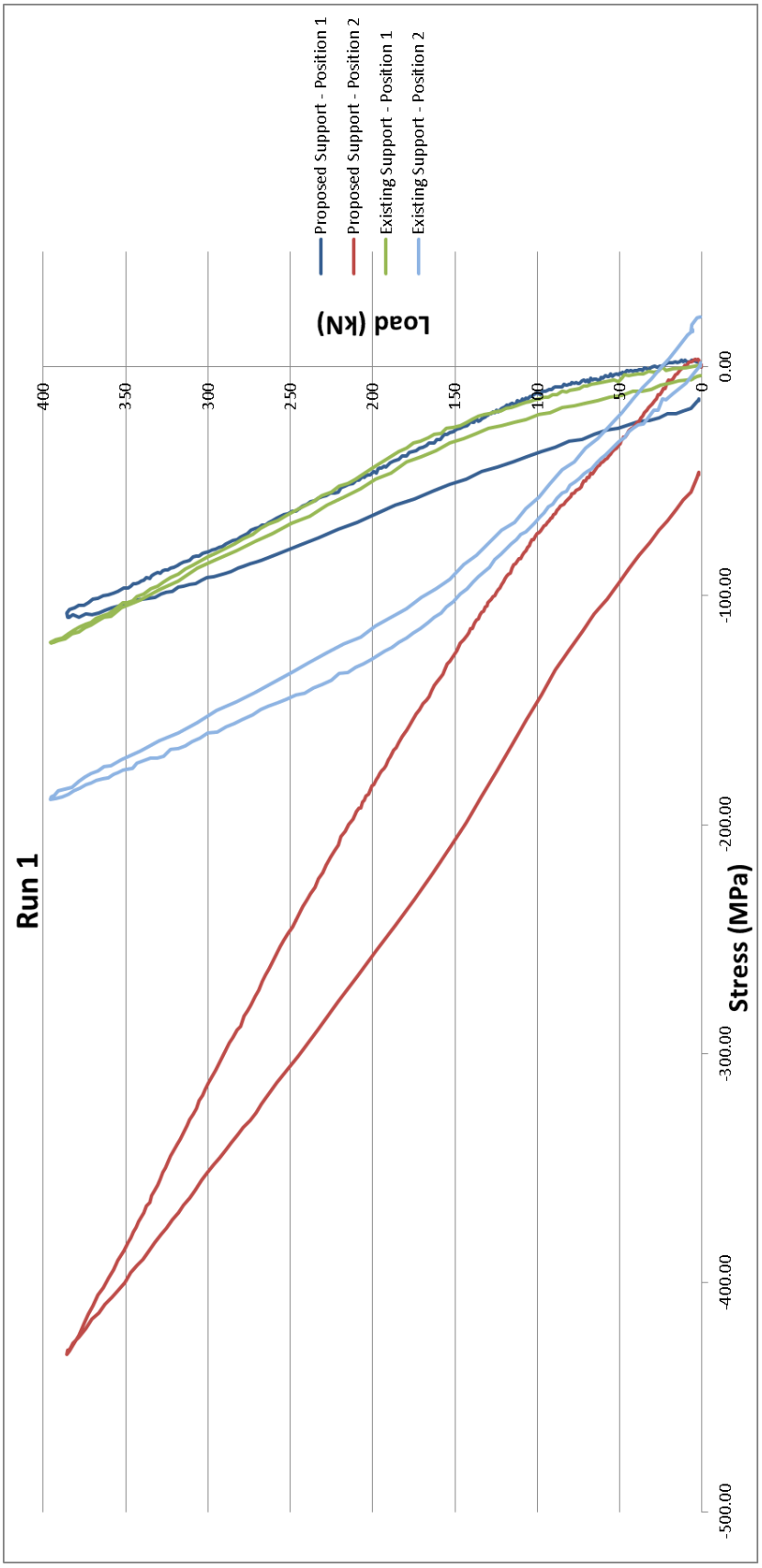

Figure 5-23 - Run 1 - Stress Plots for Positions 1 & 2 on Both Supports

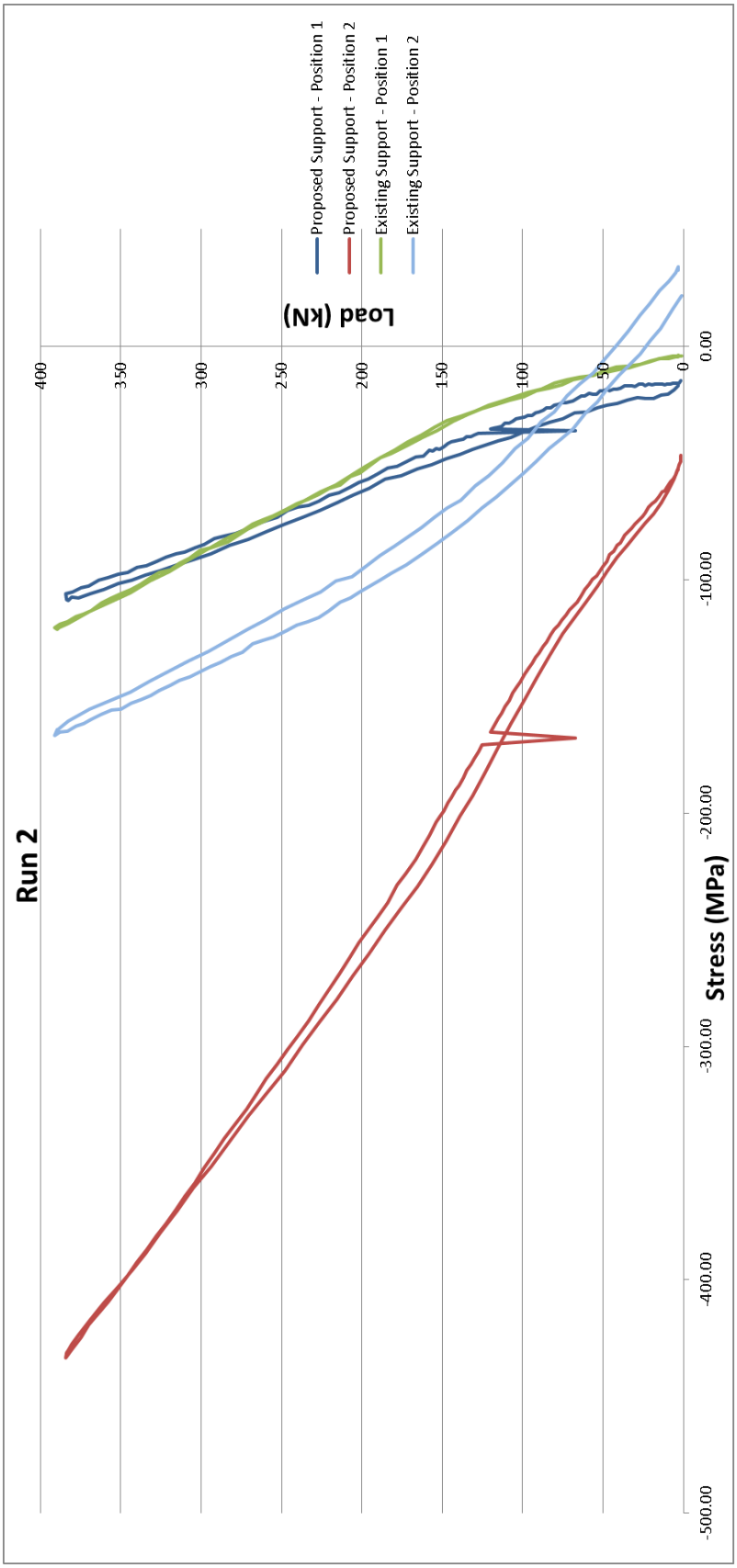

Figure 5-24 - Run 2 - Stress Plots for Positions 1 & 2 for Both Supports

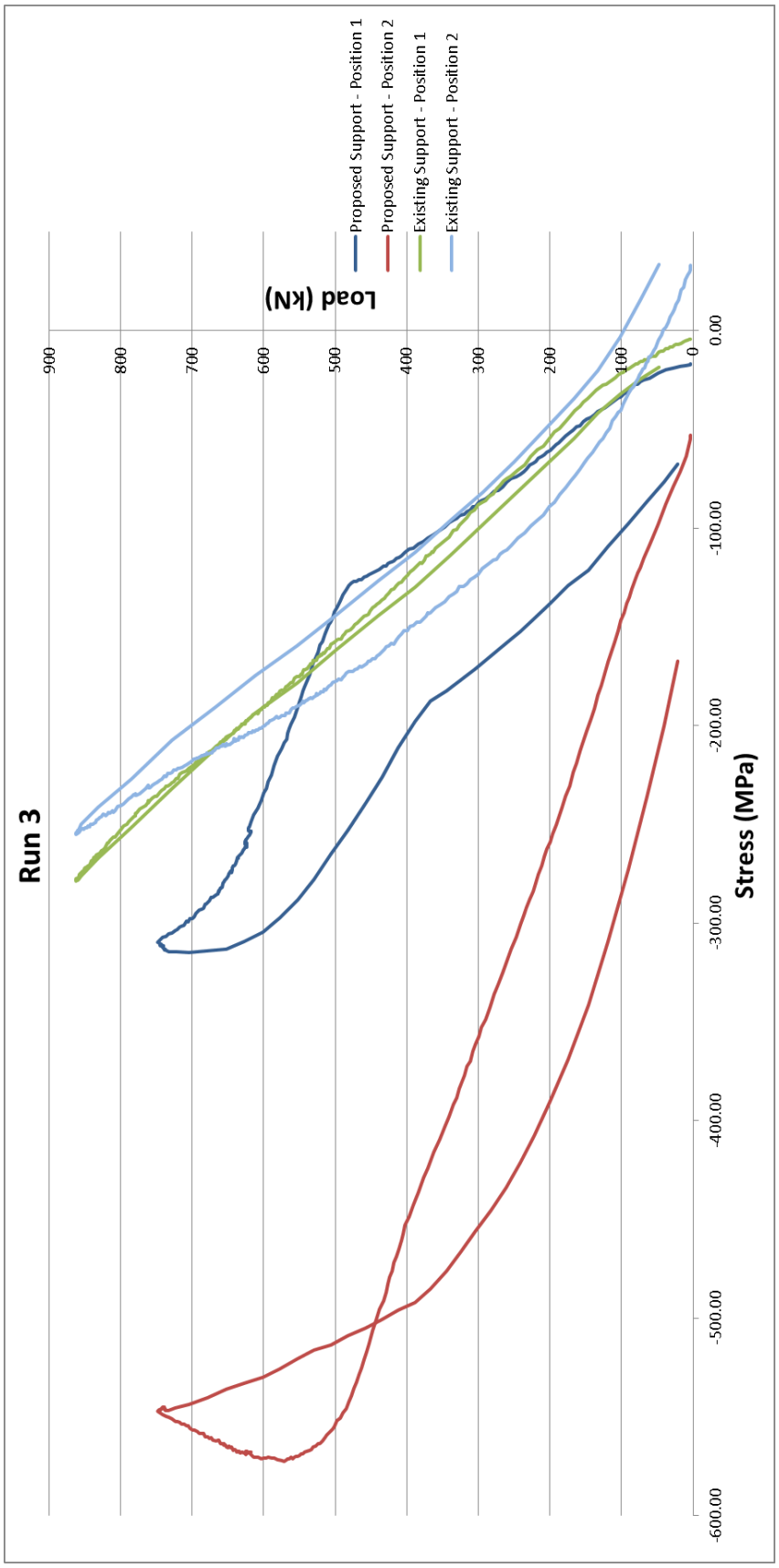

Figure 5-25 - Run 3 - Stress Plots for Positions 1 & 2 for Both Supports

The existing support withstood 870kN without any sign of deformation, apart from a slight cracking noise that was heard from inside the support. This may have been a weld splitting on one of the small stiffeners inside the support. The decision was made to end the test at this load rather than push the capabilities of the press. For a vertical load at least, the existing support exhibits a factor of safety in excess of 2.22.

There is a far greater difference in stress between positions 1 & 2 on the proposed support than on the existing support which confirms that the proposed support was loaded less evenly than the existing support. This uneven loading reduces the validity of the comparison. Despite the unfair loading, on run 3 it can be seen that the proposed support began to buckle around 470kN, 78kN above the worst-case vertical load. For the vertical load, this provides a factor of safety of 1.2. The uneven loading means that the resulting load path is in some ways more similar to the combination load. In the FEA study of the non-revised support (not shown in this thesis), the stress in the front panel peaked at 400MPa for the combination load. Gauges 1 and 2 have been placed where these high stresses in the front and rear panels occurred in the FEA study. Run 3 shows that a compressive stress of just over 500MPa occurs at position 2 before the proposed support begins to buckle. Since position 2 appeared to experience a drift of 40MPa in run 1, it would be more conservative to say that a stress of around 460MPa occurs before buckling. Therefore it could be suggested that the proposed support provides a factor of safety of around 1.15 for the combination load.

The factor of safety calculated for the vertical load is particularly skewed by the uneven loading. However, the aforementioned revisions made to the support after this test have significantly increased the buckling load. Given the improved stress distribution in the revised support, a factor of safety of 1.45 – 1.5 is estimated for both the combination load and the vertical load.

Two video stills are shown below; one from before any load was applied on the proposed support and the other from the point of maximum load. The video camera was directed at the opposite side of the support from that shown in Figure 5-21. The deformation is apparent in the upper left region.

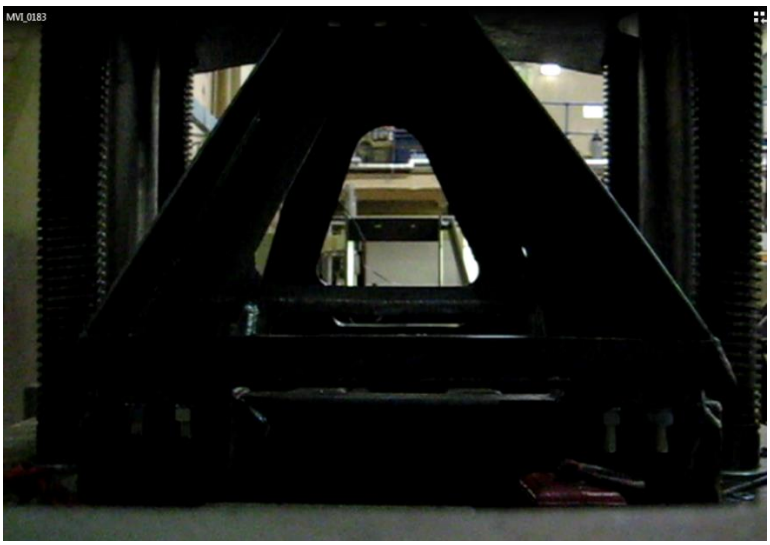

Figure 5-26 - Proposed Support before Loading

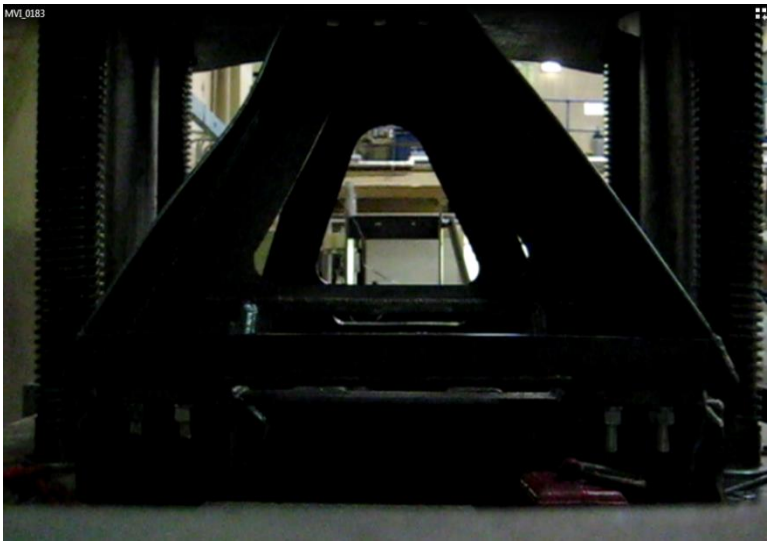

Figure 5-27 - Proposed Support at Maximum Load

Comparing the stresses calculated from the strain data to the FEA calculated stresses is of low validity due to the uneven loading. Regardless, a comparison is given below using the data for the existing support. For the FEA principal stresses, the average was taken from several nodes in the region of the strain gauge. Positions 3 and 5 have good correlation; however positions 1, 2, and 4 have unsatisfactory differences. No issues were found with the analysis; therefore the majority of the error is likely due to the uneven loading.

Table 5-1 - Test vs. FEA Stress Comparison for Existing Support

	Position 1	Position 2	Position 3	Position 4	Position 5
Press test - stress calculated from strain data (MPa)	-120.26	-168.35	-49.28	-34.16	-61.39
FEA - principal stress (MPa)	-94.5	-105.6	-48.3	-48.8	-60.55
Difference	25.76	62.75	0.98	14.64	0.84

5.1.8 Reflective Conclusion

The press test has proven that the proposed support can withstand the worst-case vertical load despite the load being applied unevenly. The revisions made to the support after testing ensure that a suitable factor of safety is achieved, as well as improving manufacturability.

The only significant downfall of this test was the uneven application of the load. Time constraints made it impossible to machine new blocks or shims. A simple solution if the test were to be performed again would be to build a basic jig for each support that would constrain the top plate at a precise angle during the assembly process. It would also have been beneficial to zero the strain gauges after each run.

The proposed front support has succeeded in improving the interaction with the sub-frame. On the other hand, the resulting design costs more to manufacture than the existing support. For the needs of this concrete mixer manufacturer, the upsides outweigh the downsides.

Alternative bolting/fixing solutions could be investigated in future. Casting the bolting blocks should also be considered as a potential cost reduction.

5.2 Rear Drum Support – Design & Analysis

The rear of the drum rests on two large roller bearings attached to the rear drum support. This arrangement means that the rear drum support practically takes no longitudinal loads. It also takes a lower overall vertical load than the front support due to the concrete collecting towards the front of the drum. However, the rear support can experience shock loadings due to the drum 'bouncing' off the rollers when the truck hits harsh bumps. Some trucks have particularly stiff rear suspension which increases the likelihood of the drum bouncing off the rollers. Failures are infrequent, however the primary cause of failures at the welded connection between the support and the sub-frame is thought to be due to these shock loadings. The rear of the chassis tends to have greater torsional rigidity than the front so chassis twist loads are of less concern.

The rear support also serves as a base for a variety of other parts and structures to be attached. The main structures attached are the discharge chute, the ladder platform, and the rear columns that support the loading chute and the collection chute. Sometimes a 'drum flap' is also attached via these rear columns (a drum flap is a semi-circular hydraulically operated flap designed to prevent spillage from the mouth of the drum).

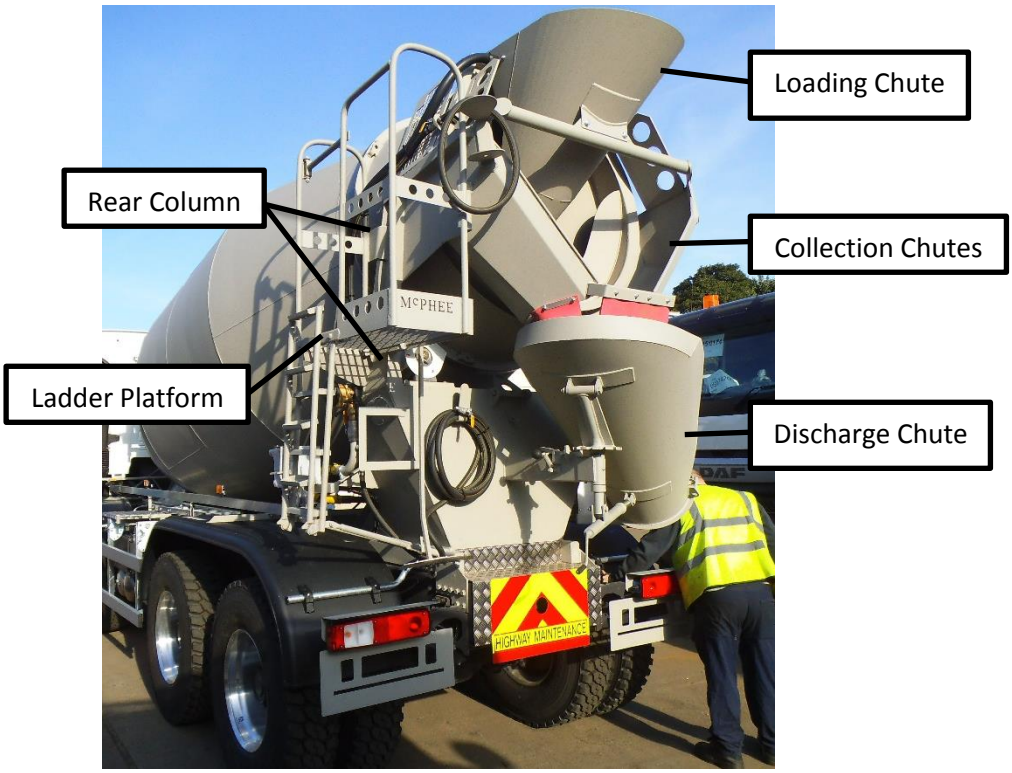

Figure 5-28 - Main Structures Supported via the Rear Drum Support

5.2.1 Design of Existing Rear Drum Support

Like the front drum support, this is a welded sheet metal structure. The main panels are 4mm S355. It is primarily constructed from a rear panel that wraps over the top, two outer side panels that wrap around to the front, two inner side panels, and an arch-shape front panel.

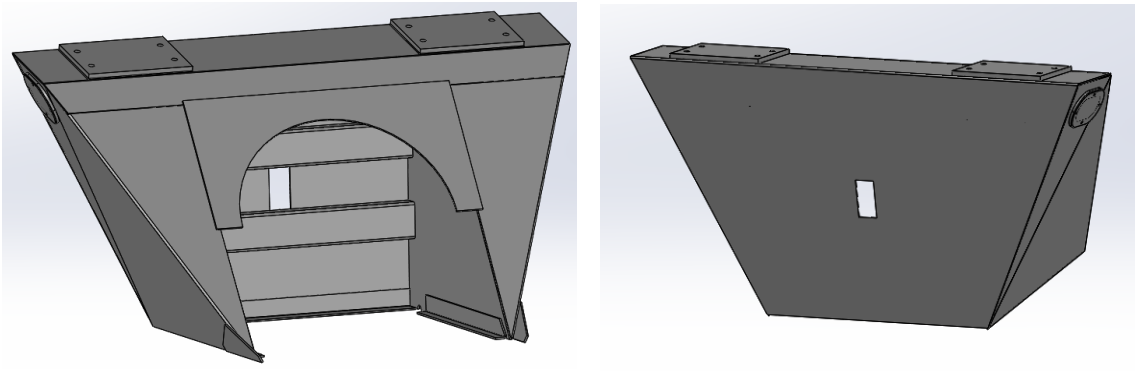

Figure 5-29 - Existing Rear Drum Support

The rectangular hole in the rear panel is for the hollow-section arm that supports the discharge chute. To strengthen this area, two C-profile sections are welded above and below the hole on the inside of the structure. There are also small strengthening plates underneath the two 10mm thick roller bearing pads. The front arch-shaped panel was not always a feature of this design. It was designed in response to cracks developing at the right angle corners that are now covered over by the panel.

The support is welded to the sub-frame legs along its full length. The angle sections on the inside are also welded to the sub-frame to help spread the load. These long weld passes along the sub-frame likely create large residual stresses. A small improvement would be to weld in short sections and allow cooling time between each weld.

The weight of the existing rear drum support for an $8m^3$ mixer is 152Kg.

5.2.2 FEA Load Cases for Rear Drum Support

As with the front support, the load cases were initially calculated using data from the literature. However, no changes were made after the dynamic testing. The calculated loadings were seen as fit for purpose. It was not clear from the dynamic testing whether the drum bounced on the rollers during the bump event, so there is a possibility that the full effect of these shock loadings has not been captured. There is therefore a small risk that

the calculated load cases provide non-conservative results. Four load cases were calculated for the rear support; a bump load (vertical), a lateral load, a chassis twist load, and a chute support arm load.

5.2.2.1 Vertical/Bump Load

With a full 8m^3 load on board, the static load supported by the rear drum support is:

$$Load\ at\ rear\ support = 90464.76N$$

See 5.1.2.2 for the calculation of the above load. As with the calculation of the bump load at the front support, the static load must be multiplied by 3 for a 2g load (the 2g acceleration does not account for 1g gravity):

$$90464.76 * 3 = 271394N$$

Divided by two for distribution between the two rollers:

$$\frac{271394}{2} = 135697N$$

The roller bearings themselves were excluded from the FEA study. The load was applied to the shaft holes in the base of the rollers at the precise angle at which the drum contacts the roller. This is illustrated by the black arrows below. The support was fixed at its base.

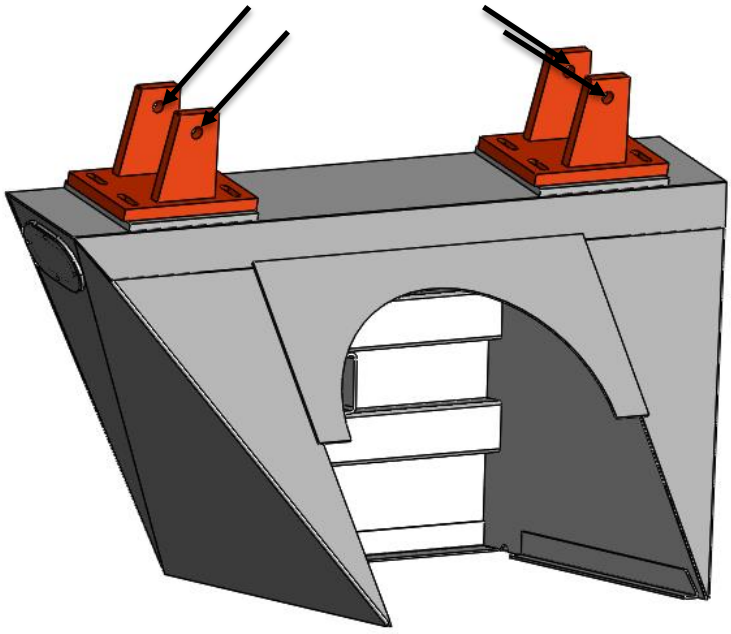

Figure 5-30 – Illustration of Vertical/Bump Load

5.2.2.2 Lateral Load

This lateral load simulates a static truck being tilted by 20°.

At an angle of 20°, the static force through the lower roller increases to 73000N, and the force through the upper roller decreases to 17465N. These forces were applied in the same way as the vertical/bump load.

5.2.2.3 Chassis Twist Load

The rear of a truck chassis does not tend to flex significantly. However, for the purpose of comparison between the existing and proposed rear supports, it was of interest to include this load case. For simplicity, no chassis sections have been included in this model. Sections of the sub-frame legs have been included.

An arbitrary forced displacement was used in this study. The two sub-frame sections were fixed at the rear. One front end was forced up by 5mm, the other forced down by 5mm as illustrated below.

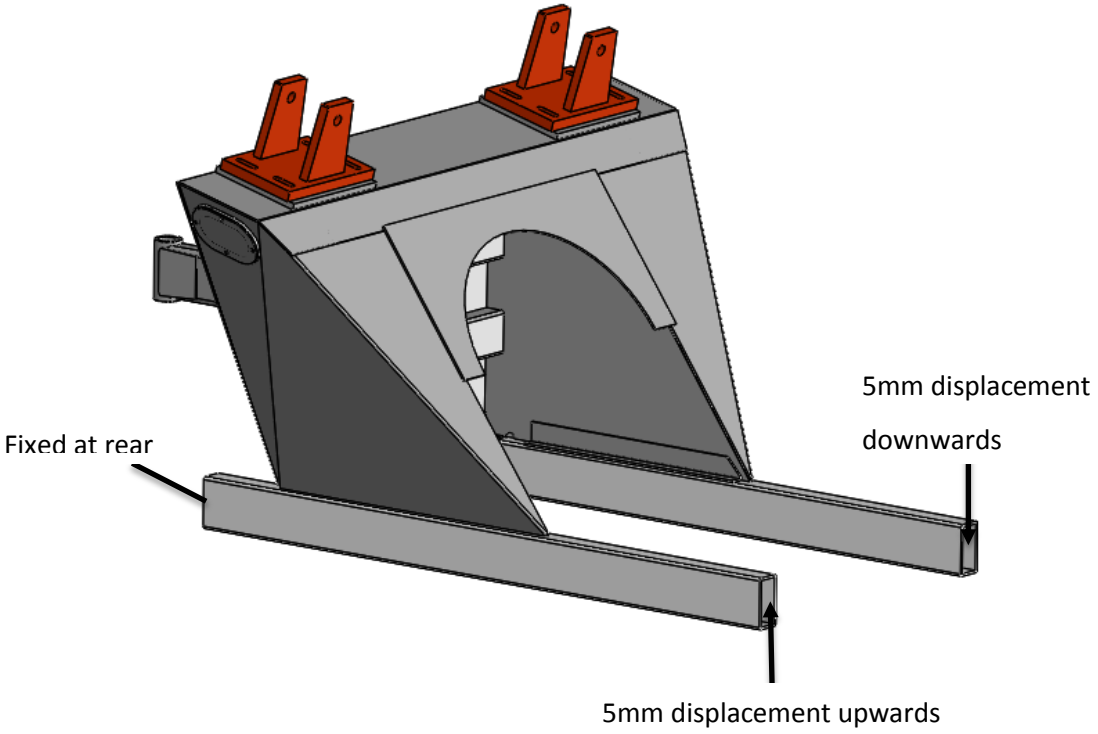

Figure 5-31 - Illustration of Twist Load

5.2.2.4 Chute Support Arm Load

Since this chute support arm could be affected by a redesign of the rear drum support, it was necessary to run an analysis and determine how much stress it generates in the support when the chutes are fully loaded. This load was calculated by finding the maximum volume of concrete that the discharge chute and its extension chutes could hold. The maximum possible load on this chute support arm was found to be 18462N. This can be considered conservative since it is highly unlikely that the chutes would ever fill to the brim during discharge.

This load was simply applied vertically on the end of the chute support arm. In reality a torque would be applied to the arm due to the way that the discharge chute is attached. The rear drum support was fixed at its base.

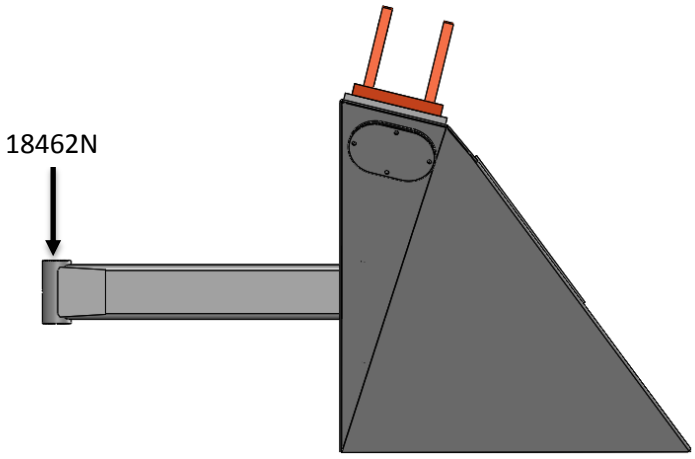

Figure 5-32 - Illustration of Chute Support Arm Load

5.2.3 FEA Results for Existing Rear Drum Support

As before, the results show Von-Mises stress with the scale set to a maximum of 355 to match the material yield strength. The colour scale in these plots is discrete rather than a smooth gradient. This can sometimes make it easier to see the load path through the structure. A solid mesh with parabolic tetrahedral elements was used. Some small modifications to the original model were required to improve the fitment of the individual parts. This rear support is sized for an $8m^3$ mixer.

Vertical/Bump Load

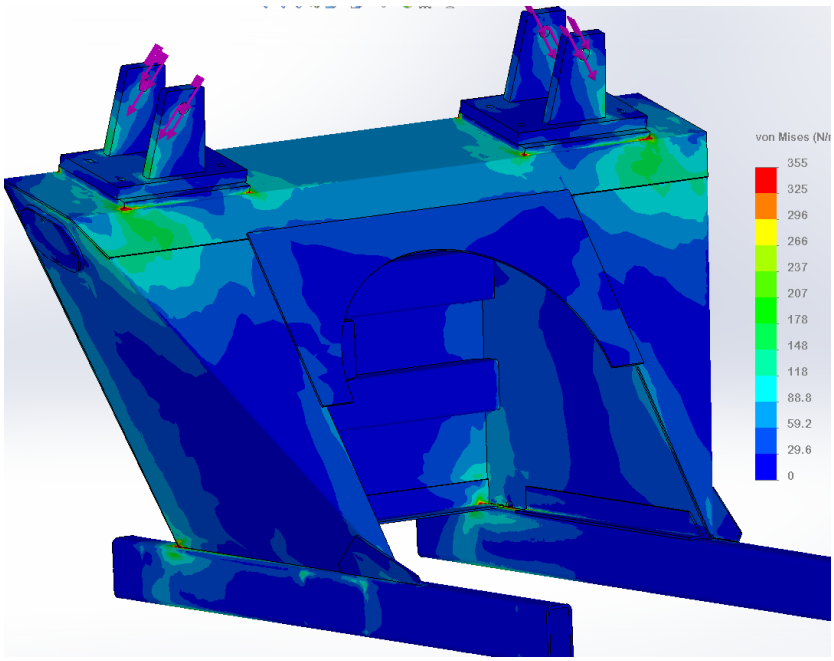

Figure 5-33 - Existing Rear Support - Vertical Load - 1

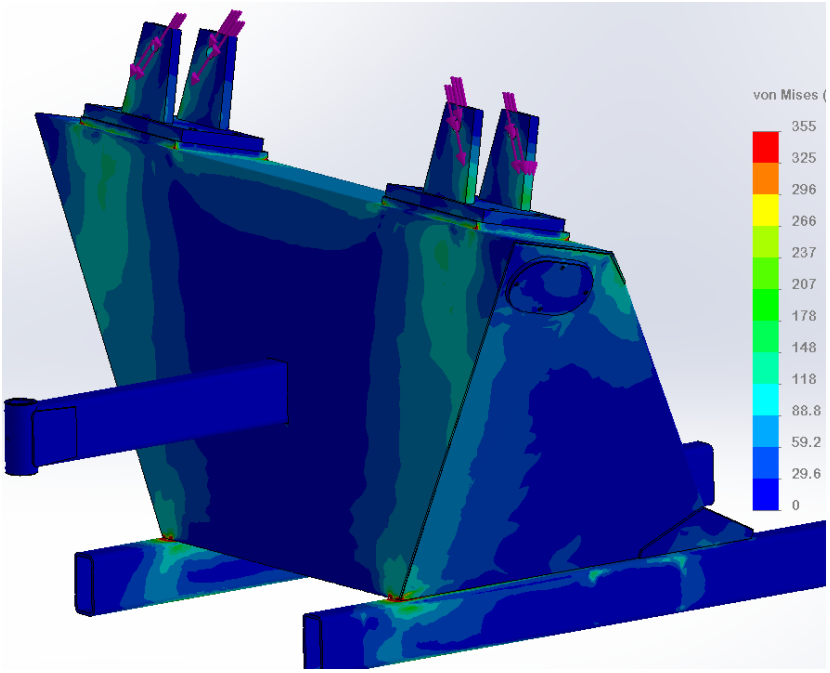

Figure 5-34 - Existing Rear Support - Vertical Load - 2

Lateral Load

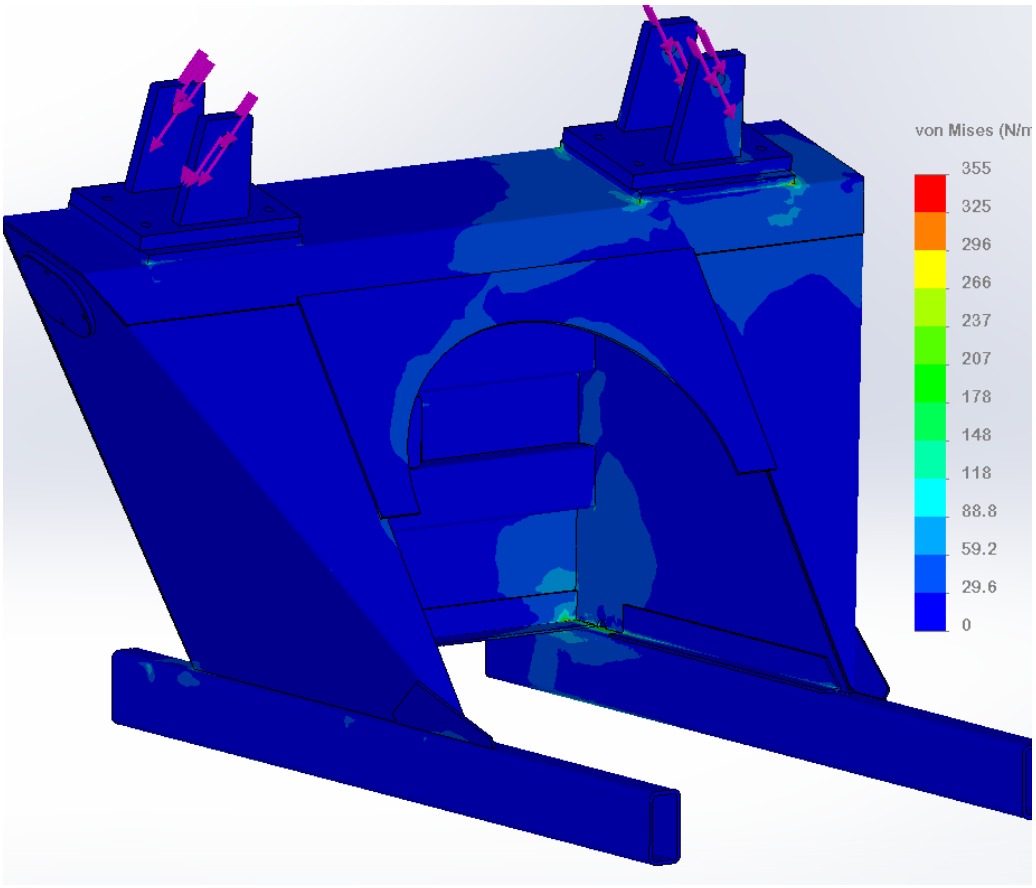

Figure 5-36 - Existing Rear Support - Lateral Load - 1

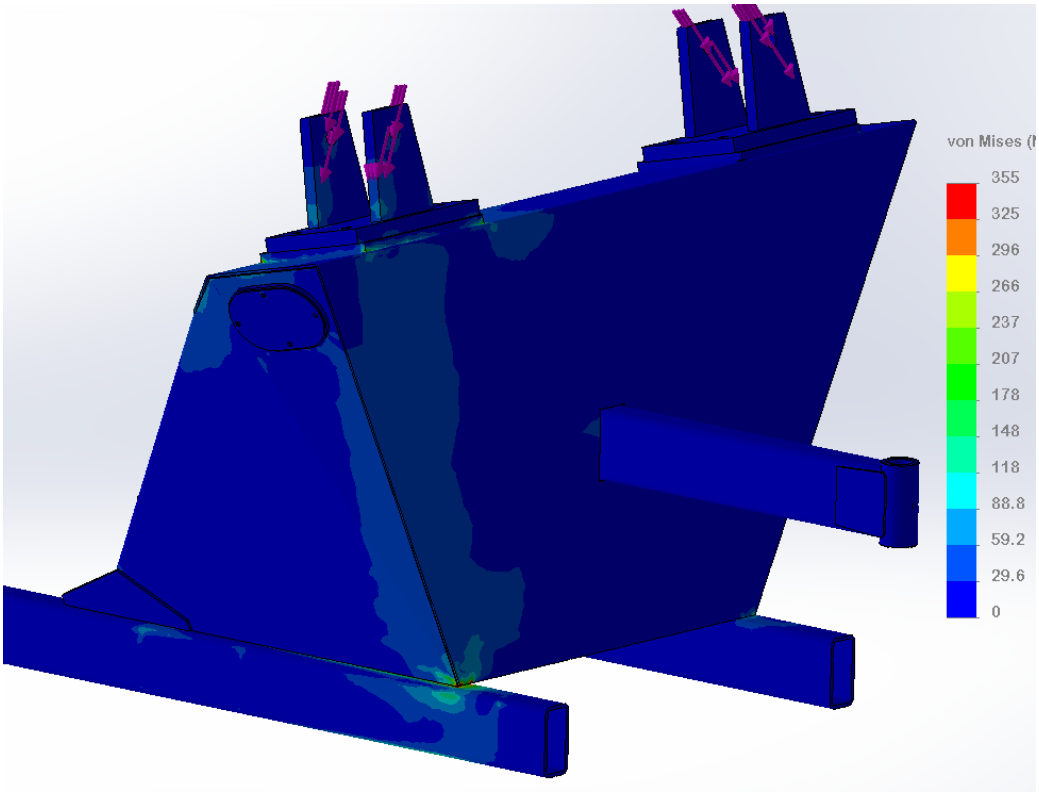

Figure 5-35 - Existing Rear Support - Lateral Load - 2

Chassis Twist Load

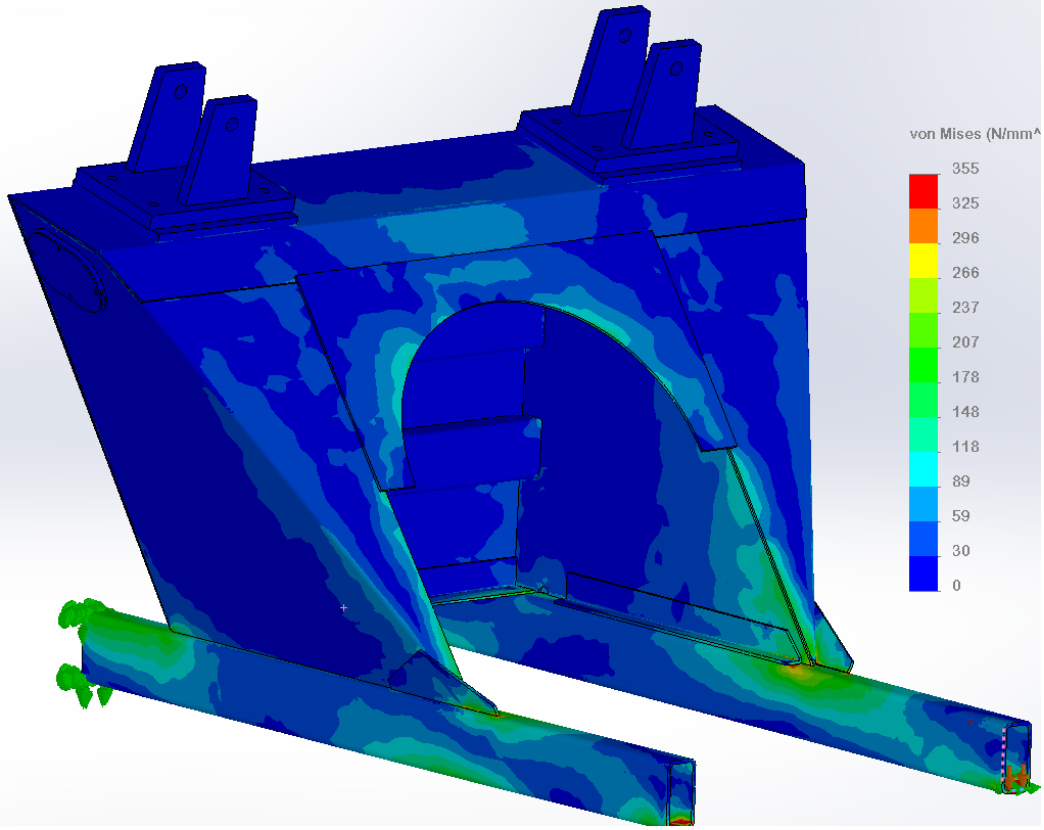

Figure 5-38 - Existing Rear Support - Twist Load - 1

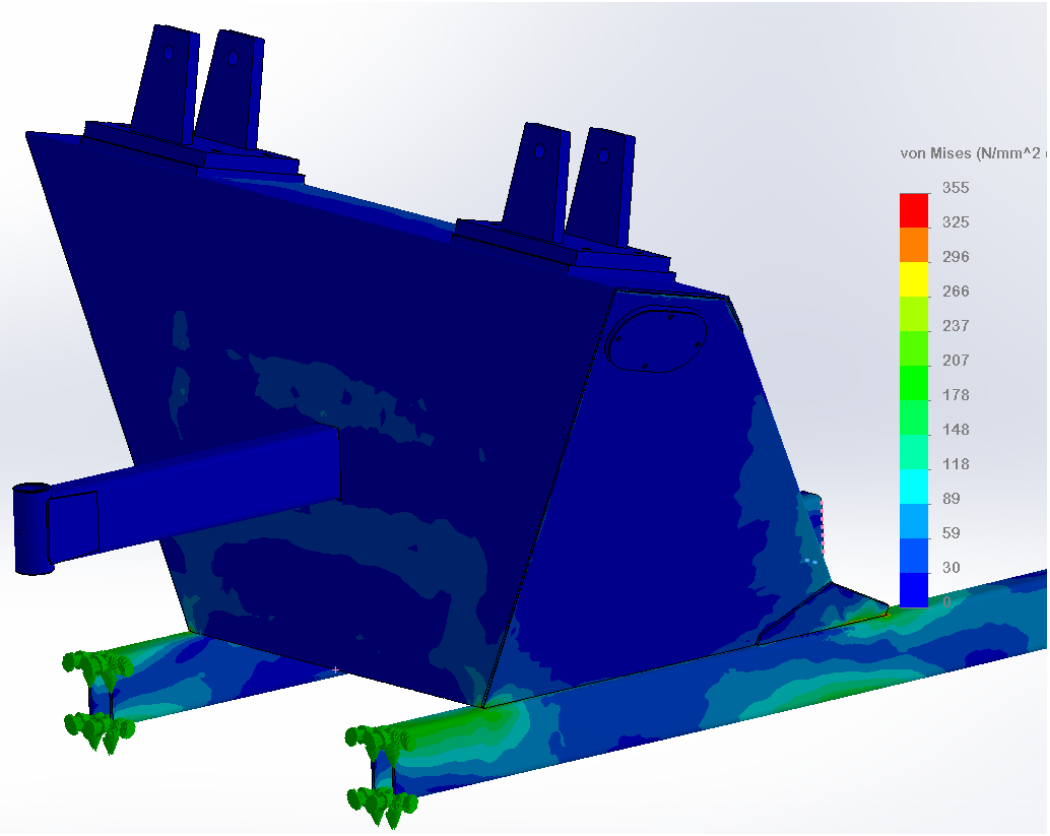

Figure 5-37 - Existing Rear Support - Twist Load - 2

Chute Support Arm Load

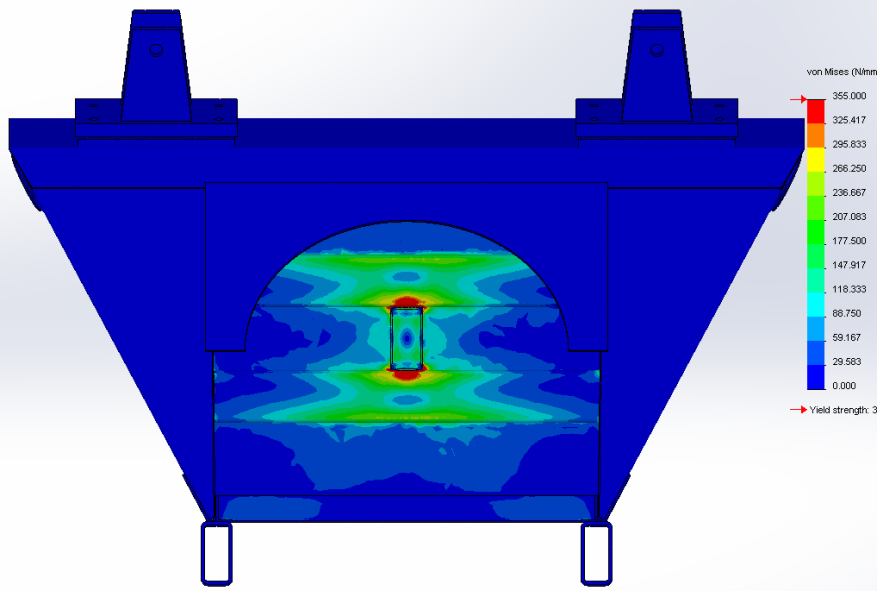

Figure 5-39 - Existing Rear Support - Chute Support Arm Load – 1

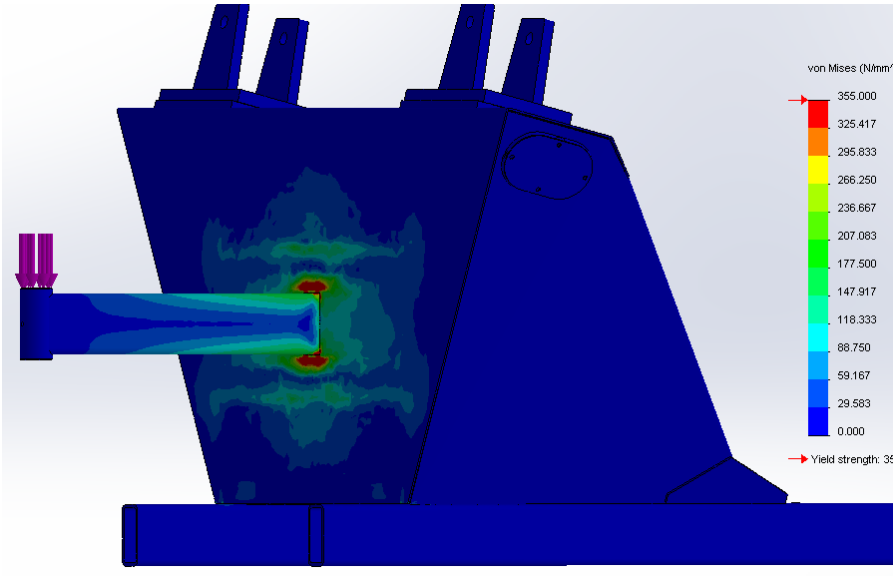

Figure 5-40 - Existing Rear Support - Chute Support Arm Load - 2

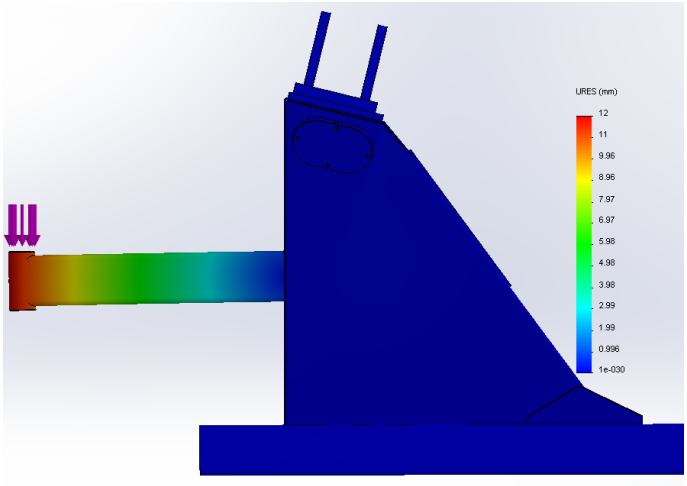

Figure 5-41 - Existing Rear Support - Chute Support Arm Load - 3 (Displacement)

5.2.3.1 Discussion of Results

A small area of high stress develops at a corner of the base of the roller bearings for the vertical loading. No failures have been known to occur in this area so this is not of great concern. Of more concern is the moderate stress in the sub-frame at the rear of the support. Given the lack of any post-weld treatments applied to this area it is thought that failures here are more likely due to poor weld geometry than moderate stress. Weld treatment here is particularly recommended for the trucks that are known to have stiffer than average rear suspension.

There are no areas of concern with the lateral loading. The arbitrary twist load suggests an acceptable interaction with the sub-frame, however the true extent of twist in this region of the chassis is unknown. Excessive stress occurs at the chute support arm's connection to the rear support. The end of the arm displaces 12mm. Although no common failures have been recognised for this particular part of the support arm, improvements here would be advisable.

5.2.4 Design of Proposed Rear Drum Support

A number of restrictions with this structure meant that it was not productive to drastically change its design. Other types of structural members were initially considered for this design such as beams, however a benefit analysis proved the original sheet metal method to be the most effective. Looking at the shape of the structure and the various parts that attach to it, it was clear that drastically changing the overall shape would require the re-design of numerous additional parts. Considering these findings, and that the current design already has good manufacturability, it was concluded that an optimisation approach should be used on this structure rather than one of total redesign.

The rear end of a concrete mixer suffers particularly badly from corrosion. It is naturally a harsh environment. Therefore it is not advisable to use thin sheet metal in this region. Considering the current level of paint protection, thicknesses of 3mm and under are at risk of corroding excessively within the lifespan of the mixer. For this reason the thickness of the panels on the proposed rear support remains 4mm. Weight reduction has been achieved by creating cut-outs in the structure. The small strengthening plates inside the structure underneath the roller bearing pads have been reduced from 5mm to 3mm and extended in length to spread the load. The two horizontal c-profile beams for the chute support arm have been replaced by a single vertical beam. This arrangement increases

stiffness and allows for large cut-outs in the rear panel. The front arch-shaped panel could have been reduced in thickness from 5mm to 4mm, however the mixer manufacturer desired to leave this panel unchanged. With the cut-outs in the side panels it was necessary to design a 'blanking plate' to fit in the gap at the bottom to prevent water from gathering inside. The shape of the cut-out in the side panel was restricted by the existence of a slight bend in the panel (viewable just to the left of the cut-out in Figure 5-43).

This proposed rear support for an $8m^3$ mixer weighs 112Kg – a 26% reduction.

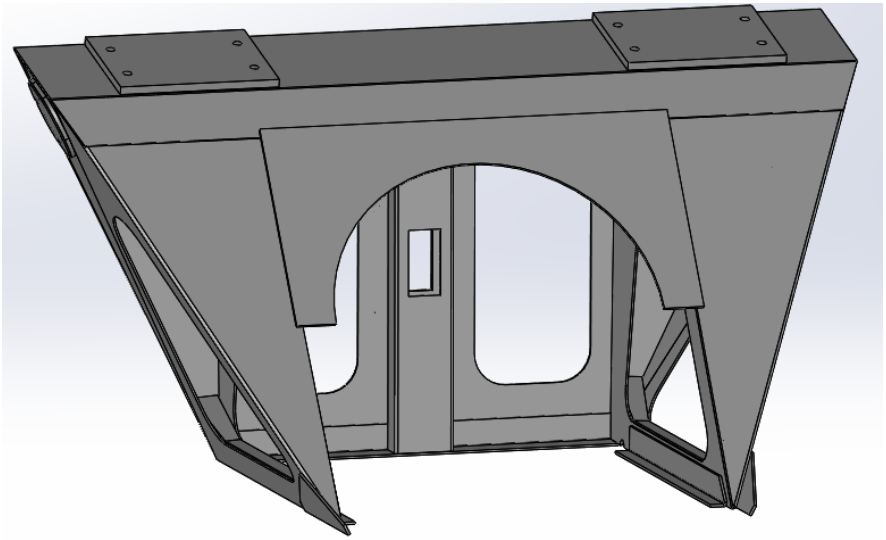

Figure 5-42 - Proposed Rear Drum Support Design - Front

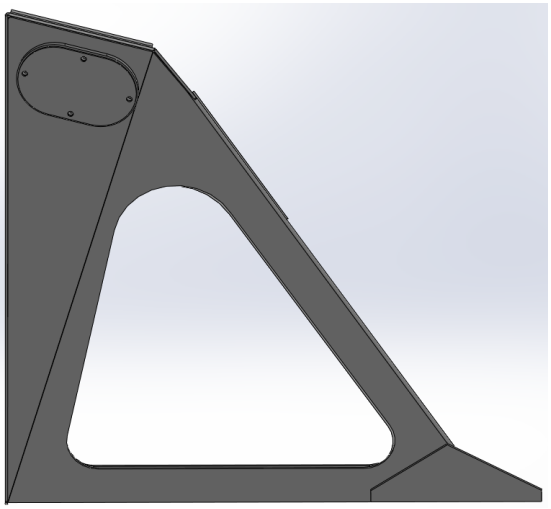

Figure 5-43 - Proposed Rear Drum Support Design - Side

5.2.5 FEA Results for Proposed Rear Drum Support

The same study and mesh parameters were used as with the analysis of the existing support.

Vertical/Bump Load

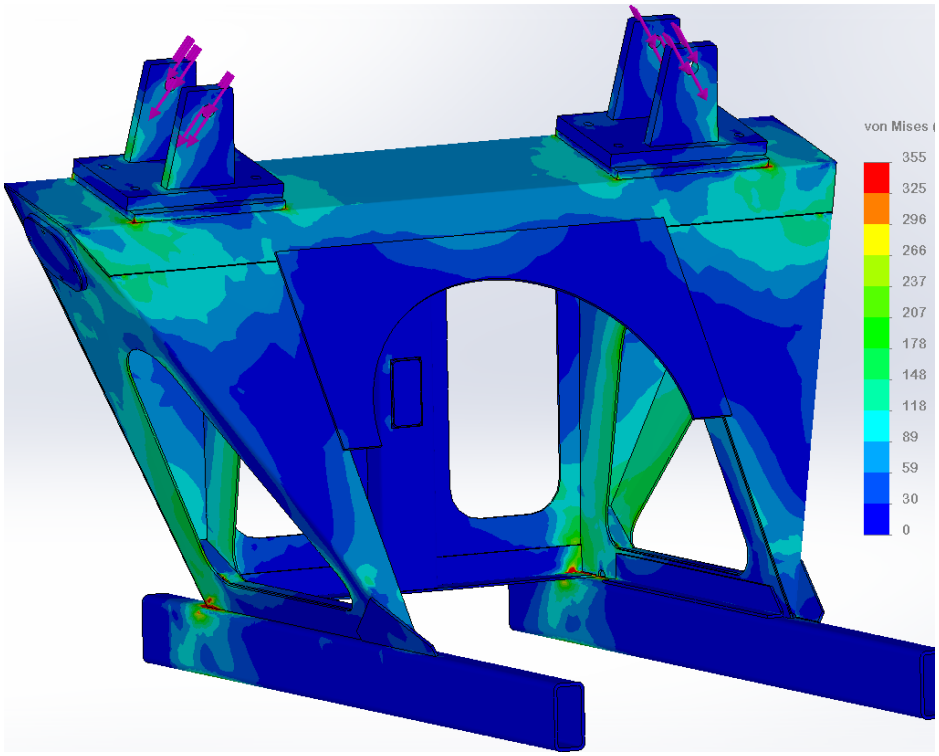

Figure 5-44 - Proposed Rear Support - Vertical Load - 1

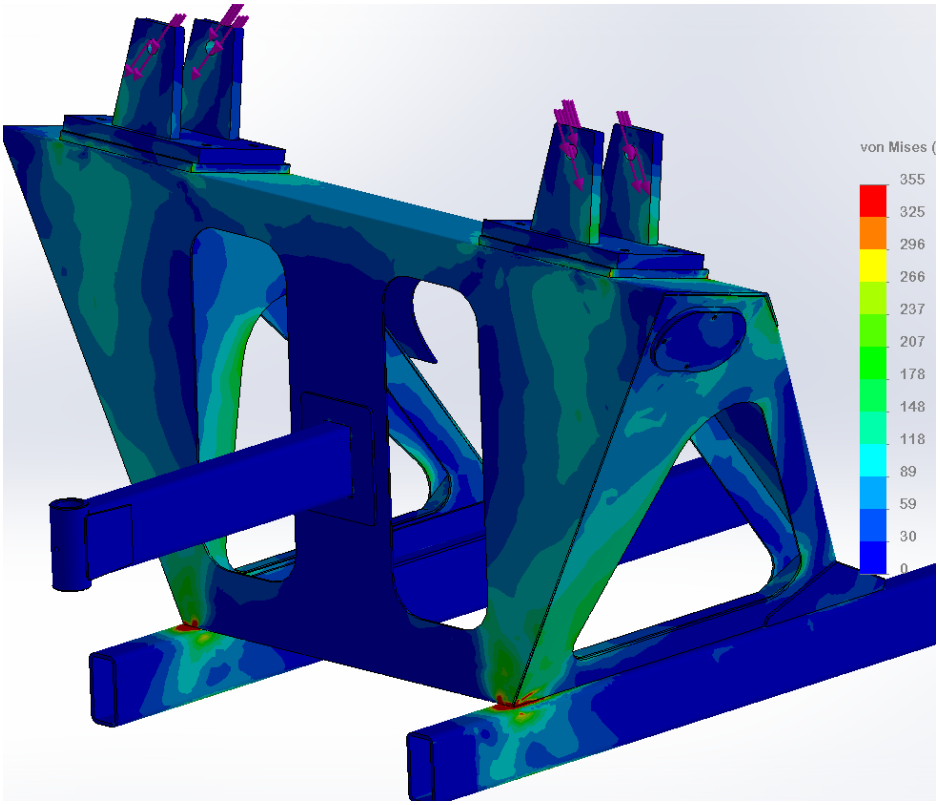

Figure 5-45 - Proposed Rear Support - Vertical Load - 2

Lateral Load

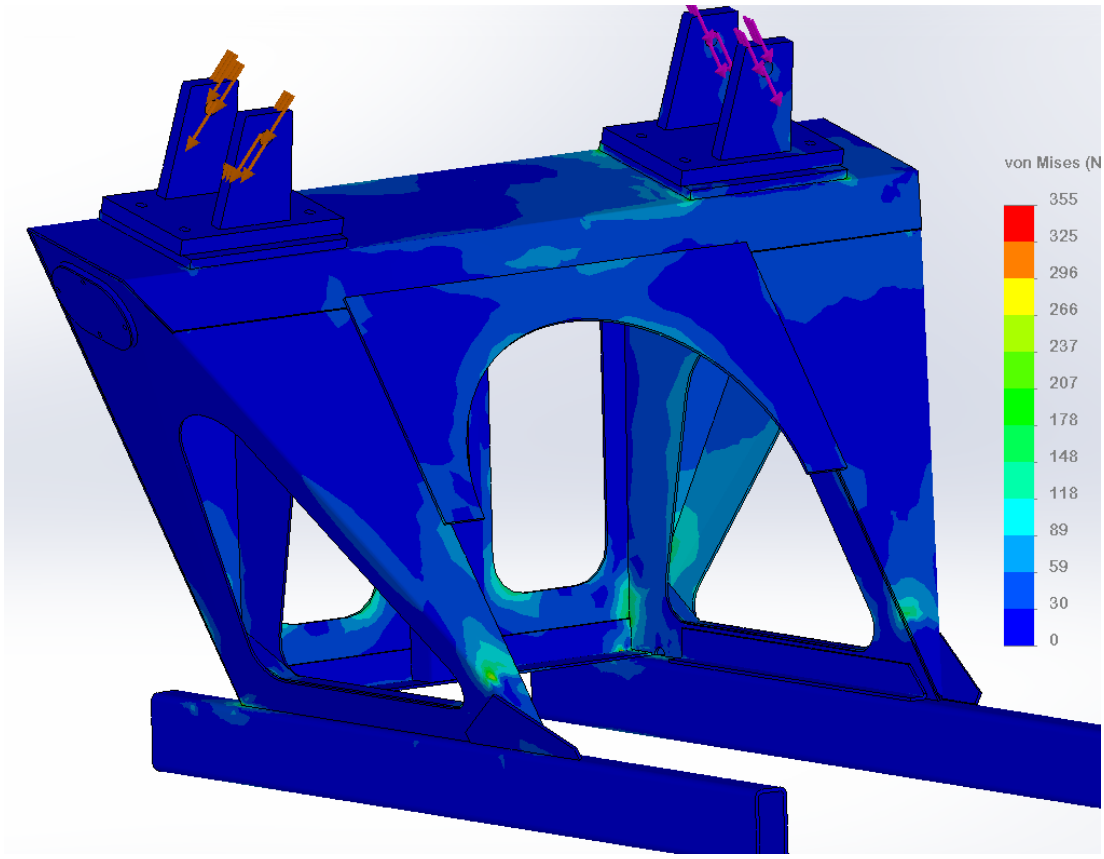

Figure 5-47 - Proposed Rear Support - Lateral Load - 1

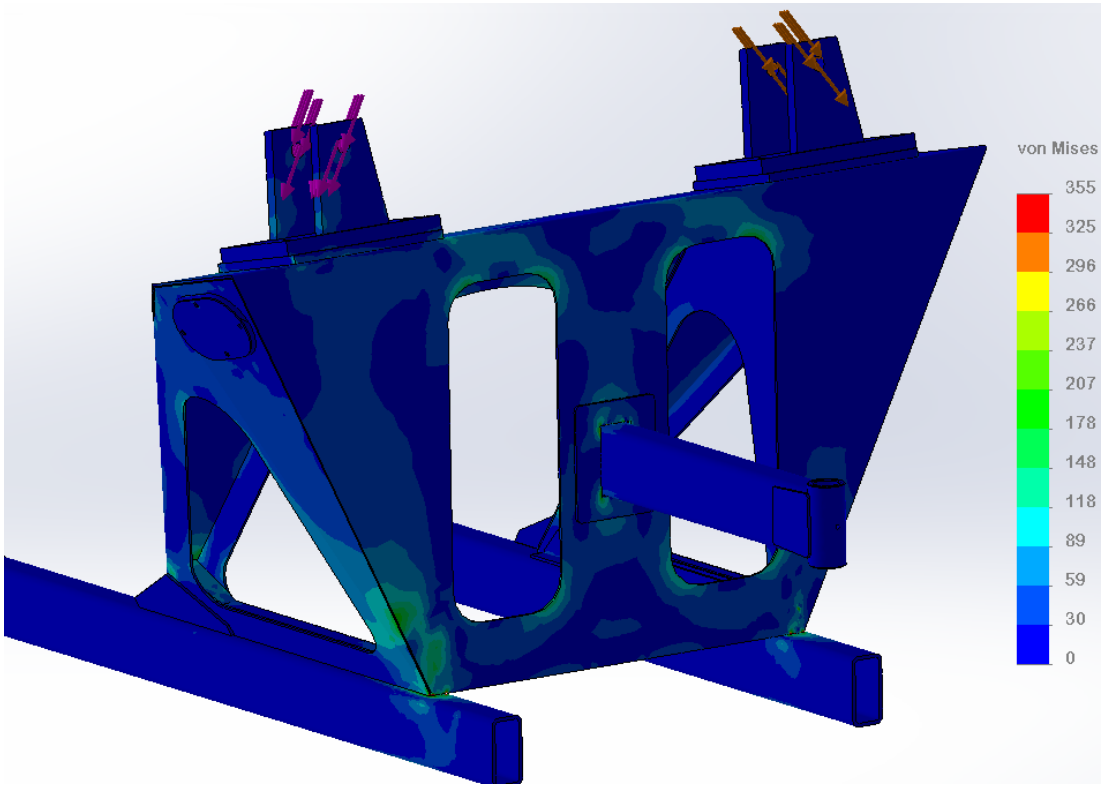

Figure 5-46 - Proposed Rear Support - Lateral Load - 2

Chassis Twist Load

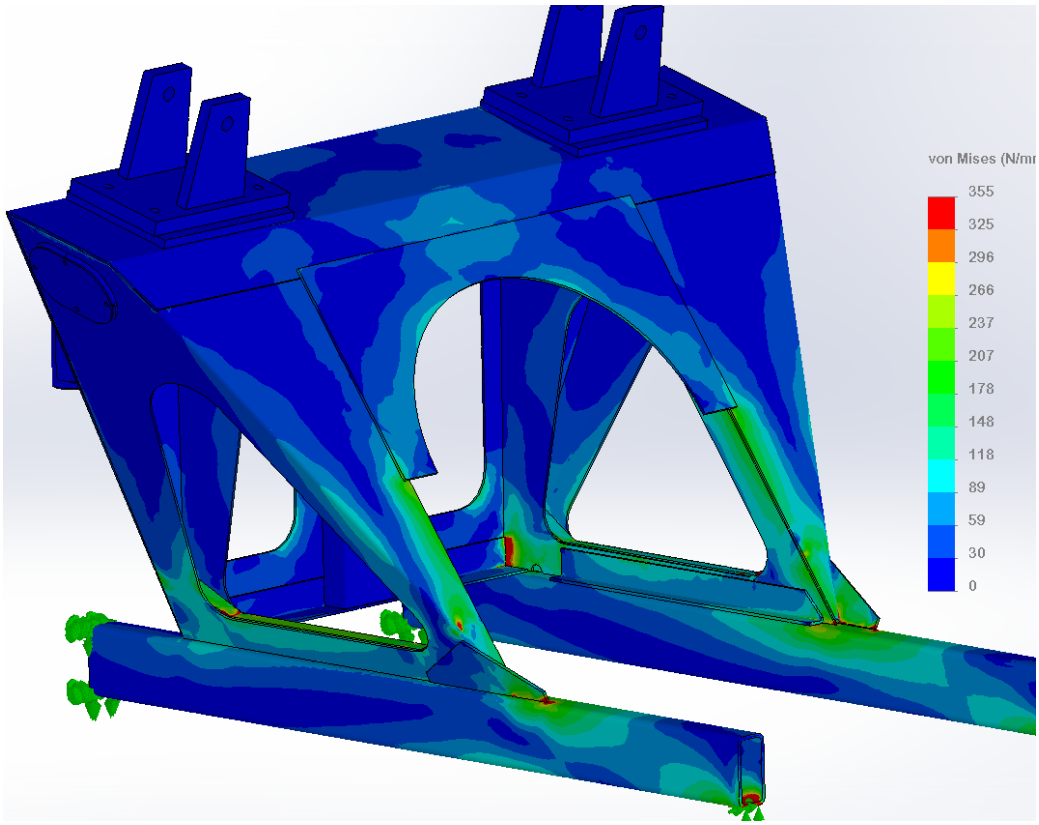

Figure 5-49 - Proposed Rear Support - Twist Load - 1

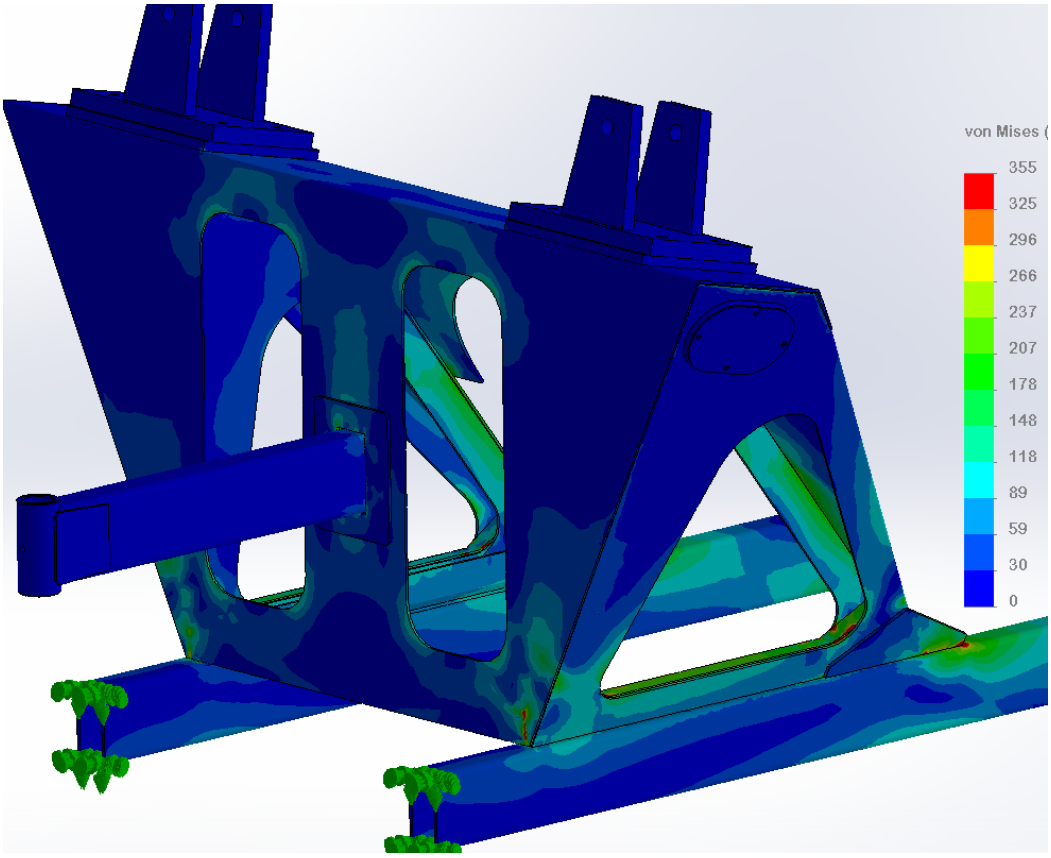

Figure 5-48 - Proposed Rear Support - Twist Load - 2

Chute Support Arm Load

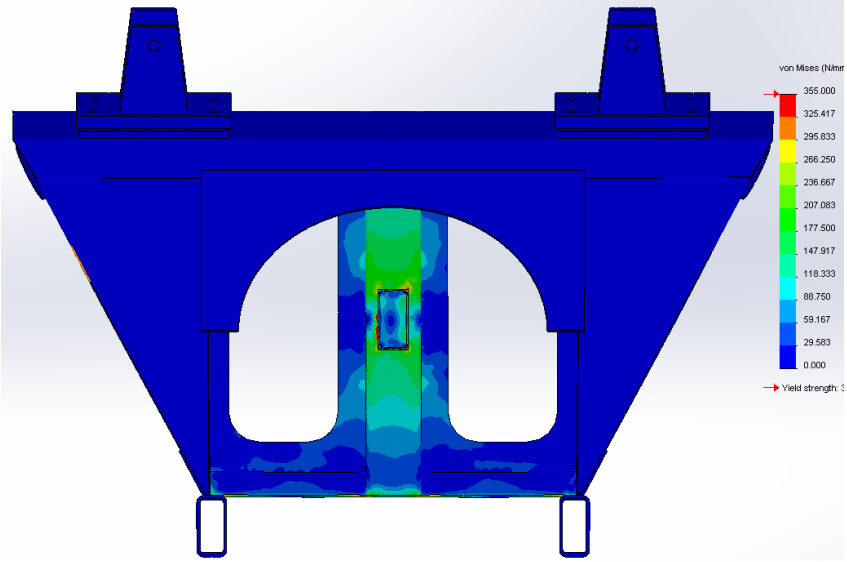

Figure 5-50 - Proposed Rear Support - Chute Support Arm Load - 1

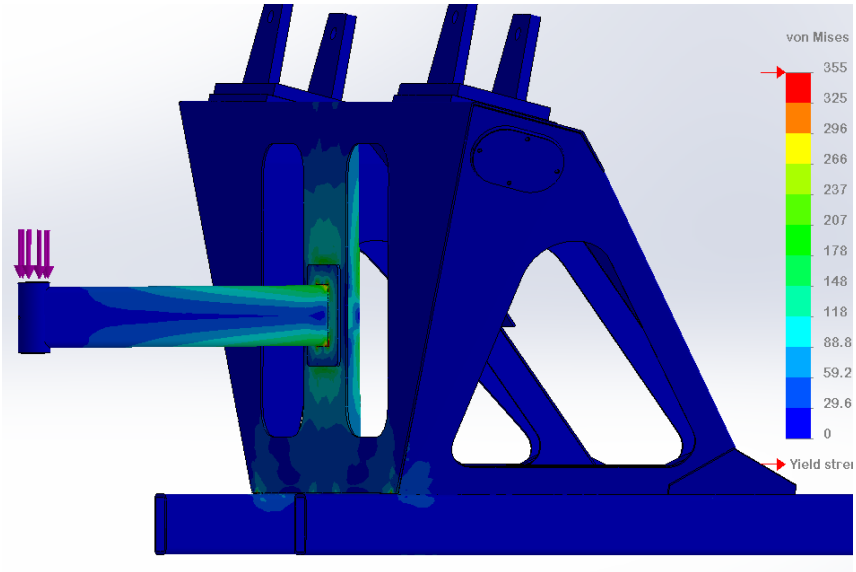

Figure 5-51 - Proposed Rear Support - Chute Support Arm Load - 2

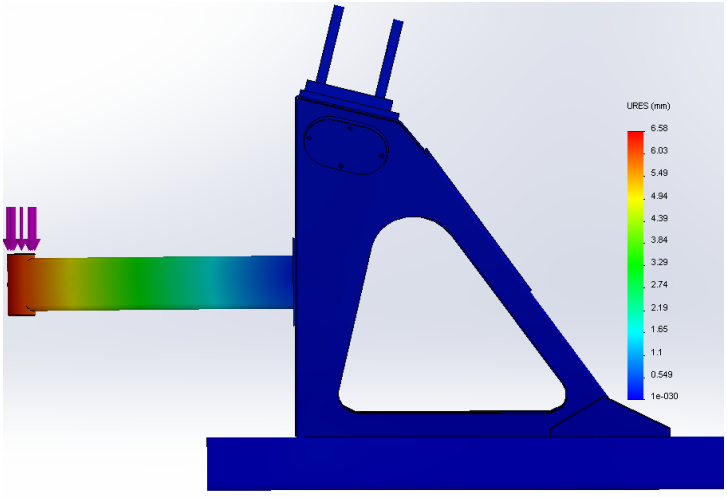

Figure 5-52 - Proposed Rear Support - Chute Support Arm Load - 3

5.2.5.1 Discussion of Results

The stress in the sub-frame at the rear of the proposed support is slightly greater for the vertical/bump load than with the existing support. Although not shown here, a plate was added to the side of the rear support to help spread the load. As mentioned before the more significant issue with this area is the lack of weld treatment. Smoothing the weld toe here will significantly improve fatigue life. The proposed support experiences higher stresses for the twist load than the existing support. The load path through the sub-frame also changes with higher stress going into the sub-frame at the front right of the support (offside), but lower stress going into the sub-frame at the rear right. The lateral load shows no areas of concern.

The chute support arm displaces far less with this vertical brace design – 6.6mm vs. 12mm for the existing design. The stress at the connection to the rear support is greatly reduced. Note the addition of a small plate surrounding the arm on the rear surface of the support. This plate helps to spread the load.

It could not be confirmed whether the dynamic testing in Chapter 3 captured the effects of the drum bouncing on the rollers. If the full extent of this has not been captured then the vertical/bump load could be underestimated. In hindsight, to ensure that no problems arise in future, it may have been beneficial to investigate a total redesign of the way the rear support attaches to the sub-frame. At the time of design, the speed and convenience of the existing welded attachment made it desirable. To combat residual stress, the existing welded attachment should be welded in small sections with cooling time allowed between welds. The possibility of adding shock absorption pads underneath the base of the rollers should also be investigated.

5.3 Sub-frame and Chassis Interaction

The sub-frame must be designed to interact effectively with both the drum supports and the chassis. DAF and Mercedes-Benz recommend that rigid connectors should be used on the sub-frame of a concrete mixer. Scania, Volvo, Renault, and MAN recommend that longitudinally flexible brackets should be used towards the front of the sub-frame. It was theorized that rigid brackets may reduce the stress in the sub-frame at the front drum support, due to the decreased flexibility of the sub-frame. This would be at the expense of increased stress at the connectors and potentially reduced ride comfort. A study has been performed to determine the differences between using flexible or rigid brackets. Two additional small scale studies have also been performed. The first of these demonstrates the potential reduction of stress by using U-profile channels for the sub-frame legs rather than RHS. The second study aims to determine whether the weld design of the Mercedes bracket reduces stress in comparison to the company's existing weld design.

5.3.1 Flexible Connectors versus Rigid Connectors

The frontal section of the sub-frame has been used in this study and is attached to a simplified chassis model. Forces have been applied to twist the chassis in the same way as with the front support analysis in section 5.1.2.2. To reduce the occurrence of stress singularities, the triangular gussets at the front of the front drum support have been modified so that they sit flush with the sub-frame. This study is purely for comparison purposes so the exact stress values are not of interest. This being a large computationally intensive analysis, issues developed when trying to use high quality elements. The analysis was therefore run with first-order tetrahedral elements, with the chassis cross-members using shell elements.

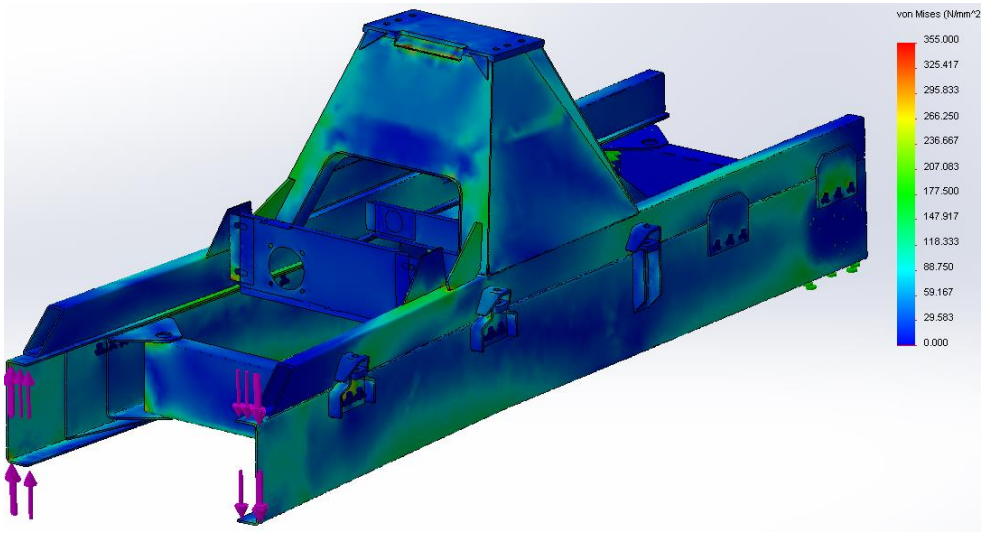

Figure 5-53 - Longitudinally Flexible Brackets - Chassis Twist

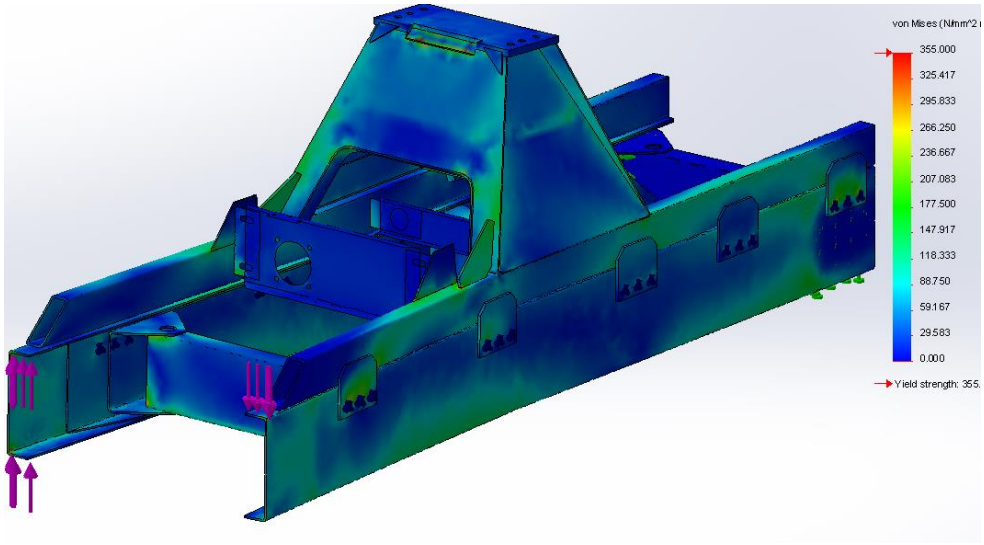

Figure 5-54 - Rigid Brackets - Chassis Twist

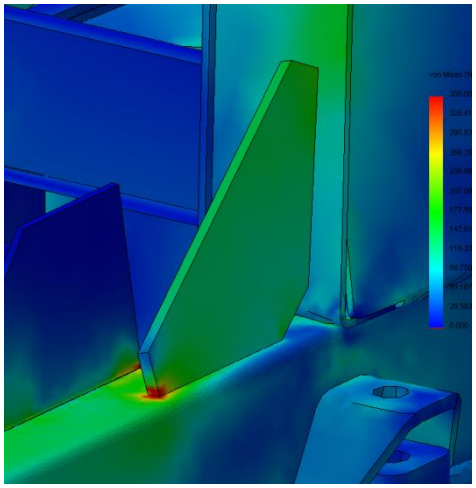

Figure 5-55 - Nearside Close-up - Flexible Brackets

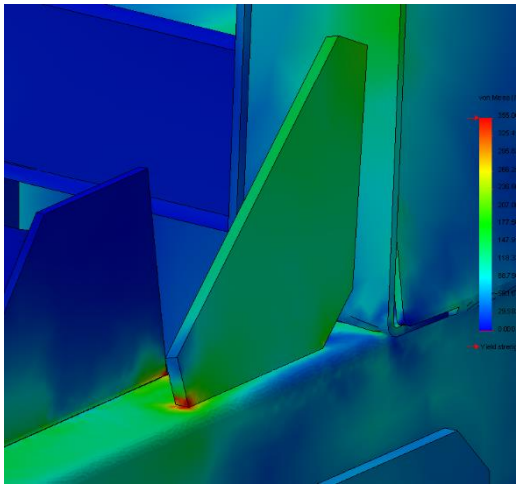

Figure 5-56 - Nearside Close-up - Rigid Brackets

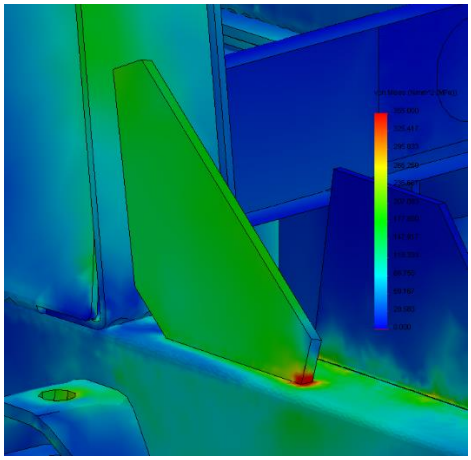

Figure 5-57 - Offside Close-up - Flexible Brackets

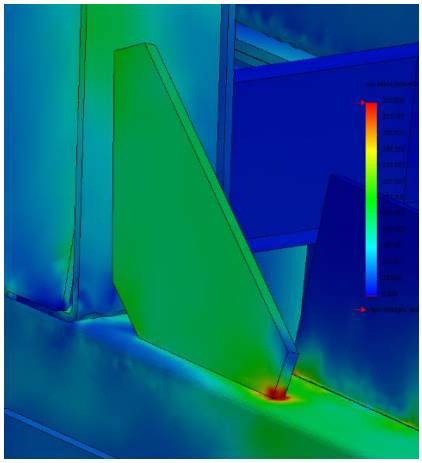

Figure 5-58 - Offside Close-up - Rigid Brackets

Table 5-2 - Stress and Displacement Comparison - Flexible vs. Rigid

	Flexible Brackets	Rigid Brackets
Max Displacement (mm)	20	18
Max Stress at Gusset – Offside (MPa)	470	451
Max Stress at Gusset –Nearside (MPa)	484	439

As stated before the stress values themselves are not relevant. However the differences between them reflect the reduced displacement of the rigid bracket arrangement. Whether this reduced displacement is of much benefit depends on the design of the structure. For the existing front support design (as above) it would help reduce the stress concentration at the front support gussets. However a greater reduction in displacement and stress would be achieved by using a larger hollow-section for the sub-frame legs. To conclude, no significant reason has been found for the differences in attachment recommendations between the various truck manufacturers.

5.3.2 U-Profile versus Rectangular Hollow Section

Truck manufacturers generally recommend that U-profile channels should be used for sub-frame legs. The existing design of this concrete mixer manufacturer uses Rectangular Hollow Section (RHS). The torsional flexibility of a U-profile channel can lead to reduced stress in the sub-frame connections, as demonstrated by the simple study below whereby the visible end of this short section of chassis was forced downwards by 3mm. A longitudinally flexible bracket has been used at the front end. “Pin” connectors have been used in the bolt holes as a simple means of connecting the brackets to the chassis.

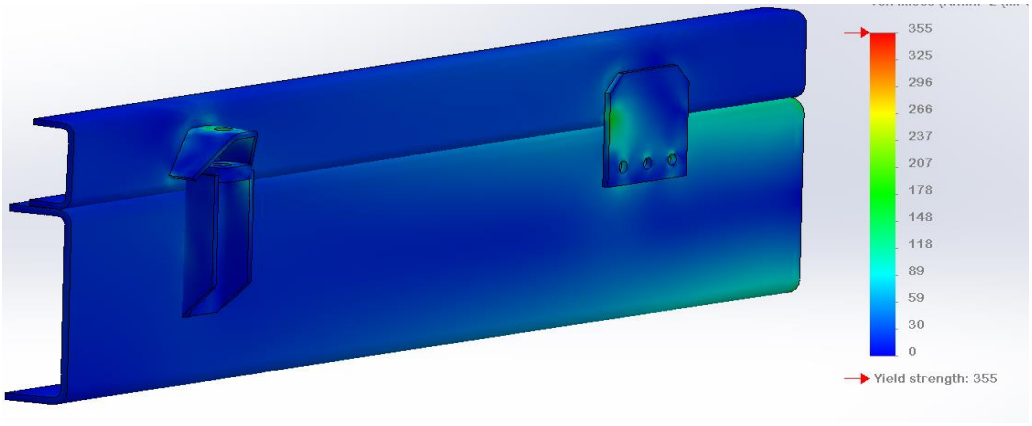

Figure 5-59 - U-Profile Stress Demonstration

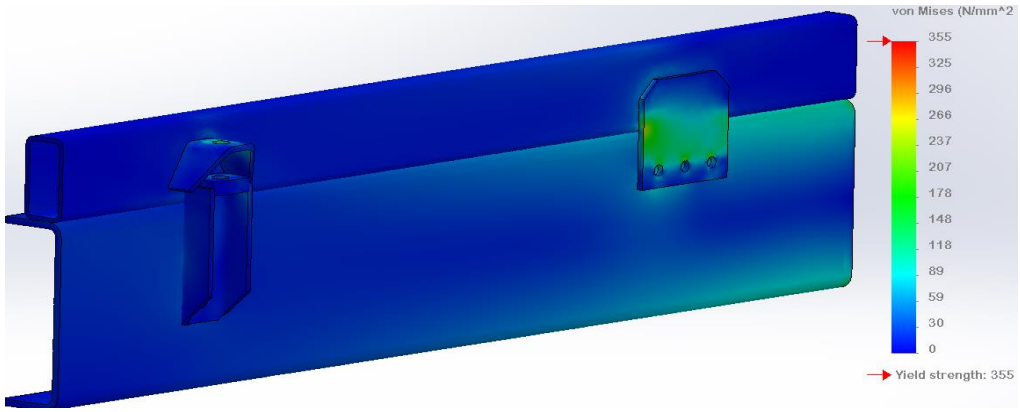

Figure 5-60 - RHS Stress Demonstration

However, it is also generally recommended by the truck manufacturers that these U-profile channels have an extra web welded in to turn them into hollow sections from the region of the front drum support to the rear end. Therefore the flexural benefits are only felt in the frontal section of the sub-frame. From the analyses performed thus far, there has been no evidence to suggest that using RHS for the entire length of the sub-frame over-stresses any of the connections. Hence the existing sub-frame design has not been changed.

5.3.3 Advantages of Mercedes-Benz Recommended Welding Technique

Traditionally, rigid attachments installed by this mixer manufacturer have been rectangular shaped plates that are welded as illustrated below on the left. The Mercedes plate and welding technique is illustrated on the right.

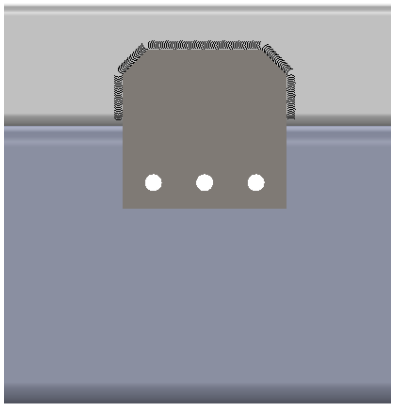

Figure 5-61 - Traditional Plate & Weld Design

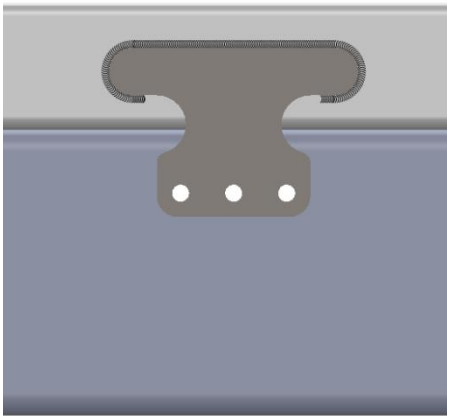

Figure 5-62 - Mercedes Plate & Weld Design

A simple analysis has been performed to determine whether the Mercedes weld design significantly reduces stress. A short section of one side of the sub-frame and chassis has been used in this study. This is not a totally realistic scenario, however it does provide a suitable basis for comparison. A longitudinally flexible bracket has been used at the front end.

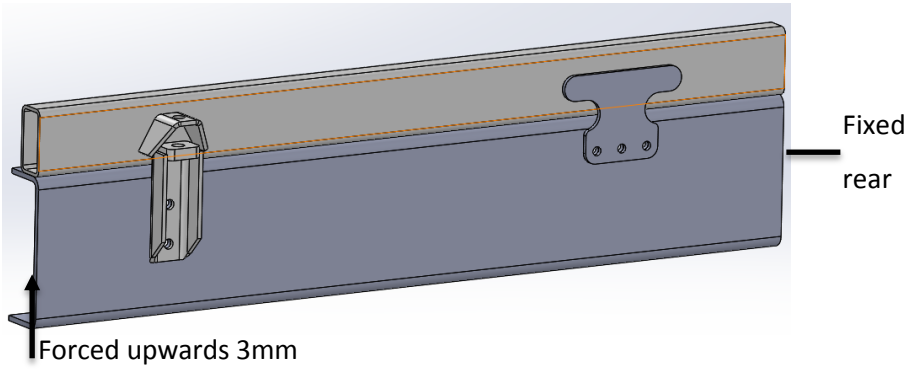

Figure 5-63 - Illustration of Applied Load for Bracket Test

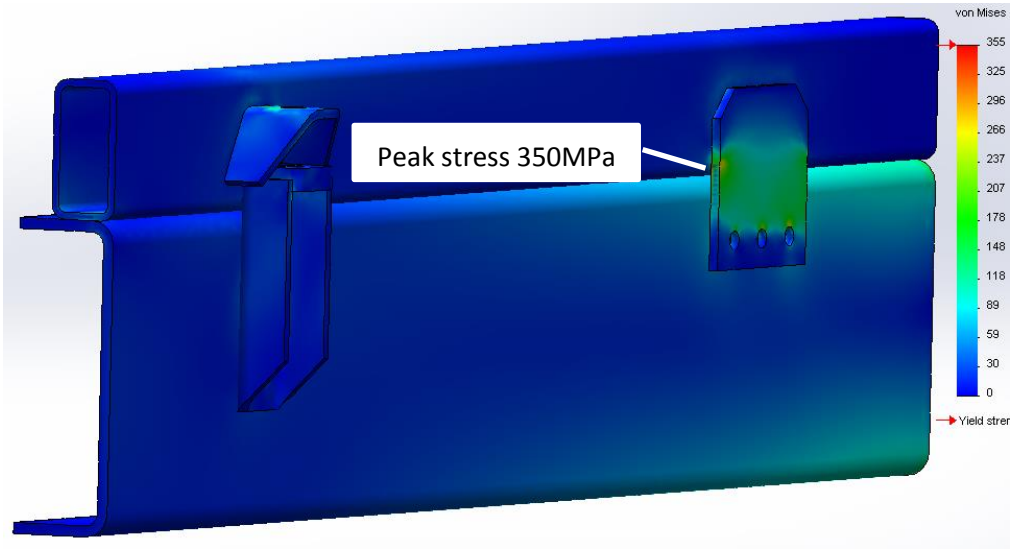

Figure 5-64 - Existing Bracket and Weld Design - Von-Mises Stress

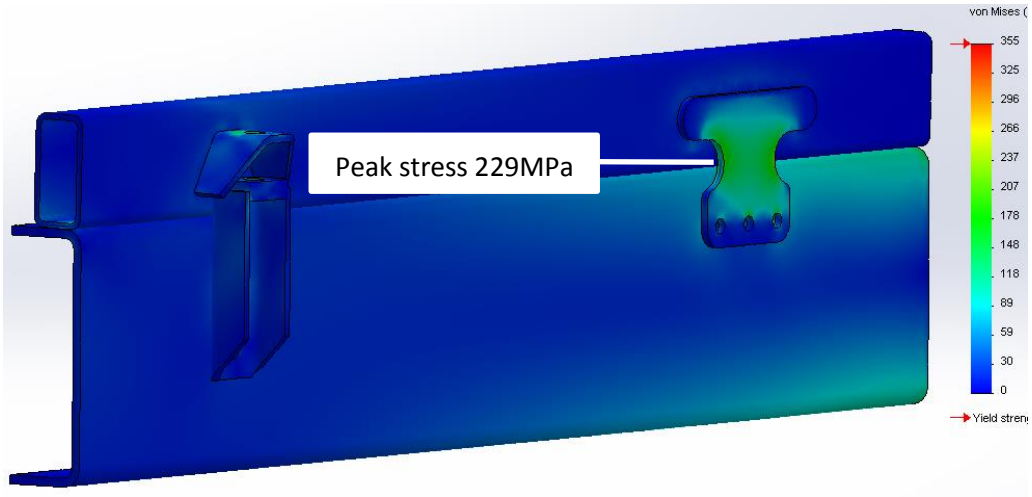

Figure 5-65 - Mercedes Brackets and Weld Design - Von-Mises Stress

Although this simplified geometry (no weld model present) is prone to creating stress singularities, there is a clear difference in peak stress. However, the most important finding from this is that the region of peak stress does not occur at the end of the weld on the Mercedes bracket. This design should therefore deliver a longer fatigue life.

6. Summary and Future Work

This research has progressed the understanding of the structural design of concrete mixers. The strains experienced by a concrete mixer during normal use have been captured. Improved designs for the front and rear drum support structures have been developed for a particular mixer manufacturer. There is scope for further weight reduction through continued redevelopment of the drum support structures and of the many other significant parts that have not been assessed in this work. However, for a relatively small manufacturer the limit of feasibility is quickly reached, i.e. structures can easily become too expensive and/or time consuming to manufacture.

In order to develop the front drum support further, it is recommended that a dynamic test similar to that in section 3.1 should be performed. In the test presented, not enough strain gauges were attached to the front support to fully understand the load paths. Future work here should focus on determining the load paths through the front support by using a large number of strain gauges positioned symmetrically on both sides. Alternative bolting methods that improve manufacturability could also be investigated.

For the rear drum support, alternative attachment designs should be considered for the purpose of spreading the load more effectively and reducing the welding effort. Shock absorption pads should also be considered for use underneath the base of the rollers.

The large scale sub-frame and chassis interaction analyses presented in this thesis were completed using low quality elements. Future work should use high quality elements to continue investigating the design of the sub-frame and its connections. The true extent of chassis twist should also be measured to allow accurate analysis.

The Design by Analysis process has proven effective in this application. The reduced weight of the concrete mixer increases the profit achievable by companies involved in the transport of concrete. Similar SME's should consider implementing this process; however the capabilities of FEA must be fully understood before making a business case.

Bibliography

Adams, V. (2006) *How to Manage Finite Element Analysis in the Design Process.* East Kilbride, UK: NAFEMS Ltd.

Anonymous (2007) *Heavy Single-Unit Truck Original Equipment and Aftermarket Brake Performance Characterization in Field, Test-Track, and Laboratory Environments* US Department of Transportation: National Highway Traffic Safety Administration.

Anonymous (2010) *Final Report on Jerkling - An Energy Saving Speed Bump.* Massachusetts Institute of Technology.

Aurell, J. (2013) '*Dynamics of Heavy Commercial Vehicles and Buses*'. *Road and Off-Road Vehicle System Dynamics Handbook.* London: CRC Press.

Billingham, J., Sharp, J.V., Spurrier, J. & Kilgallon, P.J. (2003) *Review of The Performance of High Strength Steels Used Offshore.* Cranfield University: Health and Safety Executive.

Birch, K. (2001) *Truck Braking Systems and Stopping Distances.* Royal Society for the Prevention of Accidents. Available at: http://www.ukmotorists.com/hgv%20braking%20distances.asp.

Collin, P., Moller, M., Nilsson, M. & Tornblom, S. (2007) *Undermatching Butt Welds in High Strength Steel.* International Association for Bridge and Structural Engineering.

Costa, J.D.M., Ferreira, J.A.M. & Abreu, L.P.M. (2010) *Fatigue Behaviour of Butt Welded Joints in a High Strength Steel.* Elsevier Ltd.

Dunn, A. & Hoover, R. (2004) *Class 8 Truck Tractor Braking Performance Improvement Study.* East Liberty, OH: National Highway Traffic Safety Institution, Vehicle Research and Test Centre.

Eckerlid, J., Asell, M. & Ohlsson, A. (Date unknown) *Use of Vanadium High-Strength Low-Alloy Steels in Trailers.* Borlange, Sweden: SSAB (Research sponsored by: Army Research Laboratory).

Fui, T.H. & Rahman, R.A. (2007) 'Statics and Dynamics Structural Analysis of a 4.5 Tonne Truck Chassis'. *Jurnal Mekanikal,* pp.56-57.

George, R., Gleeson, B., Elischer, M. & Ramsay, E. (1997) *Assessment of Truck/Trailer Dynamics.* ARRB Transport Research.

Kurdi, O. & Rahman, R.A. (2010) 'Finite Element Analysis of Road Roughness Effect on Stress Distribution of Heavy Duty Truck Chassis'. *International Journal of Technology,* pp.57-64.

Li, S., Yongchen, L. & Naiji, F. (2014) 'Optimization Design on Triangle Plate of Auxiliary Frame of Mixer Truck'. *The Open Mechanical Engineering Journal,* 8 pp.297-302.

Riley, W. & George, A. (2002) *Design, Analysis and Testing of a Formula SAE Car Chassis.* Society of Automotive Engineers.

Zoran, D.M., Novak, S.V. & Srbije, V. (2010) 'Analysis of Connection Element Classes and Locations and of Some Technical Requirements for The Mounting of Different Superstructure Types on Transport Vehicles'. *Military Technical Courier,* LIX, No.2 pp.120-141.

Volvo Bodybuilder Guidelines, Volvo Truck Corporation.

Renault Bodybuilder Guidelines, Renault Trucks SAS.

Scania Bodybuilder Guidelines, Scania CV AB.

MAN Bodybuilder Guidelines, MAN Trucks & Bus AG.

DAF Bodybuilder Guidelines, DAF Trucks NV.

Mercedes-Benz Bodybuilder Guidelines, Mercedes-Benz Trucks.

Appendices

Appendix A – Strain Gauge Positions

The three gauges in each rosette were given individual descriptors; A, B, C – named in clockwise direction.

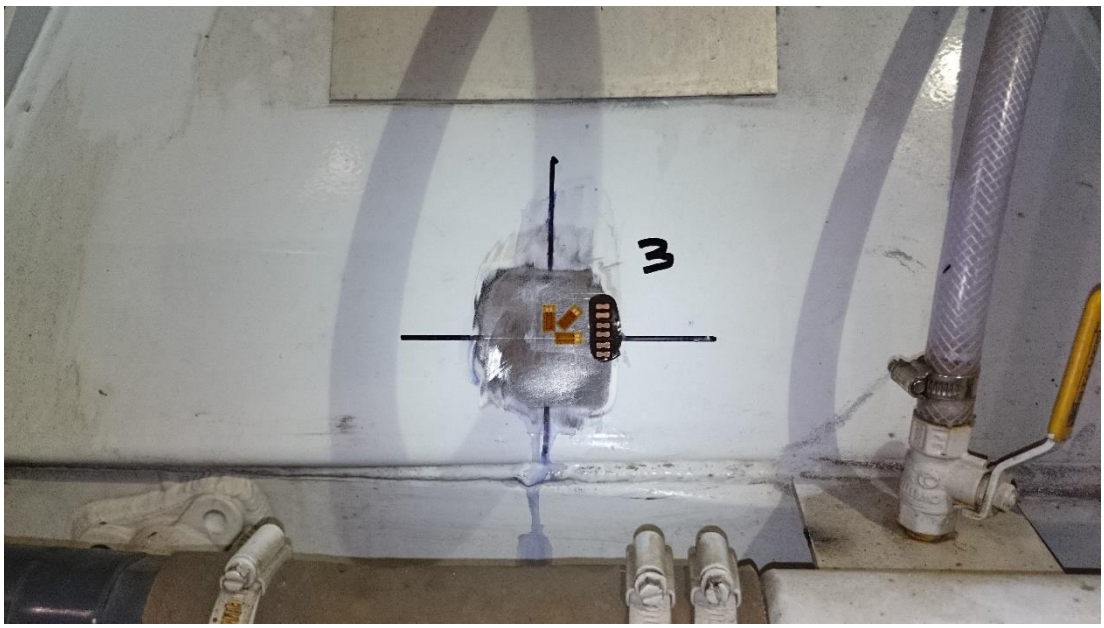
3


4


5


6


7


8

Appendix B – Additional Strain Data from Dynamic Load Test

Load case: Truck stationary – full 7.5m^3 concrete load – drum turning slowly

Explanation of gauge type: R1 indicates the rosette in position 1, S4 indicates single gauge in position 4.

Gauge type & Position	Row	Time (s)	Principal Stress (Mpa) (+ve for tension)	Principal Strain ($\mu\varepsilon$)	Shear Strain ($\mu\varepsilon$)	Principal Angle	Tensile or compressive/ notes
R1		1400	1.3	83	-229		
R1		1400	-53.8	-258	-229	21 anti-clockwise from A	
R2		1400	2.2	124	-92		
R2		1400	-79.6	-382	-92	5 clockwise from C	
R3		1400	4.6	52	25		
R3		1400	-21.1	-107	25	4.5 anti-clockwise from C	
S4		1400	-48.72				
S5		1400	7.35				
R6		1400	25.2	103	-81	38 anti-clockwise from C	
R6		1400	11.7	20	-81		
R7		1400	-31.4	-61	-76		
R7		1400	-34	-157	-76	26 clockwise from C	
R8		1400	5.9	89	-95		
R8		1400	-71.6	-308	-95	7 anti-clockwise from A	

Load case: Vertical/Bump Load – full 7.5m^3 concrete load – approx. 7mph

Gauge type & Position	Row	Time (s)	Principal Stress (Mpa) (+ve for tension)	Principal Strain ($\mu\varepsilon$)	Shear Strain ($\mu\varepsilon$)	Principal Angle	Tensile or compressive/ notes
R1	1580	1885.72	2.7	91	-222	21 anti-clockwise from C	Max tensile
R1	3962	1909.54	-60.4	-288	-241	20 anti-clockwise from A	Max compressive
R2	1524	1885.16	4	164	-98	5 clockwise from A	Max tensile
R2	3964	1909.56	-107	-513	-115	6.6 clockwise from C	Max compressive
R3	481	1874.73	24.3	107	21	4 anti-clockwise from A	Max tensile
R3	3964	1909.56	-20.9	-108	-12	2.8 clockwise C	Max compressive
S4	1593	1885.85	-26	-124			Min compressive
S4	4193	1911.85	-120.1	-572			Max compressive
S5	4184	1911.76	31.5	150			Max tensile
S5	1526	1885.18	6.5	31			Min tensile
R6	4447	1914.39	38.9	166	-157	45 clockwise from A	Max tensile
R6	493	1874.85	9.3	8	-65	43 anti-clockwise from C	Min tensile
R7	1586	1885.78	-30.7	-69	-43	20 anti-clockwise from C	Min compressive
R7	4189	1911.81	-79.8	-357	-110	15 anti-clockwise from C	Max compressive
R8	4189	1911.81	18	207	-269	8.7 anti clockwise from C	Max tensile
R8	4187	1911.79	-164	-694	-267	8.6 anti-clockwise from A	Max compressive

Load case: Longitudinal/Braking Load – 5m^3 concrete load – from 45 to 15mph

Gauge type & Position	Row	Time (s)	Principal Stress (Mpa) (+ve for tension)	Principal Strain ($\mu\varepsilon$)	Shear Strain ($\mu\varepsilon$)	Principal Angle	Tensile or compressive/ notes
R1	575	545.67	28.9	155	136	16.2 anti-clockwise from gauge A	Max tensile
R1	739	547.3	-12.9	-98.8	-63	21 anti-clockwise from A	Max compressive
R2	575	545.67	52.6	251	79	7 clockwise from C	Max tensile
R2	739	547.3	-13.75	-77	-31	11 clockwise from C	Max compressive
R3	575	545.67	12.6	54	41	27.4 clockwise from C	Max tensile
R3	739	547.3	-5	-20	5	7 anti-clockwise from C	Max compressive
S4	1489	554.8	10.7	51			Max tensile
S4	569	545.61	-37.59	-179			Max compressive
S5	594	545.86	12.81	61			Max tensile
S5	821	548.13	-0.4	-2			Max compressive
R6	473	544.65	9.2	41	-45	43 anti-clockwise from A	Max tensile
R6	723	547.15	-4	-22	24	38 anti-clockwise from C	Max compressive
R7	849	548.41	2.3	9	1	5.7 clockwise from C	Max tensile
R7	595	545.87	-19.9	-99	-44	18 anti-clockwise from C	Max compressive
R8	467	544.59	36	152	59	9 clockwise from A	Max tensile
R8	594	545.86	-37.3	-158	-59	8 anti-clockwise from A	Max compressive

Load case: Downhill – full 7.5m^3 concrete load

Gauge type & Position	Row	Time (s)	Principal Stress (Mpa) (+ve for tension)	Principal Strain ($\mu\varepsilon$)	Shear Strain ($\mu\varepsilon$)	Principal Angle	Tensile or compressive/ notes
R1	475	1459.67	7.4	132	-287	21 anti-clockwise from C	Max tensile
R1	449	1459.41	-77.5	-375	-320	20 anti-clockwise from A	Max compressive
R2	29	1455.21	23.2	180	60	14 clockwise from C	Max tensile
R2	453	1459.45	-115.9	-556	-151	6 clockwise from C	Max compressive
R3	60	1455.52	12.9	75	67		Max tensile
R3	451	1459.43	-30.2	-152	22	2 anti-clockwise from C	Max compressive
S4	484	1459.76	-11.8	-56			(Minimum compressive strain due to slope)
S4	33	1455.25	-82.7	-394			Max compressive
S5	485	1459.77	2.9	14			Min tensile
S5	8	1455	19.3	92			Max tensile
R6	513	1460.05	33.8	144	-133	41 anti-clockwise from C	Max tensile
R6	346	1458.38	8.5	6	14	45 clockwise from A	Min tensile
R7	484	1459.76	-20	-48	-48	30 clockwise from C	Min compressive
R7	420	1459.12	-49.7	-246	-121	24 clockwise from C	Max compressive
R8	25	1455.17	17.6	246	-315	8 anti-clockwise from C	Max tensile
R8	26	1455.18	-207.7	-879	-314	8 anti-clockwise from A	Max compressive

Appendix C – Bolts Tested in Section 3.2

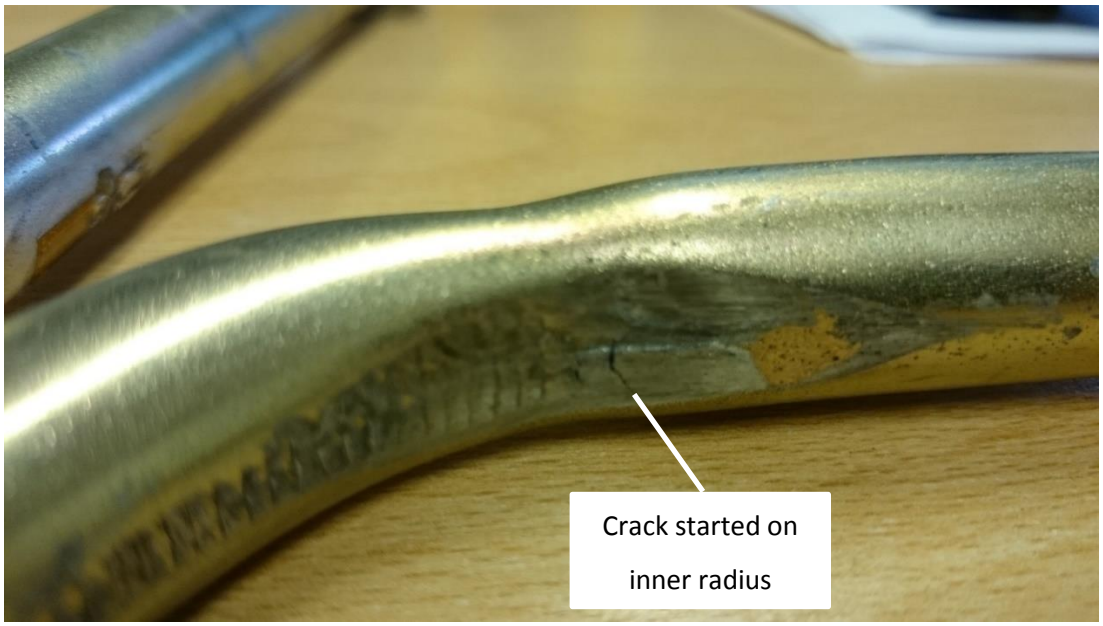
Crack started on
inner radius


Untested U-bolt for comparison

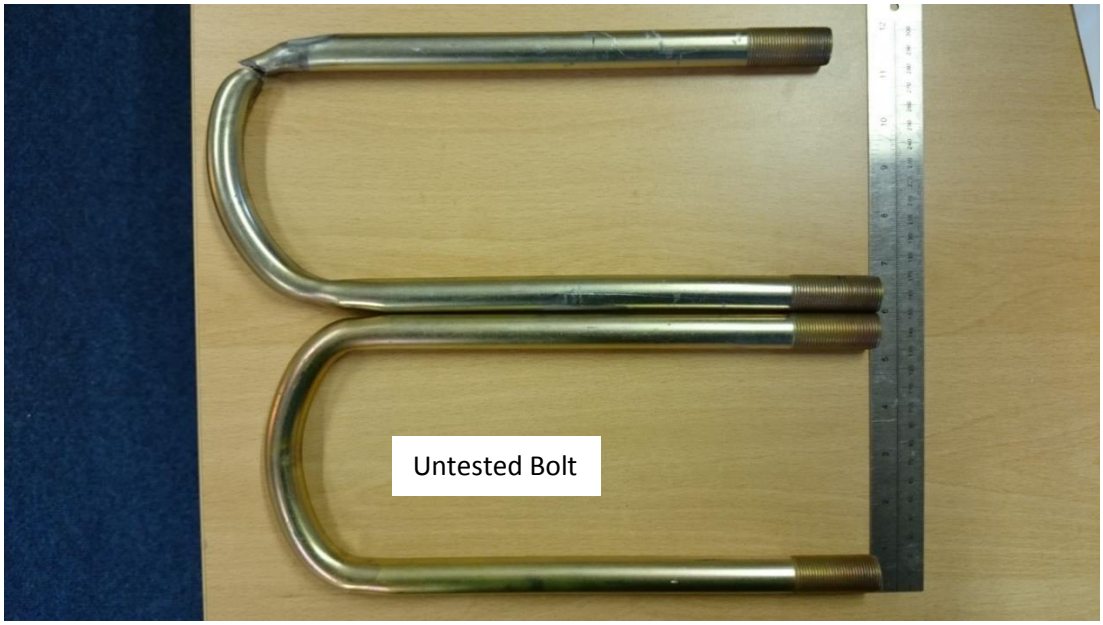
Untested Bolt